



**Ana Isabel Machado Mouquinho**  
Graduation in Chemistry

**Selective synthesis under Microwave  
Irradiation of New Monomers for potential  
applications in PDLC films**

Dissertation to obtain the degree of master in Bioorganic

Supervisor: Prof.Dr. João Carlos da Silva Barbosa Sotomayor  
(assistant professor, FCT/UNL)

President: Prof. Dr. Paula Cristina de Sérgio Branco

Examiner: Prof. Dr. Maria Madalena Alves Campos de Sousa Dionísio de Andrade  
Dr. Ana Maria Madeira Martins Faísca Phillips

Jury: Prof. Dr. João Carlos da Silva Barbosa Sotomayor  
Prof. Dr. Maria Madalena Alves Campos de Sousa Dionísio de Andrade  
Dr. Ana Maria Madeira Martins Faísca Phillips



FACULDADE DE  
CIÊNCIAS E TECNOLOGIA  
UNIVERSIDADE NOVA DE LISBOA

February, 2012



**Ana Isabel Machado Mouquinho**  
Graduation in Chemistry

**Selective synthesis under Microwave  
Irradiation of New Monomers for potential  
applications in PDLC films**

Dissertation to obtain the degree of master in Bioorganic

Supervisor: Prof. Dr. João Carlos da Silva Barbosa Sotomayor  
(FCT/UNL)

**February, 2012**





# **“Selective synthesis under Microwave Irradiation of New Monomers for potential applications in PDLC films”**

Copyright, Ana Isabel Machado Mouquinho, FCT/UNL, UNL

## **Indicação dos direitos de cópia**

A Faculdade de Ciências e Tecnologia e a Universidade Nova de Lisboa têm o direito, perpétuo e sem limites geográficos, de arquivar e publicar esta dissertação através de exemplares impressos reproduzidos em papel ou de forma digital, ou por qualquer outro meio conhecido ou que venha a ser inventado, e de a divulgar através de repositórios científicos e de admitir a sua cópia e distribuição com objectivos educacionais ou de investigação, não comerciais, desde que seja dado crédito ao autor e editor.

## **Copyright**

Faculdade de Ciências e Tecnologia and Universidade Nova de Lisboa have the perpetual right with no geographical boundaries, to archive and publish this dissertation through printed copies reproduced on paper or digital form or by any means known or to be invented, and to divulge through scientific repositories and admit your copy and distribution for educational purposes or research, not commercial, as long as the credit is given to the author and editor.



To Victor



### **Acknowledgements**

I would like to thank to my supervisor Professor João Sotomayor for his guidance, knowledge and support. Special thanks to the confidence placed in me and freedom of decision.

I also wish to thank and express my appreciation to Professor Teresa Barros for all her contribution to this work, for her insistence, her knowledge and encouragement.

I want to thank all the elements associated with this project, Krasimira Petrova, Alexandre Maiiau and Mara Saavedra for all their immense contribution to the results presented in this thesis. For all the difficulties and successes and for their friendship.

I must also thank to the colleagues of laboratory 3.15, 3.16 and 4.15 of the Chemistry Department of FCT/UNL. I am sincerely grateful to all.

I want to thank to the analysis laboratory of the Chemistry Department of FCT/UNL and especially to Carla Rodrigues and Maria do Rosário for technical support of DSC and NMR, respectively.

I want to thank to Professor Ana Isabel Ricardo for the opportunity and to Mara Silva for the technical support to use of GPC.

I would like to thank to Fundação para a Ciência e Tecnologia for the financial support through Project PTDC/CTM/69145/2006

I wish to thank to my mother, father, brother, sister in law and niece for all their love and support.

Finally, I want to thank to my husband, Victor, for all the love, support, patience, understanding, encouragement and great sense of humour. Without his love it would not be possible to accomplish this thesis.



## Abstract

Polymer dispersed liquid crystal (PDLC) films consist, commonly, on nematic liquid crystal domains dispersed in a polymeric matrix. These composites can be switched electrically from an opaque scattering state to a highly transparent state by an applied electric field. The molecular structure of the polymerisable monomers that can be incorporated as polymeric matrix plays an important role in the performance of PDLCs. Therefore, the aims of this work were to design and synthesise several new monomers that could be polymerised photochemically and thermally to be incorporated as polymeric matrices in PDLCs and investigate the influence of the molecular structure on the performance of these devices. Several monomers were synthesised in order to achieve better miscibility between the liquid crystal and the monomers during preparation of PDLC films. For this purpose, the monomers were synthesised so as to mimic some structural elements of the E7 liquid crystal molecules. Thus, several aromatic mono- and dimethacrylates with and without a linear chain spacer with five methylene units, as well as vinylic monomers were successfully synthesised. Mild and solvent free-procedures were developed with reaction times as short as 1 to 5 min, using microwave irradiation. The structures of all isolated monomers were supported by  $^1\text{H}$  NMR,  $^{13}\text{C}$  NMR and FTIR spectroscopy, elemental analysis and melting point. Of all the synthesised monomers, the monomers that included in their structure aromatic rings bearing a cyano group and/or a linear chain spacer with five methylene units were fully characterised due to their higher molecular structure affinity with the E7 liquid crystal molecules. In order to evaluate the effect of these groups, these monomers were compared with those of similar structure but without the respective groups. Thus, DSC and POM with temperature ramps were used for the thermal characterisation of the monomers. The structural morphologies of the polymeric matrices were characterised by SEM. The monomers were also copolymerised with glycidyl methacrylate and the molecular weights of the resulting polymers were evaluated by GPC. The electro-optical properties of the PDLC films were determined by measuring the voltage dependence on the transmitted light.

Keywords: Monomer synthesis, microwave irradiation, solventless reactions, liquid crystal, PDLC, electro-optical properties.





### Resumo

Filmes de cristal líquido disperso num polímero (PDLC) consistem geralmente em domínios de um cristal líquido nemático disperso numa matriz polimérica. Estes compósitos podem ser comutados electricamente de um estado opaco para um estado transparente pela aplicação de um campo eléctrico. A estrutura molecular dos monómeros que constituem a matriz polimérica desempenha um papel importante no desempenho dos PDLCs. Assim, o principal objectivo deste trabalho é sintetizar uma série de monómeros fotoquimicamente e termicamente polimerizáveis de modo a serem incorporados como matriz polimérica em PDLCs e investigar o efeito da estrutura química dos monómeros no desempenho dos respectivos dispositivos. Vários monómeros novos foram sintetizados e concebidos de modo a permitirem uma melhor miscibilidade entre o cristal líquido e o monómero na preparação dos filmes de PDLC. Assim, os monómeros sintetizados foram desenhados com uma estrutura molecular próxima à estrutura das moléculas de cristal líquido, E7. Com este propósito foram sintetizados com sucesso monómeros aromáticos, mono- e di-metacrilatos com e sem uma cadeia linear de cinco unidades de metileno (espaçador) assim como monómeros vinílicos. Para a síntese dos mesmos, foram desenvolvidos procedimentos sem recurso ou com recurso a quantidades mínimas de solvente e com tempos de reacção entre 1 a 5 minutos através de radiação por micro-ondas. A estrutura molecular de todos os monómeros isolados foi comprovada por espectroscopia de  $^1\text{H}$  RMN,  $^{13}\text{C}$  RMN e de FTIR, análise elementar e ponto de fusão. De entre os monómeros sintetizados existe um grupo que foi amplamente caracterizado devido à maior afinidade estrutural com as moléculas do cristal líquido E7. Estes monómeros incluem na sua estrutura molecular o grupo ciano ligado ao sistema aromático e/ou uma cadeia linear (espaçador). De modo a avaliar o efeito destes grupos, estes monómeros foram comparados com os de estrutura semelhante mas sem os respectivos grupos. Assim, estes monómeros foram termicamente caracterizados por DSC e POM com rampas de aquecimento. As morfologias da matriz polimérica foram caracterizadas por SEM. Os monómeros foram também co-polimerizados com metacrilato de glicidilo e o peso molecular dos respectivos polímeros foi determinado por GPC. As propriedades electro-ópticas dos filmes de PDLC produzidos foram estudadas através da sua resposta electro-óptica pela aplicação de um campo eléctrico.

Palavras-chave: Síntese de monómeros, radiação por microondas, reacções sem solvente, cristais líquidos, PDLC, propriedades electro-ópticas.



## General Index

Acknowledgements .....	IX
Abstract .....	XI
Resumo .....	XIII
General Index .....	XV
Figure Index .....	XVII
Table Index .....	XXI
Symbols and Abbreviations.....	XXIII

## Chapter I

1 Introduction .....	1
1.1 Liquid Crystals.....	1
1.1.1 Lyotropic liquid crystals.....	1
1.1.2 Thermotropic liquid crystals .....	2
1.2 Liquid crystal properties .....	4
1.3 The nematic Liquid Crystal mixture E7.....	7
1.4 Polymer Dispersed Liquid Crystals .....	8
1.5 Free radical polymerisation.....	8
1.6 Microstructure of the polymer network .....	11
1.7 PDLC films transmittance.....	13
1.7.1 Electro-optical properties of PDLCs.....	14
1.8 Parameters that influence the performance of PDLC films .....	16
1.8.1 Polymeric conditions.....	17
1.8.2 Molecular structure of polymerisable monomers.....	17
1.9 Applications .....	18

## Chapter II

2 Materials and Methods .....	19
2.1 Outline .....	19
2.2 Materials.....	19
2.2.1 Nematic liquid crystal E7 .....	19
2.2.2 Initiators of polymerisation .....	19
2.2.3 Indium tin oxide cells.....	20
2.3 Methods.....	21
2.3.1 Microwave Irradiation.....	21
2.3.2 Characterisation of compounds synthesised .....	23
2.3.3 Preparation of PDLC films by the PIPS method.....	23
2.3.3.1 Photochemical polymerisation .....	24
2.3.3.2 Thermal polymerisation .....	24
2.3.4 Gel permeation chromatography.....	24
2.3.5 Scanning Electron Microscopy (SEM) .....	26
2.3.6 Differential scanning calorimetry (DSC).....	26
2.3.7 Polarised optical microscopy .....	28
2.3.8 Electro-optical properties .....	29

## Chapter III

3 Synthesis and Characterisation.....	31
3.1 Outline .....	31
3.2 List of synthesised monomers.....	32

3.3	Synthesis of methacrylate monomers .....	33
3.3.1	Monomers without a linear chain spacer with five methacrylate units .....	33
3.3.1.1	Experimental method used for monomethacrylate monomers .....	33
3.3.1.2	Experimental method used for dimethacrylate monomers .....	34
3.3.2	Synthesis of aromatic compounds bearing an alkyl bromide chain (precursors) .....	35
3.3.2.1	Experimental method used for monobromide precursors .....	36
3.3.2.2	Experimental method used for dibrominated precursors .....	36
3.3.3	Monomers bearing a linear chain spacer with five methylene units (19-24) .....	37
3.3.3.1	Experimental method used for monomethacrylate monomers (19-22) .....	37
3.3.3.2	Experimental method used for dimethacrylate monomers (23-24) .....	38
3.3.4	Synthesis of vinylic monomers (25-26) .....	39
3.3.4.1	Experimental method used for vinylic monomers .....	39
3.4	Characterisation .....	40
3.4.1	Monomethacrylate monomers without spacer .....	40
3.4.2	Dimethacrylated monomers without spacer .....	44
3.4.3	Aromatic compounds bearing an alkyl monobromide chain (precursors) .....	46
3.4.4	Aromatic compounds bearing an alkyl dibromide chain (precursors) .....	48
3.4.5	Monomethacrylate monomers bearing a linear chain spacer with five methylene units 49	49
3.4.6	Dimethacrylate monomers bearing a linear chain spacer with five methylene units ..	51
3.4.7	Vinylic monomers (25-26) .....	52
3.5	Results obtained under classical synthetic versus microwave irradiation methodologies ..	53
3.6	Selected monomers .....	54
 <b>Chapter IV</b>		
4	Thermal Characterisation .....	55
4.1	Outline .....	55
4.2	Calorimetric characterisation .....	55
4.3	Polarised optical microscopy characterisation .....	61
 <b>Chapter V</b>		
5	Structural and electro-optical characterisation .....	71
5.1	Outline .....	71
5.2	Molecular weights and polymer structures .....	71
5.2.1	Characterisation of molecular weights .....	71
5.2.2	Microstructure of the polymer matrix .....	73
5.2.3	Electro-optical characterisation .....	77
 <b>Chapter VI</b>		
6	Conclusions .....	79
 <b>Chapter VII</b>		
7	Bibliography .....	81
 <b>Chapter VIII</b>		
8	Appendix .....	85
8.1	NMR Spectra .....	85

## Figure Index

### Chapter I

Figure 1.1 – Various aggregate morphologies: a micelle (a), cylindrical micelle (b), bilayer (c), vesicle(d) and inverted micelle(e) (adapted from ref. <sup>5</sup> ).	2
Figure 1.2 – Molecular order in a nematic liquid crystal. The director shows the direction of preferred orientation (adapted from ref. <sup>3</sup> ).	3
Figure 1.3 – Schematic representation of the sequence of phase transition between solid, nematic liquid crystal and isotropic liquid by increasing temperature (adapted from ref. <sup>3</sup> ).	4
Figure 1.4 – Schematic illustration of the refraction of unpolarised light travelling through a birefringent material (adapted from ref. <sup>8</sup> ).	5
Figure 1.5 – Temperature dependence on refractive index of a thermotropic liquid crystal (adapted from ref. <sup>3</sup> ).	5
Figure 1.6 – Schematic illustration of the effect of an electric field on liquid crystal molecules (adapted from ref. <sup>11</sup> ).	6
Figure 1.7 – Molecular structures of the components of the nematic liquid crystal mixture E7.	7
Figure 1.8 – Reaction scheme for the thermal decomposition of N, N-azobisisobutyronitrile (AIBN) in the two isobutyronitrile radicals.	9
Figure 1.9 –Reaction scheme for UV induced decomposition of 2,2-dimethoxy-2-phenylacetophenone (DMPA) into an benzoyl and an acetal radical fragments.	9
Figure 1.10 – SEM micrograph for the microstructure of the polymer matrix with a swiss cheese morphology type.	11
Figure 1.11 - Schematic illustration of bipolar (a) and radial (b) director configurations of the liquid crystals inside spherical droplets (adapted from ref. <sup>3</sup> ).	12
Figure 1.12 – SEM micrograph for the microstructure of the polymer matrix with polymer ball morphology type.	12
Figure 1.13 – Schematic representation of the averaged molecular orientation of the liquid crystal within the microdroplets without (a) and with (b) an applied electric field (adapted from ref. <sup>3</sup> ).	13
Figure 1.14 – Example of electro-optical response of PDLC with no hysteresis.	14
Figure 1.15 – Example of electro-optical response of PDLC with hysteresis.	15
Figure 1.16 –Example of electro-optical response of PDLC with permanent memory effect.	15
Figure 1.17 – Images of PDLC dives with permanent memory effect: (a) initial OFF state, (b) upon applying electric field and (c) OFF state after removed electric field.	16
Figure 1.18 – Example of application of PDLC in switchable windows in ON (a) and OFF (b) state.	18

### Chapter II

Figure 2.1 – Schematic illustration of an indium tin oxide (ITO) cell.	20
Figure 2.2 –Schematic representation of conventional (a) and microwave heating (b) (adapted from <sup>36</sup> ).	21
Figure 2.3 – A schematic representation for the preparation of PDLC films by the PIPS method.	23
Figure 2.4 – Schematic diagram of the experimental system set-up used to study electro-optical properties.	30

### Chapter III

Figure 3.1 – Molecular structures of synthesised monomers.	32
Figure 3.2 – General scheme for the synthesis of (a) monomethacrylate monomers and (b) dimethacrylate monomers.	33
Figure 3.3 – General scheme for the synthesis of (a) monobromide and (b) dibromide precursors.	35
Figure 3.4 –General scheme for the synthesis of (a) mono- and (b) dimethacrylate monomers bearing a linear chain spacer with five methylene units.	37

## Figure Index

---

Figure 3.5 – General scheme for the synthesis of vinylic monomers.....	39
Figure 3.6 – Molecular structure of synthesised monomers with and without cyano and spacer chain group.....	54

### Chapter IV

Figure 4.1 – DSC measurement obtained for monomer 19 during cycle I at 10°C min <sup>-1</sup> .....	56
Figure 4.2 – DSC measurement obtained for monomer 1 during cycle I at 10°C min <sup>-1</sup> .....	56
Figure 4.3 – DSC measurement obtained for monomer 7 during cycle I at 10°C min <sup>-1</sup> .....	57
Figure 4.4 – DSC measurement obtained for monomer 5 during cycle I at 10°C min <sup>-1</sup> .....	57
Figure 4.5 – DSC measurement obtained for monomer 22 during cycle I at 10°C min <sup>-1</sup> .....	57
Figure 4.6 – DSC measurement obtained for monomer 21 during cycle I at 10°C min <sup>-1</sup> .....	58
Figure 4.7 – DSC measurement obtained for monomer 20 during cycle I at 10°C min <sup>-1</sup> .....	59
Figure 4.8 – DSC measurement obtained for monomer 8 during cycle I at 10°C min <sup>-1</sup> .....	59
Figure 4.9 – Optical micrographs of monomer 19 at specific temperatures during the heating and cooling runs at 10°C min <sup>-1</sup> .....	61
Figure 4.10 – Optical micrographs of monomer 1 at specific temperature during the heating and cooling runs at 10°C min <sup>-1</sup> .....	62
Figure 4.11 – Optical micrographs of monomer 7 at specific temperature during the heating and cooling run at 10°C min <sup>-1</sup> .....	63
Figure 4.12 – Optical micrographs of monomer 5 at specific temperatures during the heating and cooling runs at 10°C min <sup>-1</sup> .....	64
Figure 4.13 – Optical micrographs of monomer 22 at specific temperatures during the heating and cooling runs at 10°C min <sup>-1</sup> .....	65
Figure 4.14 – Optical micrographs of monomer 21 at specific temperatures during the heating and cooling run at 10°C min <sup>-1</sup> .....	66
Figure 4.15 – Optical micrographs of monomer 20 at specific temperatures during the heating and cooling runs at 10°C min <sup>-1</sup> .....	67
Figure 4.16 - Optical micrographs of monomer 8 at specific temperatures during the first and second heating at 10°C min <sup>-1</sup> .....	68

### Chapter V

Figure 5.1 – SEM micrographs for the microstructure of the polymer matrix prepared by (a) thermal and (b) photochemical polymerisation of monomer 19. ....	73
Figure 5.2 – SEM micrographs for the microstructure of the polymer matrix prepared by (a) thermal and (b) photochemical polymerisation of monomer 1. ....	74
Figure 5.3 – SEM micrographs for the microstructure of the polymer matrix prepared by (a) thermal and (b) photochemical polymerisation of monomer 7. ....	74
Figure 5.4 – SEM micrographs for the microstructure of the polymer matrix prepared by (a) thermal and (b) photochemical polymerisation of monomer 5. ....	75
Figure 5.5 – SEM micrographs for the microstructure of the polymer matrix prepared by (a) thermal and (b) photochemical polymerisation of monomer 22. ....	75
Figure 5.6 – SEM micrograph for the microstructure of the polymer matrix prepared by (a) thermal and (b) photochemical polymerisation of monomer 21. ....	76
Figure 5.7 – SEM micrograph for the microstructure of the polymer matrix prepared by (a) thermal and (b) photochemical polymerisation of monomer 20. ....	76
Figure 5.8 – SEM micrograph for the microstructure of the polymer matrix prepared by (a) thermal and (b) photochemical polymerisation of monomer 8. ....	77
Figure 5.9 – General electro-optical response for PDLC films prepared by the PIPS method with the monomers synthesised + E7 in a ratio of 30/70 (w/w). ....	77

**Chapter VIII**

Figure 8.1 – Proton NMR spectrum of monomer 1.....	85
Figure 8.2 – Carbon NMR spectrum of monomer 1. ....	85
Figure 8.3 – Proton NMR spectrum of monomer 2.....	86
Figure 8.4 – Carbon NMR spectrum of monomer 2. ....	86
Figure 8.5 – Proton NMR spectrum of monomer 3.....	87
Figure 8.6 – Carbon NMR spectrum of monomer 3. ....	87
Figure 8.7 – Proton NMR spectrum of monomer 4.....	88
Figure 8.8 – Carbon NMR spectrum of monomer 4. ....	88
Figure 8.9 – Proton NMR spectrum of monomer 5.....	89
Figure 8.10 – Carbon NMR spectrum of monomer 5. ....	89
Figure 8.11 – Proton NMR spectrum of monomer 6.....	90
Figure 8.12 – Carbon NMR Spectrum of monomer 6.....	90
Figure 8.13 – Proton NMR spectrum of monomer 7.....	91
Figure 8.14 – Proton NMR spectrum of monomer 7.....	91
Figure 8.15 – Proton NMR spectrum of monomer 8.....	92
Figure 8.16 – Carbon NMR spectrum of monomer 8. ....	92
Figure 8.17 – Proton NMR spectrum of monomer 9.....	93
Figure 8.18 – Carbon NMR spectrum of monomer 9. ....	93
Figure 8.19 – Proton NMR spectrum of monomer 10.....	94
Figure 8.20 – Carbon NMR spectrum of monomer 10. ....	94
Figure 8.21 – Proton NMR spectrum of monomer 11.....	95
Figure 8.22 – Carbon NMR spectrum of monomer 11. ....	95
Figure 8.23 – Proton NMR spectrum of monomer 12.....	96
Figure 8.24 – Carbon NMR spectrum of monomer 12. ....	96
Figure 8.25 – Proton NMR spectrum of compound 13.....	97
Figure 8.26 – Carbon NMR spectrum of compound 13.....	97
Figure 8.27 – Proton NMR spectrum of compound 14.....	98
Figure 8.28 – Carbon NMR spectrum of compound 14.....	98
Figure 8.29 – Proton NMR spectrum of compound 15.....	99
Figure 8.30 – Carbon NMR spectrum of compound 15.....	99
Figure 8.31 – Proton NMR spectrum of compound 16.....	100
Figure 8.32 – Carbon NMR spectrum of compound 16.....	100
Figure 8.33 – Proton NMR spectrum of compound 17.....	101
Figure 8.34 – Carbon NMR spectrum of compound 17.....	101
Figure 8.35 – Proton NMR spectrum of compound 18.....	102
Figure 8.36 – Carbon NMR spectrum of monomer 18. ....	102
Figure 8.37 – Proton NMR spectrum of monomer 19.....	103
Figure 8.38 – Carbon NMR spectrum of monomer 19. ....	103
Figure 8.39 – Proton NMR spectrum of monomer 20.....	104
Figure 8.40 – Carbon NMR spectrum of monomer 20. ....	104
Figure 8.41 – Proton NMR spectrum of monomer 21.....	105
Figure 8.42 – Carbon NMR spectrum of monomer 21. ....	105
Figure 8.43 – Proton NMR spectrum of monomer 22.....	106
Figure 8.44 – Carbon NMR spectrum of monomer 22. ....	106
Figure 8.45 – Proton NMR spectrum of monomer 23.....	107
Figure 8.46 – Carbon NMR spectrum of monomer 23. ....	107
Figure 8.47 – Proton NMR spectrum of monomer 24.....	108
Figure 8.48 – Carbon NMR spectrum of monomer 24. ....	108
Figure 8.49 – Proton NMR spectrum of monomer 25.....	109
Figure 8.50 – Carbon NMR spectrum of monomer 25. ....	109
Figure 8.51 – Proton NMR spectrum of monomer 26.....	110
Figure 8.52 – Carbon NMR spectrum of monomer 26. ....	110





**Table Index**

**Chapter I**

Table 1.1 – Components and mass composition of the Merck E7 liquid crystal. .... 7

**Chapter III**

Table 3.1 – Synthesis of monomethacrylate monomers..... 34  
 Table 3.2 – Synthesis of dimethacrylate monomers..... 35  
 Table 3.3 – Synthesis of monobromide precursors. .... 36  
 Table 3.4 – Synthesis of dibrominated precursors. .... 37  
 Table 3.5 – Synthesis of monomethacrylate monomers bearing a linear chain spacer with five methylene units. .... 38  
 Table 3.6 – Synthesis of dimethacrylate monomers bearing a linear chain spacer with five methylene units. .... 39  
 Table 3.7 – Synthesis of vinylic monomers. .... 40

**Chapter IV**

Table 4.1 - Thermal properties of monomers obtained by DSC during different cooling/heating cycles ..... 60  
 Table 4.2 – Thermal properties of monomers obtained by POM during heating/cooling runs..... 69

**Chapter V**

Table 5.1 – Values of average molecular weights ( $M_n$  and  $M_w$ ) and polydispersity index (PDI) for polymers prepared with a mixture of monomer/glycidyl methacrylate (50/50 w/w) by thermal polymerisation. .... 72  
 Table 5.2 – Values of average molecular weights ( $M_n$  and  $M_w$ ) and polydispersity index (PD) for polymers prepared with a mixture of monomer/glycidyl methacrylate (50/50 w/w) by photochemical polymerisation. .... 72



## Symbols and Abbreviations

$\Delta H_{cr}$  – Enthalpy of crystallisation

$\Delta H_m$  – Enthalpy of fusion

$\Delta n$  – Optical anisotropy

$\Delta \epsilon$  – Dielectric anisotropy

$^{13}\text{C}$  NMR – Carbon - 13 Nuclear Magnetic Resonance

$^1\text{H}$  NMR – Proton Nuclear Magnetic Resonance

5CB - 4-cyano-4'-pentyl-1,1'-biphenyl

5CT – 4'-n-pentyl-4-cyanoterphenyl

7CB – 4-n-heptyl-4' cyanobiphenyl

8OCB – 4,4'-n-octyloxycyanobiphenyl

AIBN – N,N-azobisisobutyronitrile

$\text{CDCl}_3$  – Deuterated chloroform

$\text{CH}_2\text{Cl}_2$  – Dichloromethane

d – Doublet

dd – Double doublet

DMF – Dimethylformamide

DMPA – 2, 2-dimethoxy-2-phenylacetophenone

DSC – Differential Scanning Calorimetry

E7 – The nematic liquid crystal E7

$E_{90}$  – Electric field required for the PDLC to reach 90% of its maximum transmittance

FTIR – Fourier Transform Infrared

GPC – Gel Permeation Chromatography

Hz – Hertz

ITO – Indium Tin Oxide

J – Coupling constant

$\text{K}_2\text{CO}_3$  – Potassium carbonate

LC – Liquid crystal

m – Multiplet

m.p. – Melting point

MAOS – Microwave Assisted Organic Synthesis

$M_n$  – Number average molecular weight

MW – Microwave

$M_w$  – Weight average molecular weight

n – Director of the liquid crystal

- $n_e$  – Extraordinary refractive index  
NEt<sub>3</sub> – Triethylamine  
Nh $\nu$ /min – Einstein (moles of photons) per minute  
 $n_o$  – Ordinary refractive index  
 $n_p$  - Refractive index of polymer  
PDI – Polydispersity index  
PDLC – Polymer Dispersed Liquid Crystal  
PIPS – Polymerisation Induced Phase Separation  
POM – Polarised Optical Microscopy  
ppm – Parts per million  
q – quadruplet  
s – Singlet  
SEC – Size Exclusion Chromatography  
SEM – Scanning Electron Microscopy  
SIPS – Solvent Induced Phase Separation  
t – Triplet  
Tan $\delta$  – Measure of the loss factor  
T<sub>c</sub> – Crystallisation temperature  
T<sub>CC</sub> – Cold crystallisation temperature  
T<sub>g</sub> – Glass transition temperature  
TIPS - Thermally Induced Phase Separation  
TLC – Thin Layer Chromatography  
T<sub>m</sub> – Melting temperature  
T<sub>MI</sub> – Mesophase to isotropic transition temperature  
TMS – Tetramethylsilane  
T<sub>NI</sub> - Nematic to isotropic transition temperature  
T<sub>SM</sub> – Solid to mesophase transition temperature  
T<sub>SN</sub> - Solid to nematic transition temperature  
 $\gamma$  – Out-of-plane bending vibrations  
 $\delta$  – Bending vibrations  
 $\delta$  – Chemical shift  
 $\epsilon_{\perp}$  - Dielectric constant according to the direction perpendicular to the director  
 $\epsilon_{\parallel}$  - Dielectric constant according to the direction parallel to the director  
 $\epsilon'$  - Dielectric constant  
 $\epsilon''$  - Dielectric loss  
 $\nu$  – Stretching vibrations

# Chapter I

## 1 Introduction

### 1.1 Liquid Crystals

Liquid crystals (LCs) are materials which have structures between the crystalline solid state and the liquid state. In crystals the molecules maintain fixed positional and orientational order and minimal mobility; on the other hand the opposite occurs in the liquids where there is neither positional or orientational order. Between these two extremes there is the situation in which the liquid crystal molecules are free to flow like a liquid but keeping a certain direction, maintaining some degree of orientation but losing their positional order<sup>1</sup>. For this reason LCs are referred to as intermediate phases or mesophases. The mesophases are true thermodynamic stable states of matter like solids, liquids and gases. Hence LCs are also often referred to the fourth state of matter<sup>2</sup>. In a simple way, liquid crystals can be divided into two main groups according to the conditions to achieve a stable liquid crystal phase: the temperature for thermotropic LC and the concentration of the solution for lyotropic LC<sup>1</sup>.

#### 1.1.1 Lyotropic liquid crystals

Lyotropic liquid crystals display liquid crystalline behaviour only when mixed with another material (solvent). The temperature is an important variable in determining the phase present. Nevertheless, it is common to indicate the concentration of solution as the main variable to achieve lyotropic liquid crystal domain.<sup>3</sup>

Generally, molecules of lyotropic liquid crystals have two distinct parts: a polar, often ionic, head (hydrophilic group) and a nonpolar often hydrocarbon tail (hydrophobic group). In solution, when the concentration gets high enough the amphiphilic molecules form ordered structures, the molecules arrange themselves in such a way that either the polar ends are turned out in a polar solvent (figure 1.1, a,b,c,d) or the nonpolar ends are turned out in a nonpolar solvent (figure 1.1, e). The opposite end is kept isolated from the unlike solvent. For example, when dissolved in a polar solvent such as water, the hydrophobic tails assemble together and present the hydrophilic heads to the solvent. When the concentration gets high enough the molecules assemble themselves. For low concentrations, the solution looks as if it were made-up of any other particles distributed randomly throughout the solvent. Many liquid crystalline biomolecules are found in cell membranes, and such structures have properties that are dependent on liquid crystallinity for their function<sup>4</sup>.

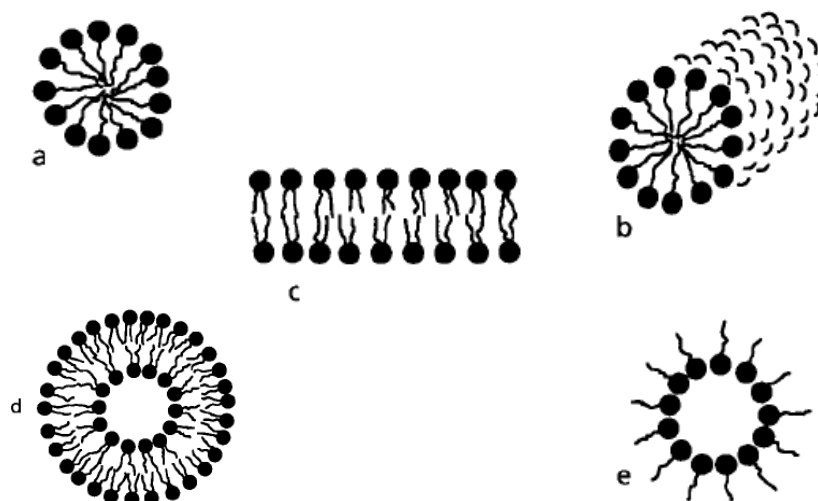


**Figure 1.1 – Various aggregate morphologies: a micelle (a), cylindrical micelle (b), bilayer (c), vesicle(d) and inverted micelle(e) (adapted from ref. <sup>5</sup>).**

The potential applications of lyotropic liquid crystals are related to the area of detergents, food emulsifiers, oil recovery and medical technology <sup>3</sup>. The optical switching properties of liquid crystals are characteristic of thermotropic liquid crystals. This type of LC has been widely used in electro-optical applications and therefore is of great interest in this work.

### 1.1.2 Thermotropic liquid crystals

In a simple way, within thermotropic liquid crystals there are four main types of LCs. These different types include the calamitic, discotic, pyramid and tetrahedral liquid crystals which, depending on the geometrical shape of the molecules resemble a rod, a disc, a pyramid and a tetrahedron, respectively. The calamitic liquid crystal is the most common type of liquid crystal and gives rise to two main phases, smetic and nematic, depending upon the amount of order in the material <sup>1, 3, 6</sup>.

The smetic liquid crystals usually do not respond to an applied electric field as easily as nematic liquid crystals. The simple application of an electric field rarely produces enough change in the optical properties of a smetic liquid crystal to be useful to apply in displays. For this reason, the nematic phase of calamitic liquid crystals has received great interested for technology applications, and are more studied in this area <sup>3, 6</sup>. The nematic phase is the simplest liquid crystal phase. In this phase the molecules maintain a preferred orientational direction as they diffuse throughout the sample. The nematic phase is characterised by long-range orientation order, the long axes of the molecules tend to align along a preferred direction.

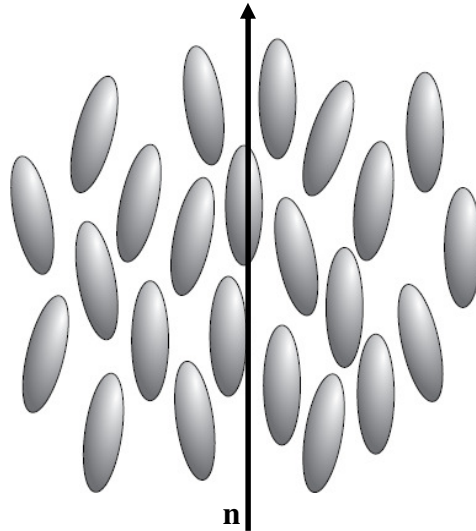


**Figure 1.2 – Molecular order in a nematic liquid crystal. The director shows the direction of preferred orientation (adapted from ref. <sup>3</sup>).**

In this phase the molecules possess only orientational but no long range positional order. The preferred alignment can be described by a unit vector  $\sim n$ , called “director”. The direction of  $\sim n$  is imposed by external forces such as the guiding effect of the wall of the container or electric and magnetic fields. The uniaxial nematic phase is characterised by rotational symmetry of the system around the director  $\sim n$ <sup>1</sup>.

As previously mentioned, the transitions involving thermotropic liquid crystal are effected by changing temperature on pure compounds or a mixture of compounds. Normally, when such a crystal melts both types of order, positional and orientational, disappear at the same temperature ( $T_m$ ). The resulting phase is an isotropic liquid where molecules move randomly. However, there are special crystalline solids that melt at  $T_{SN}$  (solid to nematic transition temperature) but to intermediate state (nematic phase) and only at higher temperature, when achieve a nematic to isotropic transition temperature,  $T_{NI}$ , to isotropic liquid state. In the intermediate state positional order disappears either fully or partially while some degree of orientational order is maintained. The liquid crystal phase obtained is stable for a certain temperature interval  $T_{SN} - T_{NI}$ <sup>1,7</sup>. Figure 1.3 illustrates the order present in the crystalline solid, nematic liquid crystal and isotropic liquid phases.

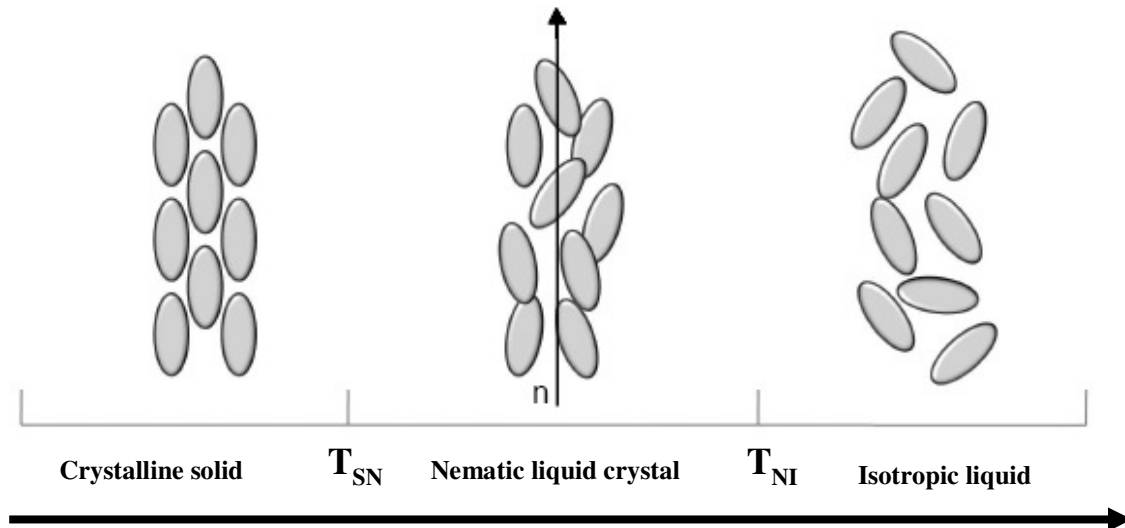


**Figure 1.3 – Schematic representation of the sequence of phase transition between solid, nematic liquid crystal and isotropic liquid by increasing temperature (adapted from ref. <sup>3</sup>).**

## 1.2 Liquid crystal properties

Liquid crystals possess many of the mechanical properties of an isotropic liquid, such as, high fluidity and the inability to support shear, but on the other hand, they have some properties similar to crystalline solids such optical anisotropy (birefringence)<sup>6</sup>.

In the liquid and gaseous states of matter, where there is no orientational order among the molecules any property measured along one direction has the same value in all directions, in other words all directions in space are equivalent. The property by which the same result is obtained regardless the direction of measurement or observation is called isotropy, and a phase that has this property is called an isotropic phase<sup>3</sup>. On the other hand, as a result of orientational order among the molecules of liquid crystals, the isotropy is destroyed and most physical properties are related to anisotropy. This means that the same properties with different values are measured along different directions. Changing the orientational order of the anisotropic molecules by the application of electric and magnetic fields it is possible to modify the original optical and the mechanical properties. The principal types of anisotropies in liquid crystals are the optic and the dielectric anisotropies.

The optic anisotropy in a nematic liquid crystal is related to birefringence. The birefringence in a nematic liquid crystal is characterised by the fact that an unpolarised light ray entering a liquid crystal is in general divided into two rays, which travel through the liquid crystal with different velocities and directions. This is due to an ordinary,  $n_o$ , and an extraordinary,  $n_e$ , indices, and having the electric vector normal and parallel to the nematic director, respectively (figure 1.4).



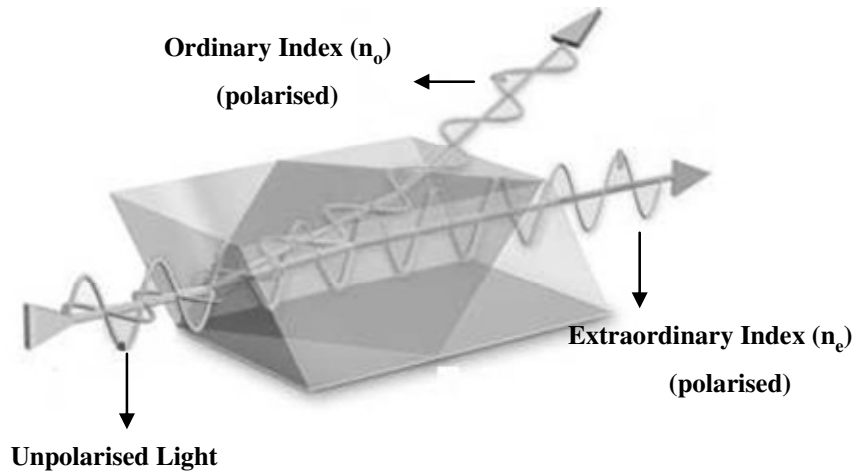


Figure 1.4 – Schematic illustration of the refraction of unpolarised light travelling through a birefringent material (adapted from ref.<sup>8</sup>).

The birefringence of a material is characterised by the difference,  $\Delta n$ , between the refractive indices for the extraordinary,  $n_e$ , and ordinary,  $n_o$ , ray<sup>9</sup>:

$$\Delta n = n_e - n_o$$

The degree of orientational order in liquid crystal varies with temperature, and therefore the refractive indices also change. At still higher temperature  $T_{NI}$  (nematic to isotropic transition temperature) a mesophase melts into an isotropic liquid with no positional and orientational order and the two indices become closer together in value. At the transition to the isotropic liquid the anisotropy disappears, and one refractive index prevails (figure 1.5)<sup>3</sup>.

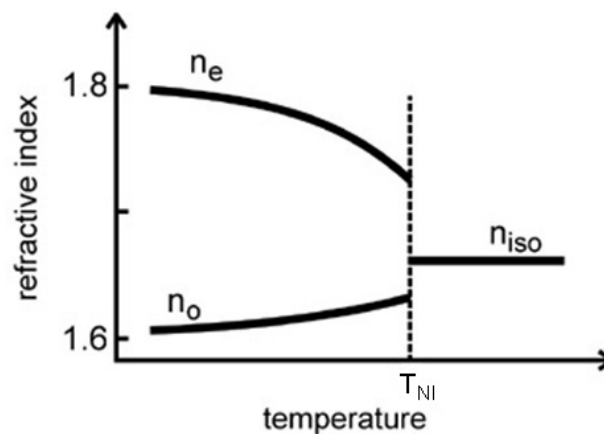
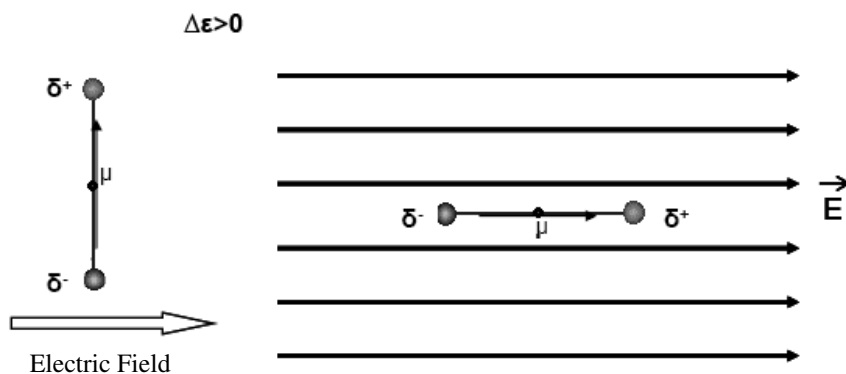


Figure 1.5 – Temperature dependence on refractive index of a thermotropic liquid crystal (adapted from ref.<sup>3</sup>).

The dielectric anisotropy determines the orientation of the liquid crystal molecules in the presence of an electric field. The electric field has a direction associated with it and when external electric fields are applied to a liquid crystal, the phase responds differently depending on direction that the electric field is applied. The freedom of the liquid crystal to change orientation (like liquids) but to do so while maintaining some orientational order among the molecules (like crystalline solids) allows this type of response with the electric field<sup>3</sup>. The dielectric anisotropy is characterised by the dielectric constants measured perpendicularly,  $\epsilon_{\perp}$ , and parallel,  $\epsilon_{\parallel}$ , to the longitudinal axis of the liquid crystal molecule. The dielectric anisotropy is given by:

$$\Delta\epsilon = \epsilon_{\parallel} - \epsilon_{\perp}$$

This difference is a measure of the tendency of the director of molecules to align parallel or perpendicular to the electric field applied. If no electric field is applied, the permanent electric dipoles on the liquid crystal molecules are not aligned, even if orientational order is present. When an electric field is applied, the molecules tend to orient according to the director of the electric field. When  $\epsilon_{\parallel} > \epsilon_{\perp}$ , the dielectric anisotropy,  $\Delta\epsilon$ , is positive and the director of molecules on the liquid crystal tends to align parallel to applied the electric field (figure 1.6), but when  $\epsilon_{\perp} > \epsilon_{\parallel}$  the dielectric anisotropy,  $\Delta\epsilon$ , is negative and the director of molecules on liquid crystal tend to align perpendicularly to the electric field applied<sup>10</sup>.



**Figure 1.6 – Schematic illustration of the effect of an electric field on liquid crystal molecules (adapted from ref.<sup>11</sup>).**

### 1.3 The nematic Liquid Crystal mixture E7

The liquid crystal used in this work is a thermotropic calamitic nematic, known as E7. It is a mixture composed by three different cyanobiphenyls and one cyanoterphenyl in different proportions. The molecular structures of the different components of the nematic liquid crystal E7 are shown in figure 1.7. The weight/weight (w/w) percentage and physical properties of E7 components are shown in table 1.1<sup>7, 12</sup>.

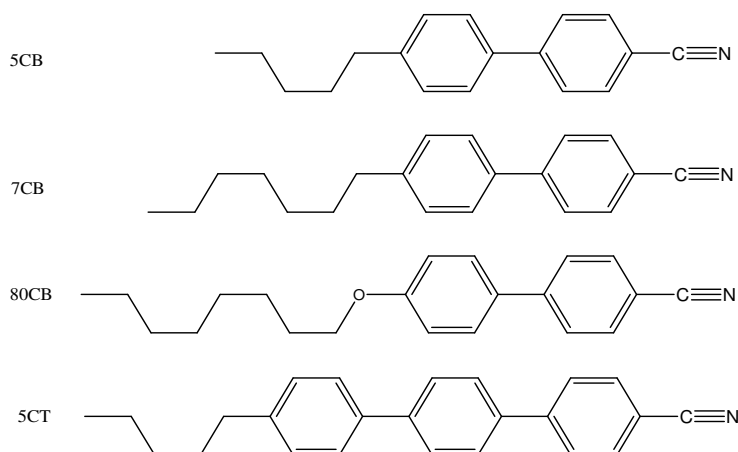


Figure 1.7 – Molecular structures of the components of the nematic liquid crystal mixture E7.

Table 1.1 – Components and mass composition of the Merck E7 liquid crystal.

Designation	Molecular formula	IUPAC name	Composition (w/w)	T <sub>NI</sub> (°C)
5CB	C <sub>18</sub> H <sub>19</sub> N	4-cyano-4'-pentyl-1,1'-biphenyl	51%	35.3
7CB	C <sub>20</sub> H <sub>23</sub> N	4-n-heptyl-4'-cyanobiphenyl	25%	42.8
80CB	C <sub>21</sub> H <sub>25</sub> NO	4, 4'-n-octyloxycyanobiphenyl	16%	80
5CT	C <sub>24</sub> H <sub>23</sub> N	4'-n-pentyl-4-cyanoterphenyl	8%	240

E7 is widely used in polymer dispersed liquid crystals, and it was selected to be studied in this work, because it offers a wide range of operating temperatures in which it maintains anisotropic characteristics. The refractive indices of E7 at T=20°C are given as: n<sub>o</sub>=1.5183, n<sub>e</sub>= 1.7378<sup>13</sup>. It exhibits a nematic to isotropic transition at nearly T<sub>NI</sub>=58°C. At room temperature it still exhibits a nematic phase and no other transitions between 58 and -62°C, where it shows a glass transition. Therefore, liquid crystalline properties are extended down to the glass transition<sup>12</sup>. These features are possible due to the multicomponent nature of E7<sup>7</sup>.

## 1.4 Polymer Dispersed Liquid Crystals

Polymer dispersed liquid crystal (PDLC) films are a mixed phase of nematic liquid crystals (LC) commonly dispersed as inclusions in a solid polymer<sup>14</sup>. They have remarkable electro-optical behaviour since they can be switched from an opaque to a transparent state simply by application of an electric field<sup>13</sup>.

PDLCs have been prepared by two general methods: one in which the system remains heterogeneous during the process, and another in which the system becomes heterogeneous during the process. The first case includes the solvent induced phase separation (SIPS): the LC is mechanically dispersed in a solution of a polymer, the solvent of which does not dissolve liquid crystal. After evaporation of the solvent, the composite structure obtained is stabilised due to the polymer morphology of the system, but is poorly controlled due to a coalescence of droplets during the preparation process. The second case is called thermally induced phase separation (TIPS) or polymerisation induced phase separation (PIPS)<sup>14</sup>.

The main advantage of preparation by the PIPS method is the possibility to obtain a composite directly between glass plates coated with conductive indium tin oxide (ITO) film without additional laminating procedures. The PDLC film is produced in one technological step. In the PIPS method the phase separation of the initially homogeneous mixture and the polymerisation occur simultaneously. The PIPS process was particularly suitable for our purpose because it is quite simple and allows for a high degree of control over the final properties of the PDLC films<sup>15</sup>

In this work the PIPS method is obtained by thermal or photochemical polymerisation of a homogeneous mixture of polymerisable monomers, initiator and liquid crystal. These types of polymerisation occur by a mechanism of free radical polymerisation initiated by radicals.

## 1.5 Free radical polymerisation

Free radical polymerisation has been a widely practiced method of chain polymerisation and was used in this work. This type of polymerisation can be described in three steps: Initiation, propagation and termination. Free radical polymerisation is initiated by radicals. These chemical species are characterised by unpaired electrons which subsequently initiate polymerisations. Radicals can be formed by monomers themselves without added initiators (self-polymerisation) but normally by the action of initiators which were added deliberately. The decomposition of initiators in radicals can be achieved electrochemically, thermally or photochemically. Depending on the polymerisation conditions, the same monomer can originate polymers that differ in configuration, molecular mass and

therefore in properties. In this work more attention was given to the thermal and photochemical polymerisation.

In thermal polymerisation the N,N-azobisisobutyronitrile (AIBN) it is one of the most common initiator which fragments mainly into isobutyronitrile radicals (figure 1.8).

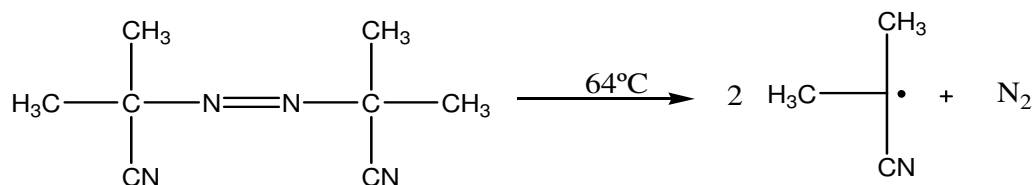


**Figure 1.8 – Reaction scheme for the thermal decomposition of N, N-azobisisobutyronitrile (AIBN) in the two isobutyronitrile radicals.**

Thermal initiator decomposition normally depends on temperature but also on the solvent and the monomer and the solubility. AIBN decomposition normally occurs to an appreciable extent at temperatures greater than 64°C.

In photochemical polymerisation light sensitive compounds are required as initiators to initiate photochemical polymerisation. These compounds absorb light in the ultraviolet / visible wavelength range and undergo fragmentation leading to the formation of radicals <sup>16</sup>. An example is the photochemical decomposition of 2,2-dimethoxy-2-phenylacetophenone (DMPA) which is illustrated in figure 1.9. The main advantage of polymerisation with UV radiation is the possibility to achieve high polymerisation rates in a fraction of seconds <sup>17</sup>.

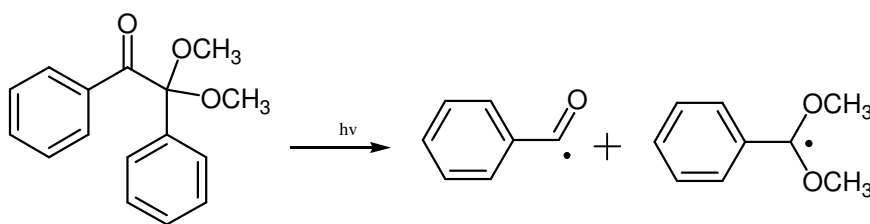


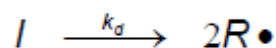
**Figure 1.9 –Reaction scheme for UV induced decomposition of 2,2-dimethoxy-2-phenylacetophenone (DMPA) into an benzoyl and an acetal radical fragments.**

However, for thermal and photochemical initiators, it is necessary to take into account that some of the radicals recombine, in secondary reactions, to form compounds that cannot decompose into radicals and therefore only some are useful radicals (not shown).

In the initiation step are included radical production (described above for the AIBN and DMPA) and the attack of these radicals to the monomer molecules. The overall mechanism for free radical chain polymerisation can be described as:

Initiation:

- i) Generation of free radicals ( $R\cdot$ ) by homolytic dissociation of the initiator (I).



( $K_d$ - rate constant for the dissociation of the initiator)

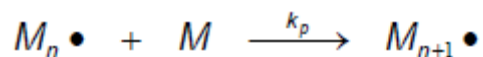
- ii) Reaction between radicals ( $R\cdot$ ) previously formed and monomer's double bond ( $M_1$ ) producing new active species ( $M_1\cdot$ ).



( $K_i$ - rate constant for the initiation step)

Propagation:

- i) Chain extension by successive addition of monomer molecules (M) to the monomer radical unities ( $M_n\cdot$ ) formed in the initiation step.

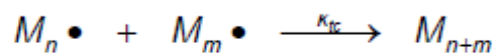


( $K_p$ - rate constant for the propagation step)

Termination:

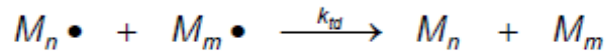
In last step, radicals combine or disproportionate to terminate the chain growth and form polymer molecules.

- i) Combination (a simple interaction between two reactive species,  $M_n\cdot$  and  $M_m\cdot$ ).



( $K_{tc}$ - rate constant for the termination step by combination)

- ii) Disproportionation (when hydrogen atom is transferred from a chain to another).



( $k_{td}$ - rate constant for the termination step by disproportionation)

## 1.6 Microstructure of the polymer network

During polymerisation of what is initially a homogeneous solution of monomers and LC molecules, the polymeric components grow in molecular weight, and when the two components become sufficiently incompatible, there is a decrease of LC solubility which induces formation of phase separation. The polymer matrix acquires a particular morphology with liquid crystal dispersed in its clusters<sup>14</sup>. The polymeric conditions<sup>18</sup>, the chemical nature of the liquid crystal<sup>19</sup> and the polymerisable monomers<sup>20</sup> determine the morphology of polymer matrix. Conventional, PDLCs have two main morphologies: swiss cheese or polymer ball types each one with different characteristics. The observation of the microstructure of the polymer matrix is carried out by scanning electron microscopy (SEM). The dark areas in the SEM microphotographs reveal the absence of the material, which would have corresponded to the original liquid crystal domains.

The swiss cheese morphology type (figure 1.10) is characterised by liquid crystal randomly dispersed in a polymer matrix, as microdroplets. The size and the shape of the LC microdroplets have strong dependence on the parameters of preparation and the type of polymeric matrix<sup>21, 22</sup>.

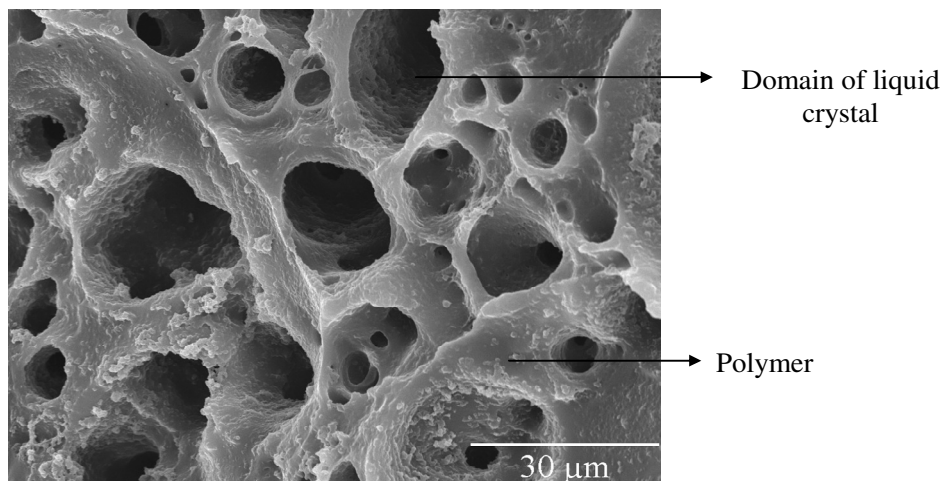
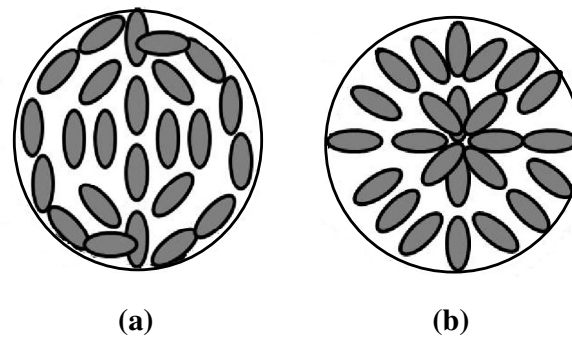


Figure 1.10 – SEM micrograph for the microstructure of the polymer matrix with a swiss cheese morphology type.

In PDLC morphologies with isolated LC microdroplets, two types of distribution of liquid crystal molecules are typically observed.



**Figure 1.11 - Schematic illustration of bipolar (a) and radial (b) director configurations of the liquid crystals inside spherical droplets (adapted from ref.<sup>3</sup>).**

The bipolar and radial configurations (figure 1.11) are related to droplet size and shape and depend on whether the liquid crystal prefers to align parallel or perpendicular to the polymer surface, respectively. Due to these different configurations, liquid crystal molecules would be randomly oriented not uniform within each droplet or from droplet to droplet causing dispersion of the incident light<sup>3</sup>.

In the polymer ball morphology type the polymerisable monomers are phase separated from the continuous liquid crystals and form micro-sized polymer balls. These micro-sized polymer balls merge and form a large polymer network structure with diverse shapes of voids in which LC exists. In this case, the LC is in a continuous phase and fills the irregular shaped voids of the polymer network, which are more or less interconnected<sup>22</sup>.

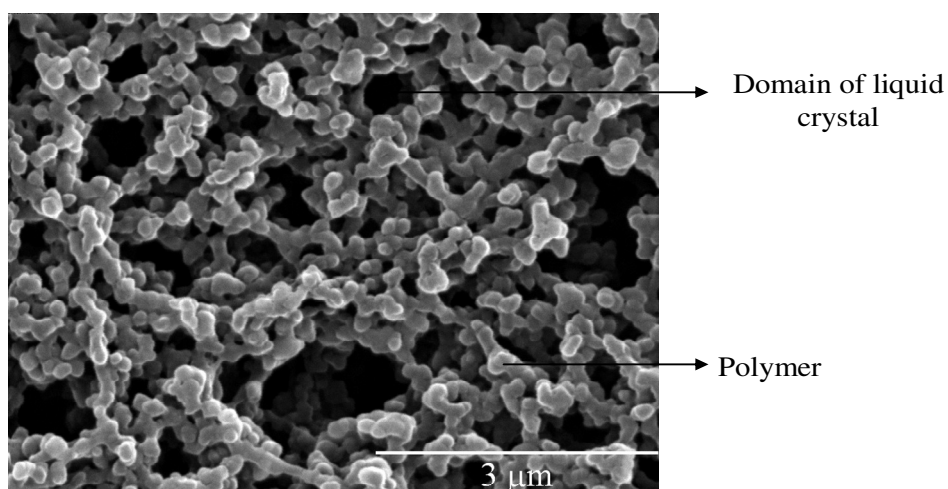


**Figure 1.12 – SEM micrograph for the microstructure of the polymer matrix with polymer ball morphology type.**



## 1.7 PDLC films transmittance

As mentioned before, PDLC devices can be switched electrically from an opaque scattering state to a highly transparent state when a film of liquid crystal-polymer mixture is sandwiched between two conductive glass slides and the electric field is applied. The polymer matrix material is optically isotropic so it has a single refractive index ( $n_p$ ). The liquid crystal within the micro-domains has an ordinary refractive index ( $n_o$ ) and an extraordinary refractive index ( $n_e$ ) when light ray travel through the liquid crystal.

When no electric field is applied although the liquid crystal molecules would be oriented within each droplet, this orientation changes from droplet to droplet and light propagation normal to the film surface will probe a range of refractive indices between ( $n_o$ ) and ( $n_e$ ). Since the optical anisotropy of LC molecules used in PDLC is sufficiently large, the effective refractive index is not generally matched with the refractive index of the polymer ( $n_p$ ), light will be scattered and the PDLC is opaque (OFF state). To maximize off-state scattering, the birefringence ( $\Delta n = n_e - n_o$ ) should be as large as possible<sup>19</sup>. On the other hand, when an electric field with sufficient strength to overcome the interactions between polymer matrix and liquid crystal at interfaces of LC domains–polymer matrix, is applied across the film liquid crystal directors within each droplet become uniformly oriented parallel to the direction of the field. If refractive index of the liquid crystal matches the refractive index of the polymeric matrix ( $n_p$ ) the film become transparent (ON state)<sup>9</sup>.

Normally, when the applied electric field is removed, the nematic directors return to their random distribution. The film begins to appear opaque again. A schematic representation of a functional PDLC film is shown in figure 1.13.

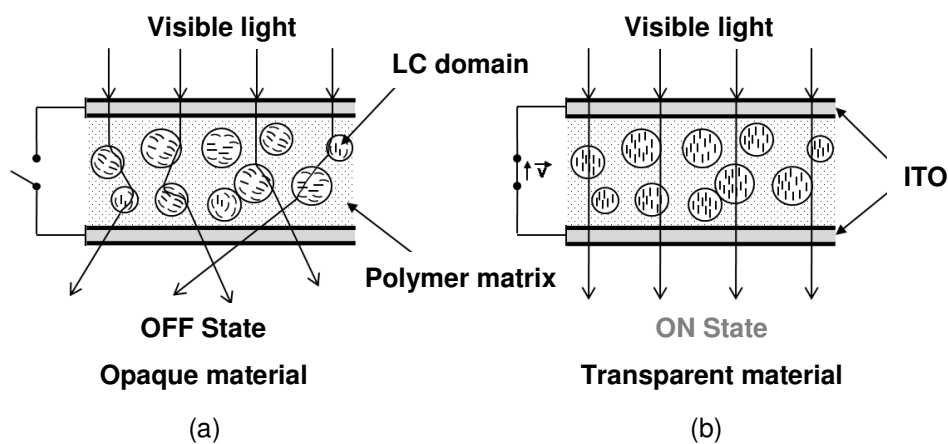


Figure 1.13 – Schematic representation of the averaged molecular orientation of the liquid crystal within the microdroplets without (a) and with (b) an applied electric field (adapted from ref. <sup>3</sup>).

### 1.7.1 Electro-optical properties of PDLCs

There are three main types of electro-optical response. The factors contributing to the different response are many and still poorly understood. Electro-optical response of PDLC is usually measured by ramping a PDLC up and down in voltage and comparing the optical response at each voltage<sup>14</sup>. The different types of change of transmittance of PDLC films as a function of the electric field are shown in figure 1.14, 1.15 and 1.16.

One of the parameters used to evaluate the efficiency of electro optical response of PDLC is the electric field required to achieve 90% of the maximum transmittance and is designated as  $E_{90}$ . Thus, the lower the value of  $E_{90}$ , the more easily PDLC devices switch from the OFF state to ON state.

The most common electro-optical response reported in the literature for PDLC is when the increasing voltage curve is coincident to the decreasing voltage curve as shown in figure 1.14. It was observed that when the electric field is removed liquid crystal molecules relax back, so that the long shaped molecules which were oriented in the same direction in each droplet return to their original random orientation.

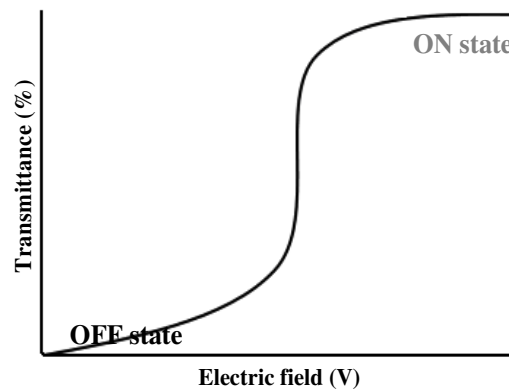


**Figure 1.14 – Example of electro-optical response of PDLC with no hysteresis.**

When these curves are not coincident the PDLC shows electrical hysteresis. The transmission with increasing voltage is lower than the transmission when the electric field is decreased. This effect is illustrated on figure 1.15 and can be defined as the difference between the increasing voltage curve and the decreasing voltage curve.

This difference is commonly attributed in literature to the fact that liquid crystal molecules have a tendency to remain with a certain degree of alignment even after removal the electric field. The PDLC

film is more transparent under decreasing field voltage than with increasing field, because liquid crystals remain with certain degree of alignment caused by the increasing field voltage. However, at the end of measured electro-optical response, the value of the transmittance for the initial opaque state is coincident with that of the final opaque state<sup>23</sup>.

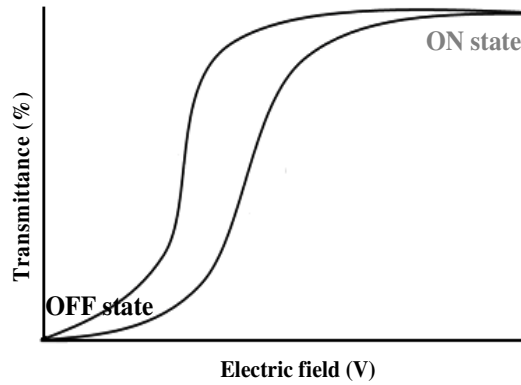


**Figure 1.15 – Example of electro-optical response of PDLC with hysteresis.**

In particular cases, not only the transmission with increasing voltage is lower than the transmission when the voltage is decreased but also a high transparency state is obtained for a long period of time at room temperature even after the applied voltage has been switched off, starting from an opaque state and after reaching a transparent state (figures 1.16-1.17)<sup>14</sup>.

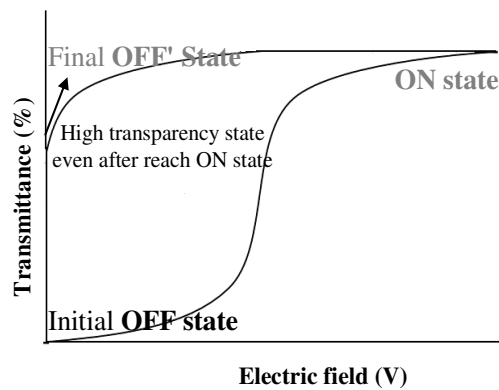


**Figure 1.16 –Example of electro-optical response of PDLC with permanent memory effect.**

In figures 1.16 and 1.17, the initial OFF state corresponds to the transmittance of the initial opaque state (zero electric field), the ON state to the transmittance upon applying electric field and the final OFF' state is the transmittance after removal of the applied field. The PDLC film with this electro-

optical response has a permanent memory effect and this still remains a poorly understood aspect of PDLC electro-optical behaviour.

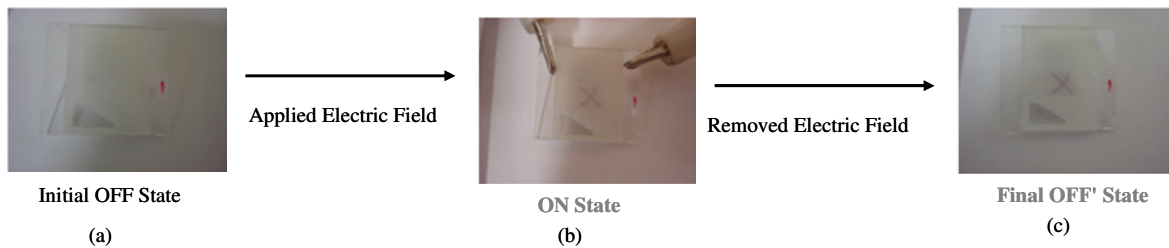


**Figure 1.17 – Images of PDLC films with permanent memory effect: (a) initial OFF state, (b) upon applying electric field and (c) OFF state after removed electric field.**

Various factors can influence the performance of a PDLC and therefore the permanent memory effect. However, the most frequently explanation mentioned in literature is related with the anchoring effect<sup>7, 21, 24, 25</sup>. This effect consists on the interaction between the liquid crystal molecules and polymer matrix at the interface of LC domains and polymer matrix. When an electric field is applied inducing the orientation of LC molecules, it opposes the anchoring effect. If this orientation remains even after the applied voltage has been switched off, the liquid crystal does not relax back completely but remains aligned with the electric field and a high transparency state is displayed without any more energy consumption. Therefore for this to happen there must be a weak force between LC molecules and the polymer surface.

The permanent memory effect is very revolutionary in the study of PDLCs because it allows a switch in transparency and the new state is kept without the need for energy to be spent. The only energy required is that needed to switch the PDLC from the OFF state to the ON state, therefore these devices become low power consumers and environmentally friendly.

## 1.8 Parameters that influence the performance of PDLC films

Despite the fact that PDLC films can be switched between a highly scattering opaque state and a clearly transparent state, these devices sometimes have disadvantages such as the high driving voltage ( $E_{90}$ ) and the insufficient maximum transmittance ( $T_{MAX}$ )<sup>26</sup>. The electro-optical properties of PDLC films prepared by the polymerisation induced phase separation (PIPS) method depend on a numbers of factors such as the type of liquid crystal, molecular structure of polymerisable monomers and polymeric conditions. These factors could seriously affect the microstructure of the polymer matrix the size and the shapes of the LC domains and molecular interactions between the LC molecules and the polymer matrix (anchoring effect)<sup>18, 27-29</sup>. In general and in a simple way, in a nematic liquid crystal there is a relationship between the size and the shape of LC domains and the anchoring effect. When

decreased the anchoring effect increase. This effect is directly related with the voltage needed to align the liquid crystal molecules in the domain. Strong anchoring forces hinder the alignment of liquid crystal molecules. Therefore a high voltage is needed to align liquid crystal molecule along the electric field, and the reverse for lower anchoring effects<sup>27</sup>. Therefore, an understanding of the relationships between preparation conditions and molecular structure of the monomers on electro-optical performance of PDLCs is crucial to control device properties.

### 1.8.1 Polymeric conditions

The phase separation phenomenon between LC and polymeric matrix in PDLCs is a rate process where the transport parameters can play an important role in determining the domain size and amount of LC separated from the polymer matrix. The rate of polymerisation and also some physical parameters, such the viscosity of the systems change the LC domain size. In general the thermal polymerisation is slower (can take several hours) which combined with the effect of temperature that significantly decreases the viscosity of the medium may cause a promotion of the growth of LC domains by diffusion and coalescence. On the other hand, photochemical polymerisation produces a higher polymerisation rate. Smaller domain size can be achieved by higher viscosity of the systems and poor diffusion of free radicals of the polymerisable monomers during polymerisation and the reduced coalescence of LC domains. Therefore, small LC domains can be obtained<sup>18, 29</sup>.

### 1.8.2 Molecular structure of polymerisable monomers

The electro-optical response of PDLC films is greatly influenced by molecular structure of the monomers to be incorporated as polymeric matrix<sup>20, 28, 29</sup>. In literature reports there is not a great variety of monomers used in research an applications for PDLC films, besides the most common commercial ones. As far as I found, published results of the synthesis of monomers to be incorporated as polymer matrix, were mainly dedicated to the preparation of monomers bearing a cyanobiphenyl group<sup>30, 31</sup>. These monomers with a molecular structure similar to the E7 liquid crystal molecules, could lead to better miscibility and compatibility between the polymeric matrix and LCs during the preparation of PDLCs. This could lead to a uniform phase separation and control of the LC domains, which could enhance the performance of PDLCs. On the other hand, the low miscibility with the LC molecules can lead to a premature separation from the matrix. Therefore, one of the main objectives of this work was the design and synthesis of new photochemical and thermal polymerisable monomers, mimicking some structural elements of the E7 liquid crystal molecules. Beyond specific cyanobiphenyl groups also aromatic systems in general with and without a linear chain spacer with five methylene units. So a number of aromatic mono- and dimethacrylates with and without a spacer, as well as vinylic monomers, were synthesised under microwave irradiation. A linear chain spacer

with five methylene units was introduced into some of the structures between the aromatic systems and the methacrylate group to mimic the structure of 5CB the liquid crystal component present with the highest percentage in E7.

## 1.9 Applications

The applications of PDLCs have received considerable attention because of their great variety of electro-optical applications. Polymer dispersed liquid crystal do not require the polarizer and alignment layers to be switched electrically to a transparent state. Beyond this, they show a quick electro-optical response, simple fabrication and low cost production<sup>29</sup>. Therefore, PDLCs are potential materials for electro-optical devices such as reflective displays, optical switches and variable transmittance windows<sup>14, 32, 33</sup>. However the most extensive application for PDLCs is in switchable windows as is shown in figure 1.18.



**Figure 1.18 – Example of application of PDLC in switchable windows in ON (a) and OFF (b) state.**

Another interesting application is related to PDLCs films with permanent memory effect. These PDLCs can be used to store optical information in PDLC film. It is possible with these PDLCs to write information (applied voltage), to read the written information (in a digital way, opaque or transparent states) and erase information by increasing temperature and converting the device into the initial opaque state. On the other hand, PDLCs with permanent memory effect allow a switch in transparency and the new state is kept without the need for any more energy to be spent, the only energy required is that needed to switch the PDLC from the OFF state to the ON state. They consume lower power and are environmentally friendly.

## Chapter II

### 2 Materials and Methods

#### 2.1 Outline

This chapter describes materials and methods used in the preparation and characterisation of the monomers synthesised and the PDLC films. A series of photochemical and thermal polymerisable monomers, mono- and dimethacrylate with and without a linear chain spacer with five methylene units and vinylic monomers were synthesised under microwave (MW) irradiation. The structures of all compounds isolated were supported by proton and carbon nuclear magnetic resonance spectroscopy ( $^1\text{H}$  and  $^{13}\text{C}$  NMR), Fourier transform infrared spectroscopy (FTIR), elemental analysis and by melting point (m.p.) determinations. On other hand, to achieve a relationship between the molecular structures of the polymerisable monomers and the performance of the PDLC film, the monomers with higher structural affinity with E7, were characterised thermally by differential scanning calorimetry (DSC) and polarised optical microscopy (POM) with temperature ramps. The morphology of the polymeric matrix was evaluated by scanning electronic microscopy (SEM). The monomers were also copolymerised with glycidyl methacrylate by photochemical and thermal polymerisation. The molecular weights of the resulting polymers were evaluated by gel permeation chromatography (GPC). The electro-optical properties of the PDLC films were determined by measuring the voltage dependence on the transmitted light.

#### 2.2 Materials

##### 2.2.1 Nematic liquid crystal E7

The liquid crystal known as E7 used was purchased from Merck and used without further purification. The chemical composition and properties of the nematic liquid crystal E7 were previously described in section 1.3.

##### 2.2.2 Initiators of polymerisation

The initiator for the thermal polymerisation was N,N-azobisisobutyronitrile (AIBN) and 2,2-dimethoxy-2-phenylacetophenone (DMPA) was used as photochemical initiator. Both initiators were used as received from Sigma-Aldrich without further purification. The molecular structures of both and the reaction for their chemical decomposition were described before in section 1.5.

### 2.2.3 Indium tin oxide cells

The commercial cells used for electro-optic studies are made-up from a transparent conducting glass coated with a thin layer of indium tin oxide (ITO). Transparent conducting electrodes with the combination of high optical transmission and good electrical conductivity are essential to electric light devices. Indium tin oxide is commonly used because of its relatively high transparency to visible light and low sheet resistance for electrical current conduction<sup>34</sup>. A schematic illustration of an indium tin oxide cell is illustrated in figure 2.1. All properties described in table 2.1 about the cells were provided by Instec. Inc.

Tabela 2.1 – Indium tin oxide (ITO) cell characteristics.

Part Number	Cell type	ITO area ( $\mu\text{m}$ )	Cell gap ( $\mu\text{m}$ )	Cell Thickness (mm)	ITO resistance ( $\Omega/\square$ )
LC2-20.0	Homogeneous alignment	5x5	20.0+0.2	1.5	100

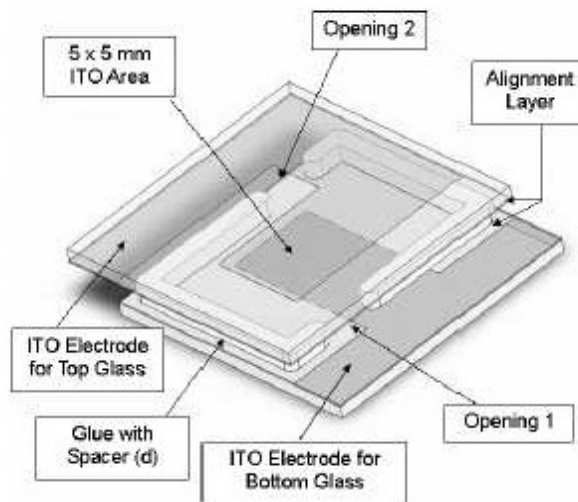


Figure 2.1 – Schematic illustration of an indium tin oxide (ITO) cell.



## 2.3 Methods

### 2.3.1 Microwave Irradiation

High-speed synthesis with microwave irradiation (MW) has attracted a considerable amount of attention in recent years. The area of microwave assisted organic synthesis (MAOS) reports the use of microwave heating to accelerate organic chemical transformations<sup>35</sup>.

Traditionally, organic synthesis is carried out by conductive heating with an external heat source, for example an oil bath. This can be an inefficient method to transfer energy into the system, since it depends on the thermal conductivity of the various materials that must be penetrated. This process can take hours. Conductive heating also hinders the chemist's control over the reaction. However, microwave irradiation produces efficient internal heating because energy is applied directly to the reagents, leading to a rapid rise in temperature (figure 2.2). Microwave enhanced chemistry is based on the efficient heating of materials by "microwave dielectric heating" effects<sup>36</sup>.

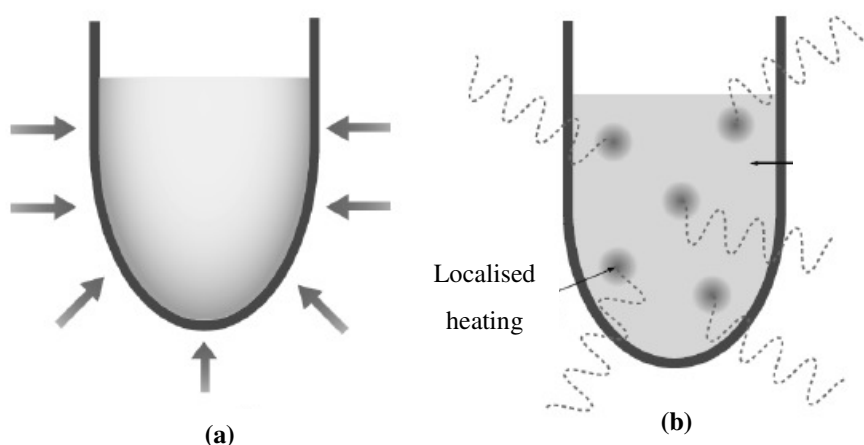


**Figure 2.2 –Schematic representation of conventional (a) and microwave heating (b) (adapted from<sup>36</sup>).**

The two main mechanisms for transfer energy from microwaves to the substance are dipolar polarisation and ionic conduction. When molecules with a permanent dipole are submitted to an electric field, they become aligned. The rapid changed of electric field of the microwave result in orientation changes with each alternation. The strong agitation provided by the reorientation of molecules cause an intense loss of energy in the form of heat. During ionic conduction, as there are free ions or ionic species which oscillate back and forth under the influence of the microwave field, colliding with the molecules. These collisions cause agitation, generating heat<sup>37</sup>.

The ability of a substance to convert electromagnetic energy into heat at a given frequency and temperature is determined by the so-called loss factor ( $\tan \delta$ ):

$$\tan \delta = \frac{\epsilon''}{\epsilon'}$$

where the dielectric loss,  $\epsilon''$ , is indicative of the amount of input microwave energy that is lost to the sample by heat and  $\epsilon'$ , the dielectric constant is describing the ability of the molecules to be polarised by the electric field<sup>36</sup>.

Therefore, to use microwave heating in organic reactions it is important to pay attention to the solvent used in the reaction mixture as for example:

- i) organic solvent with higher  $\tan \delta$  is required to convert, efficiently, microwave energy into thermal energy
- ii) higher chemical stability and inertness to minimise side reactions
- iii) high boiling point for reactions that are to be carried out at atmospheric pressure<sup>35</sup>.

An efficient choice of solvent, for reactions in microwave, should conjugate the dielectric loss values based on the general rules of synthetic organic chemistry, such as protic and aprotic solvent, to develop the specific conditions to optimize the synthesis<sup>36</sup>.

Microwave irradiation is not only applicable to standard solution-phase reactions, but also to solventless systems. Reactions in a solvent-free environment are becoming more usual in organic chemistry reducing environmental impact, costs and increasing safety. If all reagents are in the liquid state or solid reagents melt at certain temperature, then no additional liquid (solvent) may be needed. Polar or ionic reagents could be very efficient when used in the presence of microwave energy without a solvent<sup>36</sup>. New mild solvent-free procedures have been developed, with short reaction times, using microwave irradiation and which, in many cases, appears to be more selective affording higher yields compared to classical thermal heating<sup>38, 39</sup>. Throughout this work the syntheses were achieved using a microwave synthetic reactor under mild i.e. with a minimum quantity of solvent or solventless procedures with short reaction times. The reactions were performed using a MicroSynth labstation (Milestone, USA) equipped with a preprogrammed potency and time control, in open flasks and with magnetic stirring.

### 2.3.2 Characterisation of compounds synthesised

$^1\text{H}$ NMR spectra were recorded at 400 MHz on a Bruker AMX-400 instrument in deuterated chloroform ( $\text{CDCl}_3$ ) with chemical shift values ( $\delta$ ) reported in parts per million (ppm) downfield from tetramethylsilane (TMS) and coupling constants (J) in Hertz (Hz).  $^{13}\text{C}$  NMR spectra were obtained at 101 MHz in  $\text{CDCl}_3$ . FTIR spectroscopy was recorded on a PerKin-Elmer Spectrum BX apparatus, using NaCl discs as support for the sample. The measurements were carried out in the wave number range from 400 to  $4000\text{ cm}^{-1}$  accumulating 128 scans having a resolution of  $4\text{ cm}^{-1}$ . Elemental analyses were performed with a Thermo Finnigan-CE Flash EA 1112 CHNS series analyser. Melting points were determined with a capillary apparatus (Buchi 530), and are uncorrected.

### 2.3.3 Preparation of PDLC films by the PIPS method

The optimised conditions used in photochemical and thermal polymerisation such curing temperature, UV light intensity, time of polymerisation and proportions of monomer and E7 in mixtures were previously studied by the research group. The results of that complementary work that used several commercial monomers were adopted for preparation of PDLC films with monomers synthesised in this work.

For the preparation of PDLC films, mixtures of monomer and E7 with weight ratios of 30% and 70%, respectively, and 1% by weight with respect to the monomer mixture of AIBN or 1% of DMPA for thermal and photochemical polymerisations, respectively, were mixed together at room temperature until the mixture became homogeneous. Samples were prepared by introducing the mixtures into a  $20\text{ }\mu\text{m}$  ITO cell by capillarity action. Polymerisations reactions occur directly in the ITO cell. Schematic representation for preparation of PDLC is show in figure 2.3.

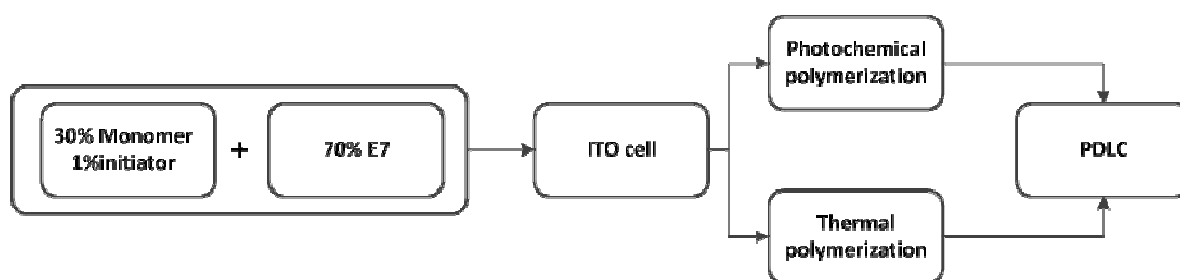


Figure 2.3 – A schematic representation for the preparation of PDLC films by the PIPS method.

### 2.3.3.1 Photochemical polymerisation

The photochemical polymerisation were carried out using Oriel 60115 equipment, with a 100W mercury medium pressure lamp powered by an Oriel 68800. The lamp is cooled by a water circuit and a rotary fan. The 366 nm UV light emission is selected by the following four filters:

- A water filter that absorbs at wavelengths higher than 2800 nm;
- A glass filter that absorbs at wavelengths lower than 300 nm;
- A BG3 filter that transmits at wavelengths between 250 and 500 nm;
- A Filter that transmits at wavelengths between 360 and 370 nm.

Photochemical polymerisation was achieved by exposing the cells filled with the mixture to UV radiation for 2000 s. All photochemical polymerisations were carried out at room temperature and an incident light intensity of  $3.91 \times 10^{-05} \text{Nhv min}^{-1}$ .

### 2.3.3.2 Thermal polymerisation

The thermal polymerisation were carried out in a handmade oven. This oven has an auto-tune temperature controller provided by CAL Controls, model CAL 3300, with a resistance thermometer, Pt100/RTD-2, whose sensor range takes temperature in the interval -200 to ~400°C. The cells filled with the mixture were kept isothermally for 8 hours at 74°C.

## 2.3.4 Gel permeation chromatography

Synthetic polymers are not constituted by macromolecules of only one single molecular weight but are composed of macromolecules having a distribution of molecular weight. Size exclusion chromatography (SEC) is an important method for the determination of molecular weights ( $M_n$  and  $M_w$ )<sup>40</sup>. It is a type of liquid chromatography that separates molecules according to sizes. In other words in SEC the separation is not done by chemical interaction of the dissolved analyte molecules with the stationary phase but through the differences in volume of the polymers associated with their different molecular weights<sup>41</sup>. Substrates consist of materials with pore sizes between 5 nm and 500 nm and an SEC with a gel as the substrate is also called gel permeation chromatography (GPC).

In polymer science, the number average molecular weight ( $M_n$ ) follows the conventional definition for the mean value of any statistical quantity. Number average molecular weight is the statistical average molecular weight of all the polymer chains in the sample according to:

$$M_n = \frac{\sum N_i M_i}{\sum N_i}$$

Where  $M_i$  is the molecular weights of a chain and  $N_i$  is the number of chains of that molecular weight. This average is only sensitive to the number of molecules present. However, polymers are composed of macromolecules of similar structure but different molecular weight. Generally, individual polymer chains rarely have exactly the same degree of polymerisation and molar mass. There is a distribution around an average value. These types of materials are called polydisperse. As a consequence of this polydispersity molecular weights are mean values only. The polymer properties depend not only on the number of polymer molecules but also on the size or weight of each polymer molecule. For a more complete characterisation it is necessary to consider the chain length distribution. This parameter is given by the weight average molecular weight ( $M_w$ ) and is defined by:

$$M_w = \frac{\sum N_i M_i^2}{\sum N_i M_i}$$

Compared to  $M_n$ ,  $M_w$  takes into account the molecular weight of a chain in determining contributions to the molecular weight average<sup>40</sup>. The polydispersity index (PDI) is a simple measure of the width of a molecular weight distribution and is given by<sup>41</sup>:

$$PDI = \frac{M_w}{M_n}$$

Gel permeation chromatography was performed on a Knauer system equipment with a HPLC Smartline Pump 1000, a light scattering detector PL-ELS 1000m and a Smartline Autosampler 3800 and controlled by Clarity and PL-ELS GPC software. Dimethylformamide (DMF) as used as eluent at a flow rate of  $1\text{ mL min}^{-1}$  on a Plus Pore 7.5 mm *ID* column at 85°C. The detectors alignment and instrument sensitivity parameters were previously calibrated using a molecular weight distribution polystyrene standard. For the calibration of the GPC column was used a calibration curve which correlates the elution time with the logarithm of the polystyrene standard molecular weight,  $\ln M$ .

Due to the fact that most of the monomers analysed are solids, a liquid was used as a co-monomer in order to solubilise the mixture (monomer and initiator). Glycidyl methacrylate was chosen as a co-

monomer because of its well-known action as a reactive solvent in polymerisation systems<sup>42</sup>. For the preparation of samples for GPC analysis, monomers and glycidyl methacrylate with weight ratios of 50:50 with 1% of initiator, AIBN or DMPA, depending on whether thermal or photochemical polymerisation was used, were placed between two KBr disks. After polymerisation these discs were immersed into water in order to dissolve the KBr. The resulting materials were dried under vacuum for 24 hours and used without purification. All sample solutions were prepared from about 0.5 mg of material dissolved in 1 mL of DMF. Then, the mixtures were filtered through a 0.20 $\mu$ m pore size membrane prior to the injection of a volume of 150 $\mu$ L the GPC column.

### 2.3.5 Scanning Electron Microscopy (SEM)

Scanning Electronic Microscopy provides images of the morphology of the polymeric matrix, of composites of liquid crystal with polymers, and allows their characterisation through parameters such as the size and the shape of voids that accommodate the liquid crystal. As mentioned before, the quantity, shape and size of LC domains in the polymer matrix have an influence on the optical properties of the composites. The scanning electron microscope has many advantages over traditional microscopes. The SEM has a greater depth of field, which allows more of a specimen to be in focus at once. The SEM also has much higher resolution images, so closely spaced specimens can be magnified at much higher levels. This technique is the most used of the surface analytical techniques<sup>41</sup>.

For SEM studies of the polymeric matrix of PDLC films the conditions for the preparation of a PDLC film were reproduced but instead of the thermal or photo-polymerisation of mixtures occurring within the ITO cell, they took place between two KBr disks. After polymerisation these discs were immersed into water in order to dissolve the KBr. To extract the LC the samples were immersed into acetonitrile and then the remaining polymer matrix was dried under vacuum for 24h. The resulting samples were mounted on aluminium stubs carbon cement (D-400, Neubaer Chemikalien) and a thick gold coating was deposited using a dual ion beam sputter coating apparatus. The measurements were obtained on a SEM Hitachi S-2400 instrument with a Rontec standard energy dispersive x-ray spectroscopy (EDS) detector.

### 2.3.6 Differential scanning calorimetry (DSC)

Differential scanning calorimetry (DSC) means the measurement of the change of the difference in the heat flow rate to the sample and to a reference sample while they are subjected to a controlled temperature program. In other words, DSC is used to obtain information on thermal changes and associated enthalpies in a sample by heating or cooling it alongside an inert reference<sup>41</sup>.

When a material is cooled below its freezing temperature it can follow different pathways. The most common is when

- i) It crystallizes losing translational and rotational degrees of freedom since the molecules are fixed in three dimensional lattices with both positional and orientational order,
- ii) It enters an intermediate metastable state between liquid and solid keeping translational and rotational degrees of freedom. This intermediate state is metastable and the liquid in such state is said to be supercooled,
- iii) if the temperature continues to decrease, the supercooled liquid can solidify becoming a glass.

The evolution from supercooled liquid to a glassy solid is called glass transition. This transition takes place in a wide temperature interval nevertheless it is common to use the term glass transition temperature ( $T_g$ ). In this state the substance presents a mechanical behaviour similar to solid materials, while keeping a disorder typical of liquids (without long-range order). Furthermore, when a material is heated above its freezing temperature it can show a cold crystallisation from the glassy state followed by a melting transition<sup>43</sup>. It should be noted that the crystallisation transition can occur from high temperature starting from the liquid state being then called melt crystallisation, or coming from low temperatures from the glassy state being then called cold crystallisation.

The result of a DSC experiment is a curve of heat flux versus temperature or versus time. By observing the difference between the heat flow of the sample and reference, it is then possible to determine the amount of heat absorbed or released during transitions. The fusion transition requires higher heat flux flowing to the sample to increase the temperature at the same rate as in the reference case. Therefore, this transition is an endothermic reaction, and the melting temperature ( $T_m$ ) corresponds to the endothermic peak of melting transition. On the other hand the crystallisation process required a smaller variation of the amount of heat to reduce the temperature of the sample and this transition is an exothermic reaction. The crystallisation temperature either for cold- or for melt-crystallisation,  $T_{cc}$  or  $T_c$ , respectively, corresponds to the exothermic peak of crystallisation transition. As mentioned before for the glass transition it is more correct to provide a temperature range instead of a defined peak. The glass transition temperature ( $T_g$ ) was taken at the inflection point of the specific heat capacity increment in the transition. The enthalpy of fusion ( $\Delta H_m$ ) and enthalpy of crystallisation ( $\Delta H_{cr}$ ) were obtained from the areas under the curve that represents the overall calorimetric enthalpy of the process.

The thermal properties of monomers were determined by DSC using a DSC 131 model Setaram calorimeter. Samples were analysed in an aluminium pan and an empty pan was used as reference. Measurements were carried out under a nitrogen atmosphere with a flow rate of around  $10^{\circ}\text{C min}^{-1}$ . In order to verify the reversibility of the thermal transitions the cooled sample were submitted at to two cycles of heating/cooling runs approximately between  $-100^{\circ}\text{C}$  and  $140^{\circ}\text{C}$  for solid sample and between  $-130^{\circ}\text{C}$  to  $25^{\circ}\text{C}$  for liquid samples.

### 2.3.7 Polarised optical microscopy

Polarised optical microscopy (POM) besides providing all the information of bright field microscopy it offers other information not available with any other optical technique. It makes it possible distinguish between isotropic and birefringent materials.

As mentioned before, isotropic materials have only one refractive index, when light passed is passed through an isotropic material it only experiences one refractive index and therefore polarised light entering the sample retains the same polarisation upon exiting it. The result, when viewed through crossed polarisers, is complete darkness as all of the light passing through the material is absorbed by the second polariser. On the other hand, when light passed through a birefringent material the light experiences more than one refractive index the ordinary index,  $n_o$ , and the extraordinary index,  $n_e$ . Therefore, the light passed through the first polarised, is refracted into waves when passing through the birefringent material. This characteristic results on a new polarisation of light compared to that incident on the sample and gone through to the second polariser. The result, when viewed through crossed polarizers is a clear image. The use of crossed polarizers allows a distinction to be made between isotropic and birefringent material<sup>41</sup>. The polarised optical microscopy is equipped with a heating/cooling stage which allows determination of the sequence of phases not only the temperature for each transition but also the different textures acquired by the sample.

The polarised optical microscopy studies were performed by an Olympus BH-2 optical polarizing microscope equipped with a Mettler Toled FP82HT hot stage ( $20$  to  $200^{\circ}\text{C}$ ). The microstructure of the samples was monitored by taking microphotographs at appropriate temperatures, using an Olympus Camedia C-5060 digital camera interfaced to a computer. Images were obtained at a magnification of  $100\times$ . The samples were introduced in the ITO cell (support with closed perimeter and thickness of  $20\mu\text{m}$ ) and inserted in the hot stage. Measurements for heating and cooling runs were carried out with a rate of around  $10^{\circ}\text{C min}^{-1}$ .



### 2.3.8 Electro-optical properties

PDLC electro-optical characterisation is one of the most important parameters to characterise the performance of PDLCs. The light transmission studies were performed using a diode array Avantes spectrophotometer (AvaLight-DHS and AvaSpec 2048) using a Halogen lamp and optical fiber connections. The wavelength was selected at 633nm. The electrical pulse is generated by a programmable waveform generator (Wavetek 20MHz Synthesised Function Generator Model 90), which creates an AC wave with a low amplitude between 0VRMS and 27VRMS, for sample excitation.

For the electro-optical measurements, an external electric field is applied across the PDLC film. The generator connected to a Vtrek TP-430 amplifier that enhances the amplitude reach a voltage of 47VRMS. A 220V/9V transformer is inversely connected and it will multiply the voltage by a factor of 22/09. The first resistance (1  $\Omega$ ) has the purpose of securing the amplifier from short-circuits and the purpose of the second resistance (150 k $\Omega$ ) purpose is to standardize the voltage wave. The amplifier is fed by a Kiotto KPS 1310 power supply. The output detector (AvaSpec-2048) is connected to a computer software data acquisition. The experimental system for electro-optical studies is shown schematically in figure 2.4.

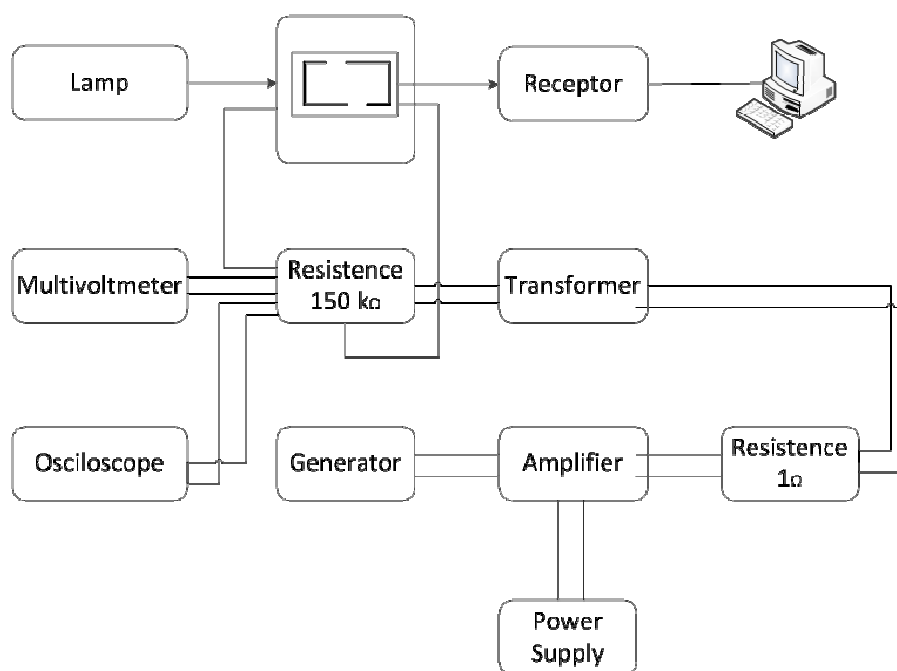


**Figure 2.4 – Schematic diagram of the experimental system set-up used to study electro-optical properties**

All measurements were performed at 1 KHz. The applied voltage is measured by a multivoltmeter (Iso-Tech IDM71) and the waveshape is observed by an oscilloscope (Tektronix TDS 210) to observe the transmittance with an applied voltage.

The study is divided in three cycles, corresponding to 1/3, 2/3 and 3/3 of the maximum voltage applied (400 V). Each cycle has 35 experimental points and each point (transmittance *versus* applied voltage) is done in 1 second. The pulse is applied to the sample 10 ms after triggered and has the duration of 200 ms.

## Chapter III

### 3 Synthesis and Characterisation

#### 3.1 Outline

As mentioned before, a number of photochemical and thermal polymerisable monomers, as well in some cases, their starting materials were prepared under microwave irradiation. In this chapter the synthetic methods and the characterisation of the compounds obtained will be described. As mentioned before, all the compounds were synthesised using a microwave synthetic reactor under mild or solventless procedures. For some reactions, it was necessary to add a small amount of DMF (dimethylformamide) to obtain a better homogenisation of the mixture. DMF was chosen because of its dipolar nature and the high ability to absorb microwave energy and convert it into heat coupled with a comparatively high boiling point of 153°C<sup>36</sup>. The protocol employed consisted in placing equivalent amounts of the corresponding reagents in an open quartz tube and then subjecting the mixture to microwave irradiation at 200W. The reaction time was optimised by following the reactions by thin layer chromatography (TLC) every minute and stopped when no starting material remained. All reactions were carried under inert atmosphere, and all the compounds synthesised were dried under vacuum, during 24 hours. Some compounds used as starting materials were acquired from Sigma-Aldrich and were used as received<sup>44</sup>. In this chapter will be described the data characterisations by <sup>1</sup>H and <sup>13</sup>C NMR, FTIR spectroscopy, elemental analysis and melting point. In this chapter, a comparison will also be made between the results described in the literature for the syntheses of the compounds under classical synthetic methods with the results obtained under microwave irradiation. All the results presented in this chapter have been published<sup>45</sup>.

### 3.2 List of synthesised monomers

The molecular structures of all synthesised monomers are shown in figure 3.1. Some of the synthesised monomers have been already mentioned in the literature, but were lacking full characterisation. The information required for compounds is provided here 1<sup>44</sup>, 2<sup>46</sup>, 3<sup>44</sup>, 4<sup>47</sup>, 5<sup>48</sup>, 6<sup>49</sup>, 7<sup>48</sup>, 9<sup>50</sup>, 10, 11<sup>51</sup>, 13<sup>52</sup>, 14<sup>53</sup>, 15<sup>54</sup>, 16<sup>55</sup>, 25<sup>56</sup>, 26<sup>57</sup>. As far as I found, the compounds 8, 12, 17, 18, 19, 20, 21, 22, 23 and 24 had not been synthesised before.

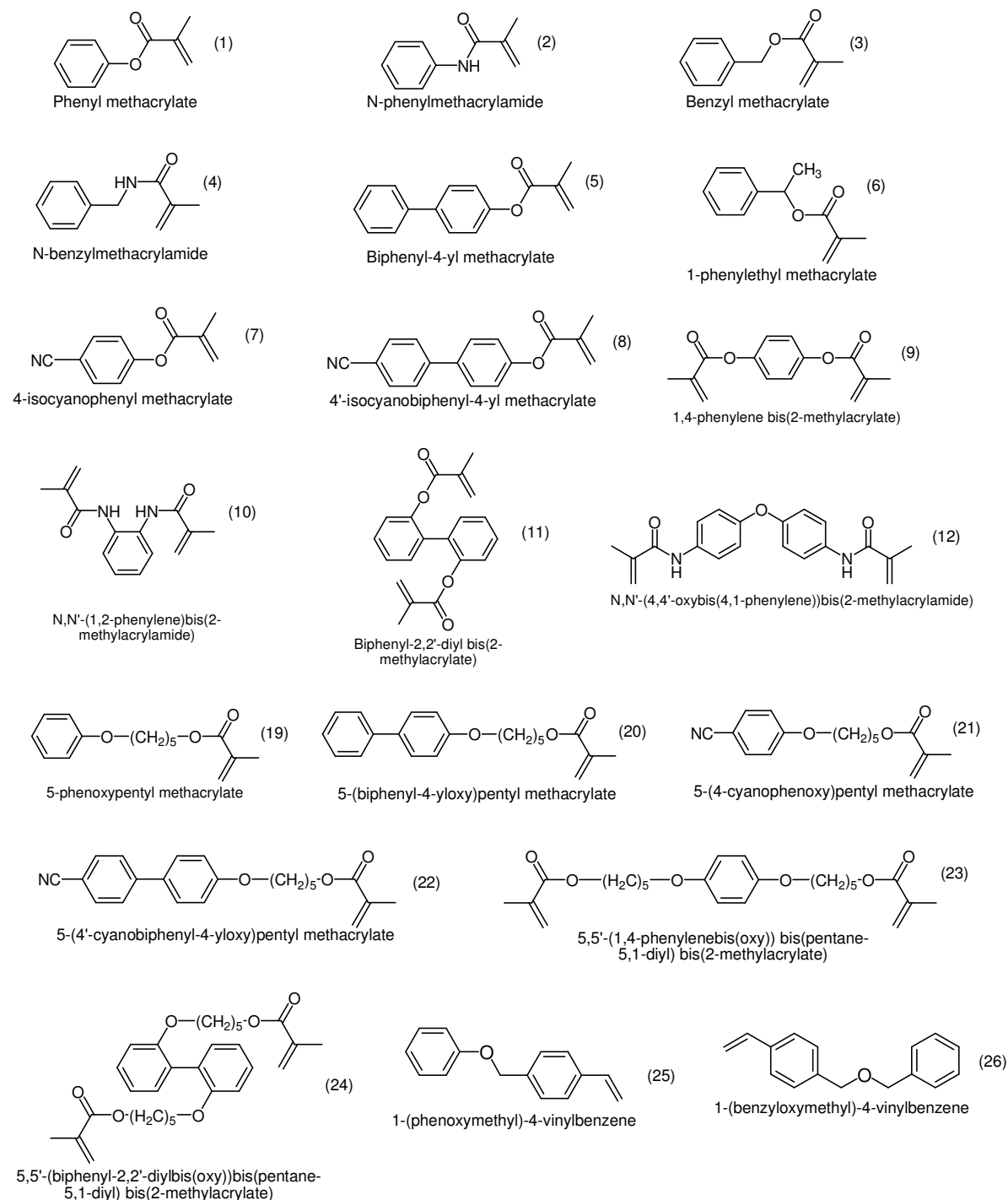


Figure 3.1 – Molecular structures of synthesised monomers.

### 3.3 Synthesis of methacrylate monomers

#### 3.3.1 Monomers without a linear chain spacer with five methacrylate units

One of the procedures reported in the literature to obtain mono- or dimethacrylate monomers is based on the reaction between the corresponding starting material and methacryl chloride in the presence of a base, usually triethylamine<sup>58</sup> as indicated in figure 3.2.

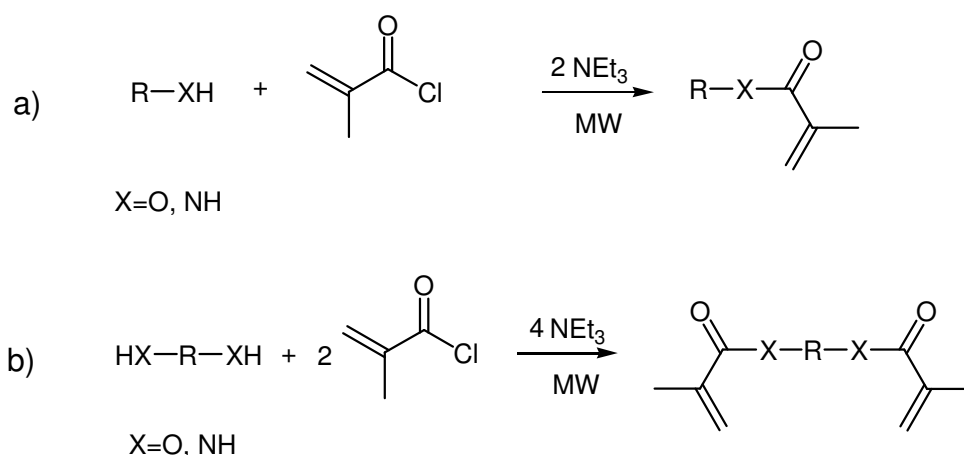
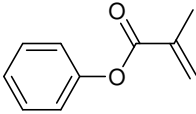
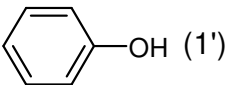
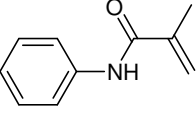
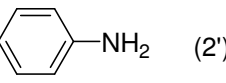
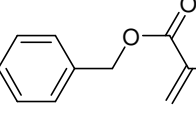
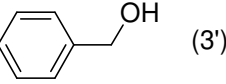
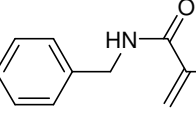
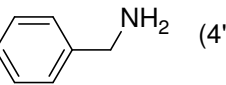
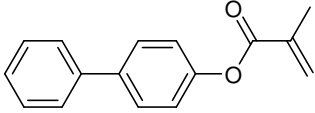
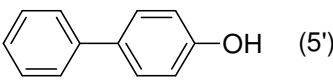
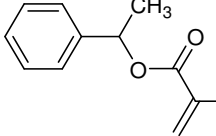
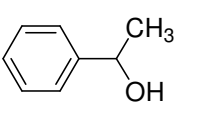
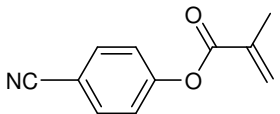
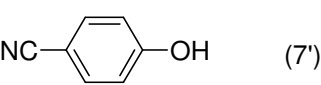
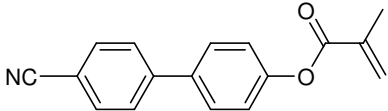
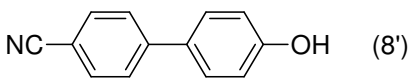


Figure 3.2 – General scheme for the synthesis of (a) monomethacrylate monomers and (b) dimethacrylate monomers.

##### 3.3.1.1 Experimental method used for monomethacrylate monomers

To prepare aromatic monomethacrylate monomers (figure 3.2 a), 1.0g of the corresponding starting material (table 3.1) and 2 equivalents of triethylamine (NEt<sub>3</sub>) were added under argon in a quartz tube. This mixture was cooled to 0-5°C (ice bath) and 1 equivalent of methacryl chloride was added slowly. The mixture was placed in the microwave cavity and subjected to a MW irradiation of 200W for the required time (table 3.1). Then, the mixture was dissolved in dichloromethane (CH<sub>2</sub>Cl<sub>2</sub>) and washed with distilled water until a neutral pH was obtained and the organic phase was dried with anhydrous sodium sulfate, filtered and concentrated. The residue was purified by flash column chromatography with hexane/ethyl acetate to afford monomers 1, 2, 3 and 4 (gradient from 1:1 to 1:2) and the monomers 5, 6, 7 and 8 (gradient from 5:1 to 1:1) as indicated in table 3.1.

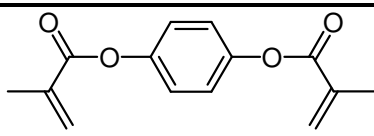
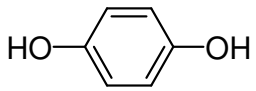
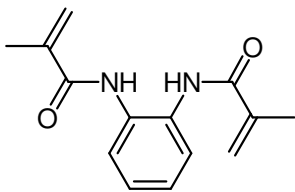
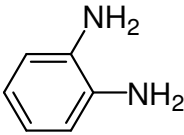
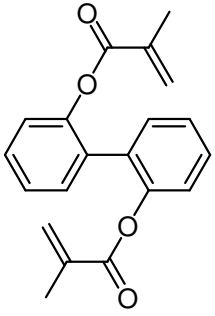
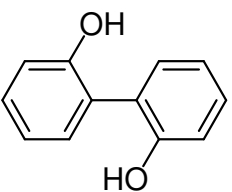
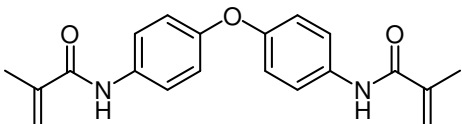
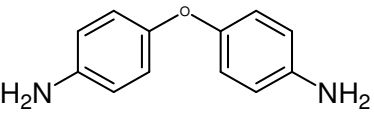
Table 3.1 – Synthesis of monomethacrylate monomers.

Monomer (n°)	Starting material (n°)	Reaction time (min)
 (1)	 (1')	1
 (2)	 (2')	5
 (3)	 (3')	1
 (4)	 (4')	5
 (5)	 (5')	1
 (6)	 (6')	5
 (7)	 (7')	2
 (8)	 (8')	1

### 3.3.1.2 Experimental method used for dimethacrylate monomers

The procedure used to prepare aromatic dimethacrylate monomers (figure 3.2 b) was similar to that used for the monomethacrylate monomers but different proportions were used. Thus, to 1.0g of the corresponding starting material (table 3.2) and 4 equivalents of triethylamine ( $\text{NEt}_3$ ) were added under argon. The mixture was cooled to 0-5°C (ice bath) and 2 equivalent of methacryl chloride were added slowly. This mixture was subjected to MW irradiation of 200W for the required time (table 3.2). The mixture was dissolved in  $\text{CH}_2\text{Cl}_2$  and washed with distilled water until a neutral pH was obtained and the organic phase was dried with anhydrous sodium sulfate, filtered, and concentrated. The residue was purified by flash column chromatography with hexane/ethyl acetate to afford monomers 9, 12 (gradient from 1:1 to 1:2) and the monomers 10 and 11 (gradient from 5:1 to 1:1) as indicated in table 3.2.

Table 3.2 – Synthesis of dimethacrylate monomers.

Monomer (n°)	Starting material (n°)	Reaction time (min)
 (9)	 (9')	1
 (10)	 (10')	1
 (11)	 (11')	1
 (12)	 (12')	3

### 3.3.2 Synthesis of aromatic compounds bearing an alkyl bromide chain (precursors)

One of the procedures reported in the literature for synthesis of methacrylate monomers bearing a linear chain spacer with five methacrylate units requires the prior preparation of the corresponding precursors. The procedures to obtain mono- and di-bromide compounds involve the reaction of the corresponding starting material and an alkylating agent, in the presence of an inorganic base, usually potassium carbonate ( $K_2CO_3$ ) as indicated in figure 3.3<sup>30,59</sup>.

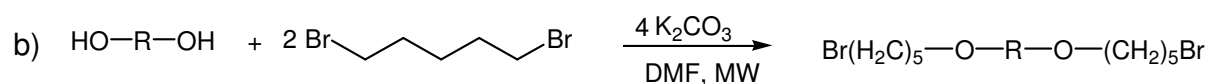
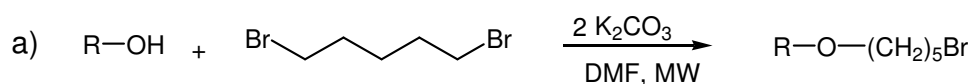
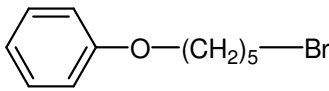
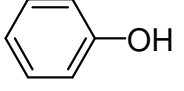
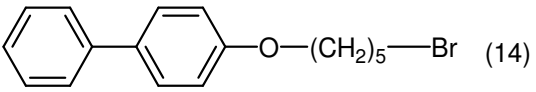
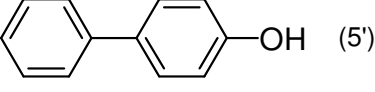
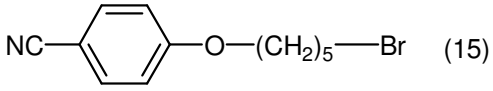
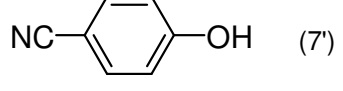
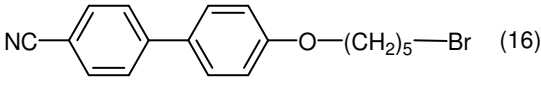
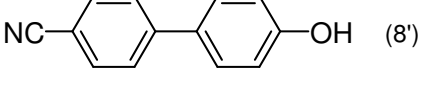


Figure 3.3 – General scheme for the synthesis of (a) monobromide and (b) dibromide precursors.

### 3.3.2.1 Experimental method used for monobromide precursors

To prepare monobrominated compounds (figure 3.3 (a)), to 1.0 g of the corresponding starting material (table 3.3) in 1 mL of DMF under argon and 2 equivalents of the base ( $K_2CO_3$ ) were added and then 1 equivalent of 1,5-dibromopentane was added slowly. This mixture was subjected to MW irradiation of 200W for the required times (table 3.3). Afterwards the mixture was dissolved in diethyl ether and washed with distilled water until a neutral pH was obtained. The organic phase was dried with anhydrous sodium sulfate, filtered and concentrated. The residue was purified by flash column chromatography with hexane/ethyl acetate to afford the compounds 13-16 (gradient from 5:1 to 1:1) as indicated in table 3.3.

Table 3.3 – Synthesis of monobromide precursors.

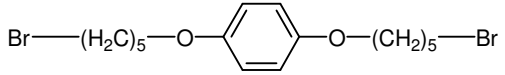
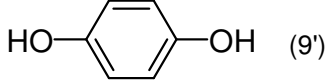
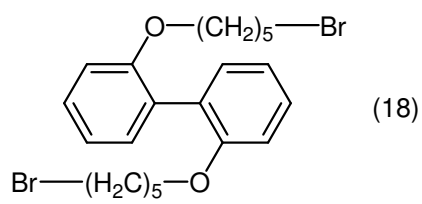
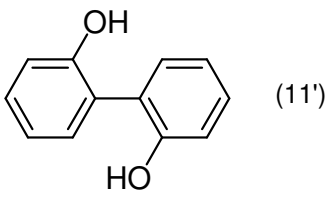
Precursor (n°)	Starting material (n°)	Reaction time (min)
 (13)	 (1')	5
 (14)	 (5')	3
 (15)	 (7')	5
 (16)	 (8')	2

### 3.3.2.2 Experimental method used for dibrominated precursors

The procedure to prepare dibrominated compounds (figure 3.3 b)) was similar to that described for monobrominated compounds, but different proportions were used. Thus, to 1.0g of the corresponding starting material (table 3.4) in 1mL of DMF under argon, 4 equivalents of the base ( $K_2CO_3$ ) were added and then 1 equivalent of 1,5-dibromopentane was added slowly. This mixture was subjected to MW irradiation of 200W for the required times (table 3.4). The mixture was then dissolved in diethyl ether and washed with distilled water until a neutral pH was obtained. The organic phase was dried with anhydrous sodium sulfate, filtered and concentrated. The residue was purified by flash column chromatography with hexane/ethyl acetate to afford the compounds 17 and 18 (gradient from 5:1 to 1:1) as indicated in table 3.4.



Table 3.4 – Synthesis of dibrominated precursors.

Precursor (n°)	Starting material (n°)	Reaction time (min)
 (17)	 (9°)	5
 (18)	 (11°)	5

### 3.3.3 Monomers bearing a linear chain spacer with five methylene units (19-24)

The procedure of synthesis, of mono- and dimethacrylate monomers bearing a linear chain spacer with five methylene units was adopted from the literature<sup>30,59</sup> and it involves the reaction of the corresponding precursors previously prepared (aromatic compounds bearing an alkyl bromide chain) with methacrylic acid in the presence of a base,  $K_2CO_3$ , as indicated in figure 3.4.

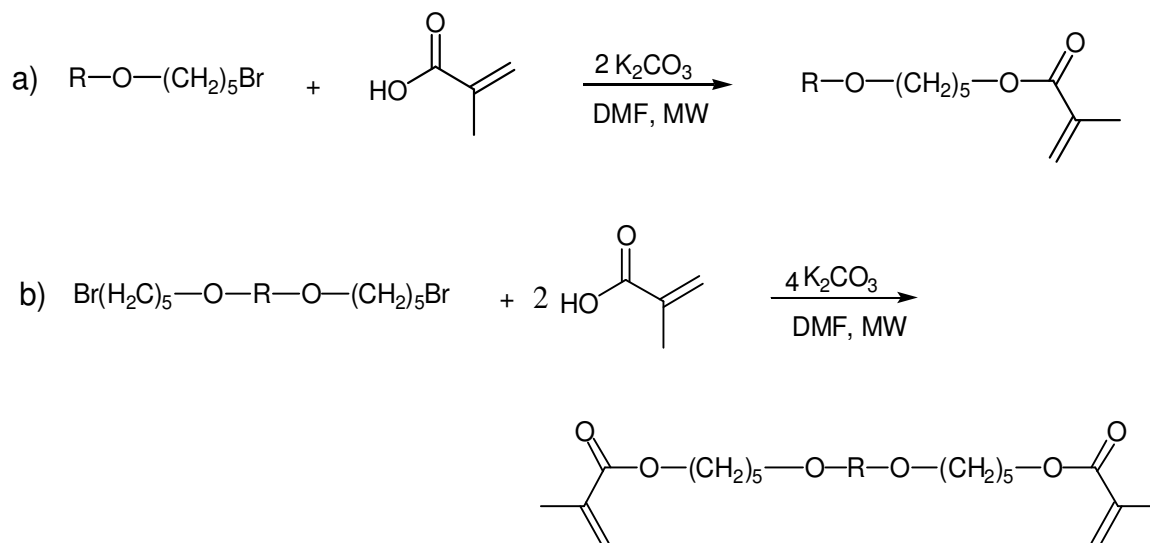


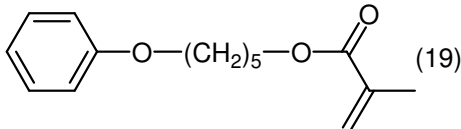
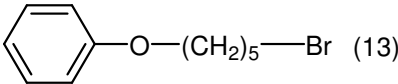
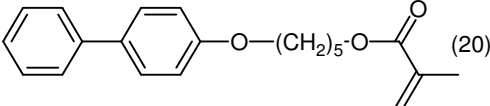
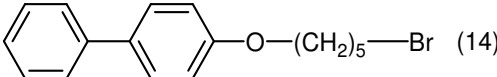
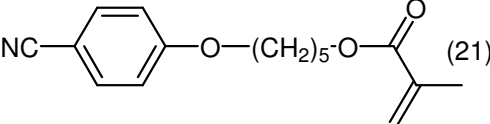
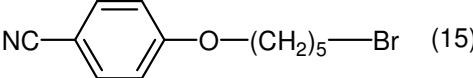
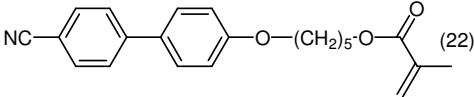
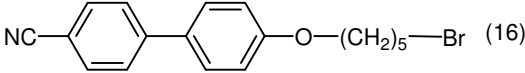
Figure 3.4 –General scheme for the synthesis of (a) mono- and (b) dimethacrylate monomers bearing a linear chain spacer with five methylene units.

#### 3.3.3.1 Experimental method used for monomethacrylate monomers (19-22)

To prepare monomethacrylate monomers bearing a linear chain spacer with five methylene units (figure 3.4 (a)), to 1.0g of the starting material previously prepared (table 3.5) in 1 ml of DMF under argon was added slowly a suspension of 2 equivalents of the base ( $K_2CO_3$ ) and 1 equivalent of methacrylic acid. The mixture was subjected to MW irradiation of 200W for the required time (table

3.5). After that the reaction mixture was dissolved in diethyl ether and washed with distilled water until a neutral pH was obtained. The organic phase was dried with anhydrous sodium sulfate, filtered and concentrated. The residue was purified by flash column chromatography with hexane/ethyl acetate to afford monomer 19 (gradient from 1:1 to 1:2) and the monomers 20-22 (gradient from 5:1 to 1:1) as indicated in table 3.5.

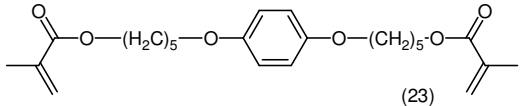
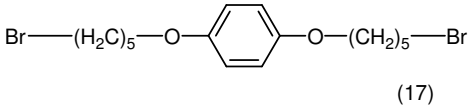
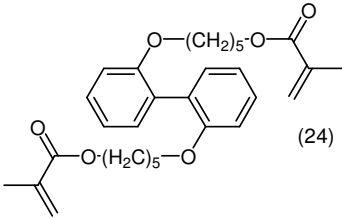
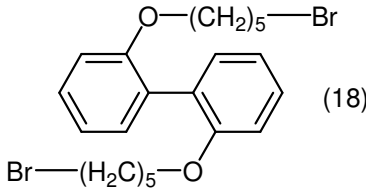
**Table 3.5 – Synthesis of monomethacrylate monomers bearing a linear chain spacer with five methylene units.**

Monomer (n <sup>o</sup> )	Precursors (n <sup>o</sup> )	Reaction time (min)
 (19)	 (13)	5
 (20)	 (14)	1
 (21)	 (15)	5
 (22)	 (16)	1

### 3.3.3.2 Experimental method used for dimethacrylate monomers (23-24)

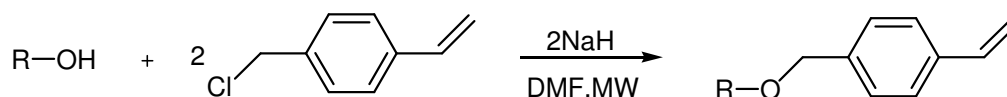
The procedure to prepare dimethacrylate monomers bearing a linear chain spacer with five methylene chain units (figure 3.4 (b)) was similar to that used for the monomethacrylate bearing a linear chain spacer with five methylene units but different proportions were used. Thus, to 1.0g of the starting material previously prepared (table 3.6) in 1 mL of DMF under argon was added slowly to a suspension of 4 equivalents of the base ( $K_2CO_3$ ), and 2 equivalent of methacrylic acid. The mixture was subjected to MW irradiation of 200W for the required time (table 3.6). After that the reaction mixture was dissolved in diethyl ether and washed with distilled water until a neutral pH was obtained. The organic phase was dried with anhydrous sodium sulfate, filtered and concentrated. The residue was purified by flash column chromatography with hexane/ethyl acetate gradient from 5:1 to 1:1) to afford monomers 23 and 24 as indicated in table 3.6.

**Table 3.6 – Synthesis of dimethacrylate monomers bearing a linear chain spacer with five methylene units.**

Monomer (n°)	Precursors (n°)	Reaction time (min)
 (23)	 (17)	5
 (24)	 (18)	5

### 3.3.4 Synthesis of vinylic monomers (25-26)

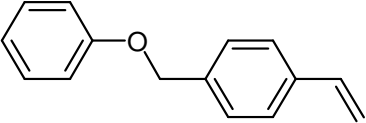
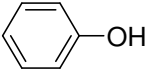
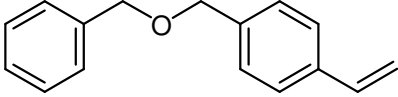
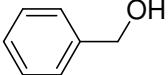
The common method reported in the literature for the synthesis of vinylic monomers involves the reaction of the corresponding starting material with 4-vinylbenzyl chloride using a catalytic amount of  $\text{Bu}_4\text{N}^+\text{I}^-$  in the presence of sodium hydride as a base as indicated in figure 3.5<sup>60</sup>.

**Figure 3.5 – General scheme for the synthesis of vinylic monomers.**

#### 3.3.4.1 Experimental method used for vinylic monomers

To a mixture of 1.0 g of the corresponding starting material (table 3.7) with a catalytic amount of  $\text{Bu}_4\text{N}^+\text{I}^-$  and 1mL of DMF at 0-5°C (ice bath), 2 equivalents of sodium hydride (NaH) were added and the resulting mixture was stirred under argon. After 20 minutes 2 equivalents of 1-(chloromethyl)-4-vinylbenzene were added slowly. Then, the reaction mixture was placed in the microwave cavity, and subjected to MW irradiation of 200 W for the required time (table 3.7). Next, the mixture was dissolved in  $\text{CH}_2\text{Cl}_2$ , and washed with distilled water until a neutral pH was obtained. The organic phase was dried with anhydrous sodium sulfate, filtered and concentrated. The residue was purified by flash column chromatography using hexane/ethyl acetate (gradient from 5:1 to 1:1) to afford monomers 25 and 26 as indicated in table 3.7.

Table 3.7 – Synthesis of vinylic monomers.

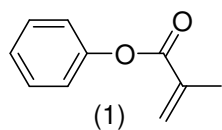
Monomer (n°)	Starting material (n°)	Reaction time (min)
 (25)	 (1')	1
 (26)	 (3')	2

### 3.4 Characterisation

The NMR analysis was done as follows: solvent (deuterated chloroform ( $\text{CDCl}_3$ )), chemical shifts ( $\delta$ ), multiplicity of spin (s-singlet, d-doublet, t-triplet, dd- double duplets, q- quadruplet, m- multiplet), coupling constant (J), relative intensity and the structural assignment. The chemical shifts ( $\delta$ ) are expressed in parts per million (ppm) and coupling constants (J) in Hertz (Hz). For FTIR spectroscopy analysis the data is presented as follows: support of the sample (sodium chloride (NaCl) discs), type of molecular vibrations ( $\delta$ - bending vibrations,  $\nu$ - stretching vibrations,  $\gamma$ - out of plane bending vibrations), and its wave number of maximum absorption ( $\text{cm}^{-1}$ ) and the assignment of the functional group involved. The assignments were based on literature data<sup>61</sup>. All  $^1\text{H}$  and  $^{13}\text{C}$  NMR spectra are presented in chapter VIII – appendix.

#### 3.4.1 Monomethacrylate monomers without spacer

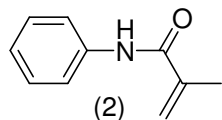
##### Phenyl methacrylate (1)<sup>44</sup>



According to the experimental method, the starting material 1' (1 g, 10.63 mmol) and methacryl chloride (1.11 g, 10.63 mmol) were reacted to afford monomer 1 (1.64 g, 95 % yield), as a colourless oil.

$^1\text{H}$  NMR ( $\text{CDCl}_3$ , ppm)  $\delta$  7.39 (t,  $J = 7.9$  Hz, 2H, Ar-H), 7.23 (t,  $J = 7.4$  Hz, 1H, Ar-H), 7.12 (d,  $J = 7.6$  Hz, 2H, Ar-H), 6.35 (s, 1H,  $\text{CH}_2$ ), 5.75 (s, 1H,  $\text{CH}_2$ ), 2.06 (s, 3H,  $\text{CH}_3$ ).

$^{13}\text{C}$ -RMN ( $\text{CDCl}_3$ , ppm)  $\delta$  165.8 (C=O), 150.9 ( $\text{C}_{\text{Ar}}\text{-O}$ ), 135.9 (C=), 129.4 ( $\text{C}_{\text{Ar}}$ ), 127.1 ( $=\text{CH}_2$ ), 125.7 ( $\text{C}_{\text{Ar}}$ ), 121.6 ( $\text{C}_{\text{Ar}}$ ), 18.4 ( $\text{CH}_3$ ).

**N-Phenylmethacrylamide (2)** <sup>46</sup>

According to the experimental method, the starting material 2' (1 g, 10.75 mmol) and methacryl chloride (1.12 g, 10.75 mmol) were reacted to afford monomer 2 (1.21 g, 70% yield), as a white solid.

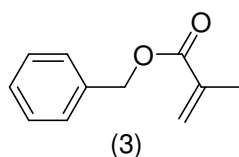
<sup>1</sup>H NMR (CDCl<sub>3</sub>, ppm) δ 7.56 (d, *J* = 7.9 Hz, 2H, Ar-*H*), 7.363 (t, *J*=7.8 Hz, 2H, Ar-*H*), 7.12 (t, *J* = 7.3 Hz, 1H, Ar-*H*), 5.79 (s, 1H, CH<sub>2</sub>), 5.45 (s, 1H, CH<sub>2</sub>), 2.06 (s, 3H, CH<sub>3</sub>).

<sup>13</sup>C-RMN (CDCl<sub>3</sub>, ppm) δ 166.6 (C=O), 140.9 (C=), 137.8 (C<sub>Ar</sub>-NH), 129.0 (C<sub>Ar</sub>), 124.4 (C<sub>Ar</sub>), 120.0 (=CH<sub>2</sub>), 119.8 (C<sub>Ar</sub>), 18.7 (CH<sub>3</sub>).

FTIR (NaCl, cm<sup>-1</sup>): ν 3290 (NH), δ 1595 (NH), γ 891 (NH), ν 1660 (C=O), ν 1620 and 1494 (aromatic C=C), ν 1436 (C-N), ν 1373 (CH<sub>3</sub>).

**m.p.** 186-189 °C.

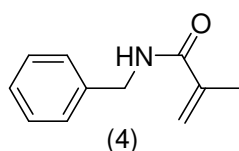
**Analysis calculated for:** C<sub>10</sub>H<sub>11</sub>NO: C,73.92; H, 6.96; N,8.61. Found: C, 74.01; H,6.88; N,8.69.

**Benzyl methacrylate (3)** <sup>44</sup>

According to the experimental method, the starting material 3' (1 g, 9.25 mmol) and methacryl chloride (0.96 g, 9.25 mmol) were reacted to afford monomer 3 (1.56 g, 96% yield), as a white oil.

<sup>1</sup>H NMR (CDCl<sub>3</sub>, ppm) δ 7.34 (m, 5H, Ar-*H*), 6.16 (s, 1H, =CH<sub>2</sub>), 5.58 (s, 1H, =CH<sub>2</sub>), 5.19 (s, 2H, CH<sub>2</sub>), 1.97 (s, 3H, CH<sub>3</sub>).

<sup>13</sup>C-RMN (CDCl<sub>3</sub>, ppm) δ 167.2 (C=O), 136.2 (C<sub>Ar</sub>-CH<sub>2</sub>), 136.1 (C=), 128.5 (C<sub>Ar</sub>), 128.1 (C<sub>Ar</sub>), 127.9 (C<sub>Ar</sub>), 125.7 (=CH<sub>2</sub>), 66.3 (CH<sub>2</sub>), 18.3 (CH<sub>3</sub>).

**N-benzylmethacrylamide (4)** <sup>47</sup>

According to the experimental method, the starting material 4' (1 g, 9.34 mmol) and methacryl chloride (0.97 g, 9.34 mmol) were reacted to afford monomer 4 (1.11 g, 68 % yield), as a white soil.

<sup>1</sup>H NMR (CDCl<sub>3</sub>, ppm) δ 7.32 (m, 5H, Ar-*H*), 5.72 (s, 1H, =CH<sub>2</sub>), 5.35 (s, 1H, =CH<sub>2</sub>), 4.50 (d, *J* = 5.5 Hz, 2H, CH<sub>2</sub>), 1.99 (s, 3H, CH<sub>3</sub>).

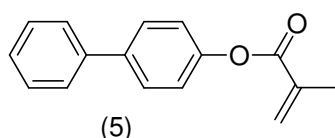
<sup>13</sup>C-RMN (CDCl<sub>3</sub>, ppm) δ 168.3 (C=O), 139.8 (C=), 138.2 (C<sub>Ar</sub>-CH<sub>2</sub>), 128.7 (C<sub>Ar</sub>), 127.8 (C<sub>Ar</sub>), 127.5 (C<sub>Ar</sub>), 119.7 (=CH<sub>2</sub>), 43.7 (CH<sub>2</sub>), 18.7 (CH<sub>3</sub>).

**FTIR** (NaCl,  $\text{cm}^{-1}$ ):  $\nu$  3450 (NH),  $\delta$  1515 (NH),  $\gamma$  736 (NH),  $\nu$  1667 (C=O),  $\nu$  1625 (aromatic C=C),  $\nu$  1454 (C-N),  $\nu$  1422 ( $\text{CH}_2$ ),  $\nu$  1375 ( $\text{CH}_3$ ).

**m.p.** 81-84 °C.

**Analysis calculated for:**  $\text{C}_{11}\text{H}_{13}\text{NO}$ : C,75.40; H,7.48; N,7.99. Found: C,74.94; H,7.60; N,8.15.

### Biphenyl-4-yl methacrylate (5) <sup>48</sup>



According to the experimental method, the starting material 5' (1 g, 5.88 mmol) and methacryl chloride (0.61g, 5.88 mmol) were reacted to afford monomer 5 (1.15 g, 76 % yield) as a white solid.

**<sup>1</sup>H NMR** ( $\text{CDCl}_3$ , ppm)  $\delta$  7.59 (dd,  $J_1 = 10.6$ ,  $J_2 = 8.45$  Hz, 4H, Ar-*H*), 7.44 (t,  $J = 7.6$  Hz, 2H, Ar-*H*), 7.36 (t,  $J = 7.3$  Hz, 1H, Ar-*H*), 7.22 (d,  $J = 8.5$  Hz, 2H, Ar-*H*), 6.38 (s, 1H, = $\text{CH}_2$ ), 5.78 (s, 1H, = $\text{CH}_2$ ), 2.09 (s, 3H,  $\text{CH}_3$ ).

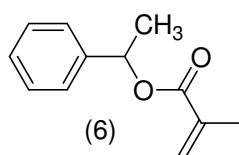
**<sup>13</sup>C NMR** ( $\text{CDCl}_3$ , ppm)  $\delta$  165.9 (C=O), 150.3 ( $\text{C}_{\text{qAr-O}}$ ), 140.4 ( $\text{C}_{\text{Ar-Ar}}$ ), 138.9 (C=), 135.9 ( $\text{C}_{\text{Ar-Ar}}$ ), 128.8 ( $\text{C}_{\text{Ar}}$ ), 128.1 ( $\text{C}_{\text{Ar}}$ ), 127.3 ( $\text{C}_{\text{Ar}}$ ), 127.1 ( $\text{C}_{\text{Ar}}$ ), 121.9 (=CH<sub>2</sub>), 18.4 ( $\text{CH}_3$ ).

**FTIR** (NaCl,  $\text{cm}^{-1}$ ):  $\nu$  1734 (C=O),  $\nu$  1638 and 1485 (aromatic C=C),  $\nu$  1378 ( $\text{CH}_3$ ),  $\nu$  1128 (C-O).

**m.p.** 102-106 °C.

**Analysis calculated for:**  $\text{C}_{16}\text{H}_{14}\text{O}_2$ : C, 80.65; H, 5.92. Found C, 80.70; H, 6.05.

### 1-Phenylethyl methacrylate (6) <sup>49</sup>



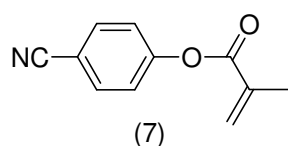
According to the experimental method, the starting material 6' (1 g, 8.19 mmol) and methacryl chloride (0.85 g, 8.19 mmol) were reacted to afford monomer 6 (0.76 g, 49 % yield) as a colourless oil.

**<sup>1</sup>H NMR** ( $\text{CDCl}_3$ , ppm)  $\delta$  7.47-7.21 (m, 5H, Ar-*H*), 6.16 (s, 1H, = $\text{CH}_2$ ), 5.94 (q,  $J = 6.54$  Hz, 1H, CH), 5.56 (s, 1H, = $\text{CH}_2$ ), 1.96 (s, 3H,  $\text{CH}_3\text{-C=}$ ), 1.57 (d,  $J = 6.57$  Hz, 3H,  $\text{CH}_3\text{-CH}$ ).

**<sup>13</sup>C NMR** ( $\text{CDCl}_3$ , ppm)  $\delta$  166.6 (C=O), 141.9 ( $\text{C}_{\text{Ar-CH}}$ ), 136.6 (C=), 128.4 ( $\text{C}_{\text{Ar}}$ ), 127.7 ( $\text{C}_{\text{Ar}}$ ), 125.9 ( $\text{C}_{\text{Ar}}$ ), 125.4 (=CH<sub>2</sub>), 72.5 (CH), 22.3 ( $\text{CH}_3\text{-CH}$ ), 18.4 ( $\text{CH}_3\text{-C=}$ ).

**FTIR** (NaCl,  $\text{cm}^{-1}$ ):  $\nu$  1713 (C=O),  $\nu$  1637 and 1495 (aromatic C=C),  $\nu$  1378 ( $\text{CH}_3$ ).

**Analysis calculated for:**  $\text{C}_{12}\text{H}_{14}\text{O}_2$ : C, 76.17; H, 6.92. Found: C, 76.24; H, 7.07.

**4-Isocyanophenyl methacrylate (7)** <sup>48</sup>

According to the experimental method, the starting material 7' (1 g, 8.4 mmol) and methacryl chloride (0.87 g, 8.4 mmol) were reacted to afford monomer 7 (1.10 g, 70 % yield), as a yellow solid.

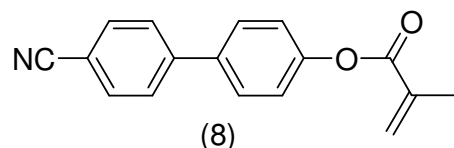
<sup>1</sup>H NMR (CDCl<sub>3</sub>, ppm) δ 7.71 (d, *J* = 8.44 Hz, 2H, Ar-*H*), 7.27 (d, *J* = 8.13 Hz, 2H, Ar-*H*), 6.38 (s, 1H, =CH<sub>2</sub>), 5.83 (s, 1H, =CH<sub>2</sub>), 2.07 (s, 3H, CH<sub>3</sub>).

<sup>13</sup>C NMR (CDCl<sub>3</sub>, ppm) δ 164.8 (C=O), 154.2 (C<sub>Ar</sub>-O), 135.2 (C=), 133.7 (C<sub>Ar</sub>), 128.4 (=CH<sub>2</sub>), 123.6 (C<sub>Ar</sub>), 118.2 (CN), 109.7 (C<sub>Ar</sub>-CN), 18.2 (CH<sub>3</sub>).

FTIR (NaCl, cm<sup>-1</sup>): ν 2232 (CN), ν 1736 (C=O), ν 1637 (=CH<sub>2</sub>), ν 1602 and 1451 (aromatic C=C), ν 1378 (CH<sub>3</sub>), ν 1266 (C-O).

m.p. 81-85 °C

Analysis calculated for: C<sub>11</sub>H<sub>9</sub>NO<sub>2</sub>: C, 70.58; H, 4.85; N, 7.48. Found: C, 70.45; H, 5.01; N, 7.35.

**4'-Isocyanobiphenyl-4-yl methacrylate (8)**

According to the experimental method, the starting material 8' (1 g, 5.13mmol) and methacryl chloride (0.53 g, 5.13 mmol) were reacted to afford monomer 8 (1.19 g, 88 % yield), as a white solid.

<sup>1</sup>H NMR (CDCl<sub>3</sub>, ppm) δ 7.69 (dd, *J*<sub>1</sub> = 23.74 Hz, *J*<sub>2</sub> = 8.19 Hz, 4H, Ar-*H*), 7.60 (d, *J* = 8.48 Hz, 2H, Ar-*H*), 7.24 (d, *J* = 8.51 Hz, 1H, Ar-*H*), 6.38 (s, 1H, =CH<sub>2</sub>), 5.80 (s, 1H, =CH<sub>2</sub>), 2.08 (s, 3H, CH<sub>3</sub>).

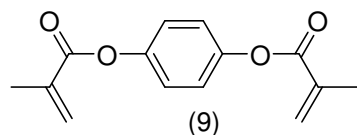
<sup>13</sup>C NMR (CDCl<sub>3</sub>, ppm) δ 165.7 (C=O), 151.4 (C<sub>Ar</sub>-O), 144.7 (C<sub>Ar</sub>-Ar), 136.7 (C<sub>Ar</sub>-Ar), 135.6 (C=), 132.6 (C<sub>Ar</sub>), 128.3 (C<sub>Ar</sub>), 127.6 (=CH<sub>2</sub>), 122.3 (C<sub>Ar</sub>), 118.8 (CN), 110.9 (C<sub>Ar</sub>-CN), 18.3 (CH<sub>3</sub>).

FTIR (NaCl, cm<sup>-1</sup>): ν 2229 (NC), ν 1732 (C=O), ν 1608 and 1421 (aromatic C=C), ν 1320 (CH<sub>3</sub>), ν 1169 (C-O).

m.p. 125-129 °C

Analysis calculated for: C<sub>17</sub>H<sub>13</sub>NO<sub>2</sub>: C, 77.55; H, 4.98; N, 5.32; O 12.15. Found: C, 77.70; H, 5.10; N, 5.43.

## 3.4.2 Dimethacrylated monomers without spacer

1,4-Phenylene bis(2-methylacrylate) (9) <sup>50</sup>

According to the experimental method, the starting material 9' (1 g, 9.08 mmol) and methacryl chloride (2 equiv., 1.89 g, 18.17 mmol) were reacted to afford monomer 9 (1.90 g, 85 % yield), as a white solid.

<sup>1</sup>H NMR (CDCl<sub>3</sub>, ppm) δ 7.14 (s, 4H, Ar-H), 6.34 (s, 2H, =CH<sub>2</sub>), 5.75 (s, 2H, =CH<sub>2</sub>), 2.05 (s, 6H, CH<sub>3</sub>).

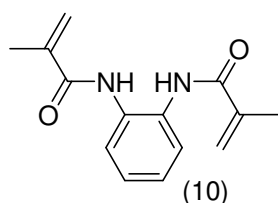
<sup>13</sup>C NMR (CDCl<sub>3</sub>, ppm) δ 165.6 (C=O), 148.2 (C<sub>Ar</sub>-O), 135.6 (C=), 127.3 (=CH<sub>2</sub>), 122.3 (C<sub>Ar</sub>), 18.3 (CH<sub>3</sub>).

FTIR (NaCl, cm<sup>-1</sup>) ν 1736 (C=O), ν 1638 (=CH<sub>2</sub>) ν 1638 and 1502 (aromatic C=C), ν 1380 (CH<sub>3</sub>), ν 1265 (C-O).

m.p. 89-93 °C.

Analysis calculated for: C<sub>14</sub>H<sub>14</sub>O<sub>4</sub>: C, 68.28; H, 5.73. Found: C, 68, 17; H 5.86.

## N,N'-(1,2-phenylene)bis(2-methylacrylamide) (10)



According to the experimental method, the starting material 10' (1 g, 9.25 mmol) and methacryl chloride (2 equiv., 1.92 g, 18.5 mmol) were reacted to afford the monomer 10 (1.81 g, 80 % yield), as a yellow solid.

<sup>1</sup>H NMR (CDCl<sub>3</sub>, ppm) δ 8.86 (s, 2H, NH), 7.28 (dd, *J* = 5.75, 3.74 Hz, 2H, Ar-H), 7.07 (dd, *J* = 5.83, 3.56 Hz, 2H, Ar-H), 5.92 (s, 2H, =CH<sub>2</sub>), 5.48 (s, 2H, =CH<sub>2</sub>), 2.00 (s, 6H, CH<sub>3</sub>).

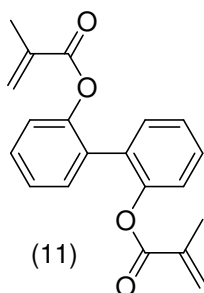
<sup>13</sup>C-RMN(CDCl<sub>3</sub>, ppm) δ 167.3 (C=O), 139.1 (C=), 130.6 (C<sub>Ar</sub>-NH), 125.9 (C<sub>Ar</sub>), 125.7 (=CH<sub>2</sub>), 121.8 (C<sub>Ar</sub>), 18.5 (CH<sub>3</sub>).

FTIR (NaCl, cm<sup>-1</sup>) ν 3419 (NH), δ 1509 (NH), γ 739 (NH), ν 1654 (C=O), ν 1626 and 1478 (aromatic C=C), ν 1446 (C-N), ν 1375 (CH<sub>3</sub>).

m.p. 119-123 °C

Analysis calculated for: C<sub>14</sub>H<sub>16</sub>N<sub>2</sub>O<sub>2</sub>: C, 68.83; H, 6.60; N, 11.47. Found: C, 68.75; H, 6.68; N, 11.53.



**Biphenyl-2,2'-diyl bis(2-methylacrylate) (11)** <sup>51</sup>

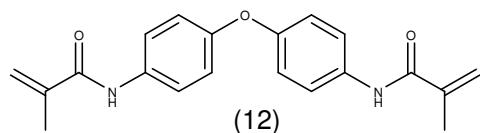
According to the experimental method, the starting material 11' (1 g, 5.37 mmol) and methacryl chloride (2 equiv., 1.12 g, 10.74 mmol) were reacted to afford monomer 11 (1.49 g, 86 % yield), as a colourless oil.

<sup>1</sup>H NMR (CDCl<sub>3</sub>, ppm) δ 7.3 (m, 8H, Ar-H), 6.02 (s, 2H, =CH<sub>2</sub>), 5.53 (s, 2H, =CH<sub>2</sub>), 1.83 (s, 6H, CH<sub>3</sub>).

<sup>13</sup>C NMR (CDCl<sub>3</sub>, ppm) δ 165.4 (C=O), 148.3 (C<sub>Ar</sub>-O), 135.4 (C=), 131.1 (C<sub>Ar</sub>-Ar), 128.8 (C<sub>Ar</sub>), 126.9 (=CH<sub>2</sub>), 125.6 (C<sub>Ar</sub>), 122.2 (C<sub>Ar</sub>), 18.1 (CH<sub>3</sub>).

FTIR (NaCl, cm<sup>-1</sup>) ν 1734 (C=O), ν 1678 (=CH<sub>2</sub>), ν 1638 and 1504 (aromatic C=C), ν 1378 (CH<sub>3</sub>), ν 1267 (C-O).

**Analysis calculated for:** C<sub>20</sub>H<sub>18</sub>O<sub>4</sub>: C, 74.52; H, 5.63. Found: C, 74.68; H, 5.69.

**N,N'-(4,4'-oxybis(4,1-phenylene))bis(2-methylacrylamide) (12)**

According to the experimental method, the starting material 12' (1 g, 4.99 mmol) and methacryl chloride (2 equiv., 1.04 g, 9.99 mmol) were reacted to afford monomer 12 (0.67 g, 40 % yield), as a white solid.

<sup>1</sup>H NMR (CDCl<sub>3</sub>, ppm) δ 7.72 (d, *J* = 8.96 Hz, 4H, Ar-H), 6.95 (d, *J* = 8.97 Hz, 4H, Ar-H), 5.81 (s, 2H, =CH<sub>2</sub>), 5.45 (s, 2H, =CH<sub>2</sub>), 1.99 (s, 6H, CH<sub>3</sub>).

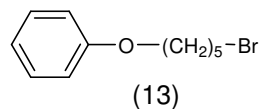
<sup>13</sup>C-RMN (CDCl<sub>3</sub>, ppm) δ 166.5 (C=O), 153.9 (C<sub>Ar</sub>-O), 140.8 (C=), 133.1 (C<sub>Ar</sub>-NH), 121.8 (C<sub>Ar</sub>), 119.8 (=CH<sub>2</sub>), 119.2 (C<sub>Ar</sub>), 18.7 (CH<sub>3</sub>).

FTIR (NaCl, cm<sup>-1</sup>) ν 3281 (NH), δ 1529 (NH), γ 837(NH), ν 1663 (C=O) ν 1625 and 1452 (aromatic C=C), ν 1371 (CH<sub>3</sub>), ν 1226 (C-O).

**m.p.** 79-83 °C.

**Analysis calculated for:** C<sub>20</sub>H<sub>20</sub>N<sub>2</sub>O<sub>3</sub>: C, 71.41; H, 5.99; N, 8.33. Found: C, 71.55; H, 6.04; N, 8.24.

## 3.4.3 Aromatic compounds bearing an alkyl monobromide chain (precursors)

(5-Bromopentyloxy) benzene (13) <sup>52</sup>

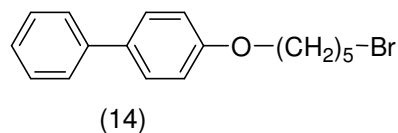
According to the experimental method, the starting material 1' (1 g, 10.63 mmol) and 1,5-dibromopentane (2.42 g, 10.63 mmol) were reacted to afford compound 13 (2.09 g, 81 % yield), as a colourless oil.

<sup>1</sup>H NMR (CDCl<sub>3</sub>, ppm) δ 7.27 (m, 2H, Ar-H), 6.9 (m, 3H, Ar-H), 4.0 (t, J=6.31, 2H, CH<sub>2</sub>-O), 3.4 (t, J=6.71, 2H, CH<sub>2</sub>-Br), 1.9 (m, 2H, CH<sub>2</sub>), 1.8 (m, 2H, CH<sub>2</sub>), 1.6 (m, 2H, CH<sub>2</sub>).

<sup>13</sup>C NMR (CDCl<sub>3</sub>, ppm) δ 159.0 (C<sub>Ar</sub>-O), 129.4 (C<sub>Ar</sub>), 120.6 (C<sub>Ar</sub>), 114.4 (C<sub>Ar</sub>), 67.4 (CH<sub>2</sub>-O), 33.5 (CH<sub>2</sub>-Br), 32.5 (CH<sub>2</sub>), 28.4 (CH<sub>2</sub>), 24.8 (CH<sub>2</sub>).

FTIR (NaCl, cm<sup>-1</sup>) ν 1598 and 1473 (aromatic C=C), ν 1389(CH<sub>2</sub>), ν 1171(C-O), ν 1152 (CH<sub>2</sub>-Br).

Analysis calculated for: C<sub>11</sub>H<sub>15</sub>BrO: C, 54.34; H, 6.22; Br, 32.86; Found: C, 54.40; H, 6.34; Br, 32.92.

4-(5-Bromopentyloxy) biphenyl (14) <sup>53</sup>

According to the experimental method, the starting material 5' (1g, 5.88mmol) and 1,5-dibromopentane (1.34 g, 8.5 mmol) were reacted to afford compound 14 (1.48 g, 79 % yield), as a white solid.

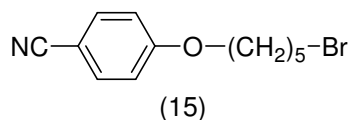
<sup>1</sup>H NMR (CDCl<sub>3</sub>, ppm) δ 7.52 (dd, J<sub>1</sub> = 13.54, J<sub>2</sub> = 8.06 Hz, 4H, Ar-H), 7.40 (t, J = 7.60 Hz, 2H, Ar-H), 7.28 (t, J = 7.30 Hz, 1H, Ar-H), 6.94 (d, J = 8.63 Hz, 2H, Ar-H), 3.98 (t, J = 6.29 Hz, 2H, CH<sub>2</sub>-O), 3.40 (t, J = 6.72 Hz, 2H, CH<sub>2</sub>-Br), 1.94 (m, 2H, CH<sub>2</sub>), 1.82 (m, 2H, CH<sub>2</sub>), 1.59 (m, J = 1.63 Hz, 2H, CH<sub>2</sub>).

<sup>13</sup>C NMR (CDCl<sub>3</sub>, ppm) δ 158.5 (C<sub>Ar</sub>-O), 140.8 (C<sub>Ar</sub>-Ar), 133.6 (C<sub>Ar</sub>-Ar), 128.7 (C<sub>Ar</sub>), 128.1 (C<sub>Ar</sub>), 126.6 (C<sub>Ar</sub>), 114.7 (C<sub>Ar</sub>), 67.58 (CH<sub>2</sub>-O), 33.6 (CH<sub>2</sub>-Br), 32.4 (CH<sub>2</sub>), 28.4 (CH<sub>2</sub>), 24.8 (CH<sub>2</sub>).

FTIR (NaCl, cm<sup>-1</sup>): ν 1610 and 1519 (aromatic C=C), 1487 ν (CH<sub>2</sub>), 1285 ν (CH<sub>2</sub>-Br), 1246 ν (C-O).

m.p. 50-53 °C

Analysis calculated for: C<sub>17</sub>H<sub>19</sub>BrO: C, 63.96; H, 6.00; Br, 25.03. Found: C, 64.00; H, 6.09, Br, 25.07.

**4-(5-Bromopentyloxy)benzonitrile (15)**<sup>54</sup>

According to the experimental method, the starting material 7' (1 g, 8.4 mmol) and 1,5-dibromopentane (1.91 g, 8.4 mmol) were reacted to afford compound 15 (1.57 g, 70 % yield), as a white solid.

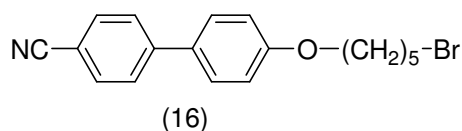
<sup>1</sup>H NMR (CDCl<sub>3</sub>, ppm) δ 7.58 (d, *J* = 8.57 Hz, 2H, Ar-*H*), 6.93 (d, *J* = 8.57 Hz, 2H, Ar-*H*), 4.02 (t, *J* = 6.25 Hz, 2H, CH<sub>2</sub>-O), 3.45 (t, *J* = 6.65 Hz, 2H, CH<sub>2</sub>-Br), 2.00-1.90 (m, 2H, CH<sub>2</sub>), 1.89-1.79 (m, 2H, CH<sub>2</sub>), 1.71-1.58 (m, 2H, CH<sub>2</sub>).

<sup>13</sup>C NMR (CDCl<sub>3</sub>, ppm) δ 162.2 (C<sub>Ar</sub>-O), 133.9 (C<sub>Ar</sub>), 119.2 (CN), 115.1 (C<sub>Ar</sub>), 103.8 (C<sub>Ar</sub>-CN), 67.9 (CH<sub>2</sub>-O), 33.4 (CH<sub>2</sub>-Br), 32.3 (CH<sub>2</sub>), 28.1 (CH<sub>2</sub>), 24.7 (CH<sub>2</sub>).

FTIR (NaCl, cm<sup>-1</sup>): ν 2226 (NC), ν 1606 and 1508 (aromatic C=C), ν 1470 (CH<sub>2</sub>), ν 1264 (C-O), ν 1172 (CH<sub>2</sub>-Br).

m.p. 53-56 °C

Analysis calculated for: C<sub>12</sub>H<sub>14</sub>BrNO: C, 53.75; H, 5.26; Br, 29.80; N, 5.22. Found: C, 53.79; H, 5.27; Br, 29.88; N, 5.20.

**4'-(5-Bromopentyloxy)biphenyl-4-carbonitrile (16)**<sup>55</sup>

According to the experimental method, the starting material 8' (1 g, 5.12 mmol) and 1,5-dibromopentane (1.16 g, 5.12 mmol) were reacted to afford compound 16 (1.32 g, 75 % yield), as a white solid.

<sup>1</sup>H NMR (CDCl<sub>3</sub>, ppm) δ 7.66 (dd, *J*<sub>1</sub> = 20.90, *J*<sub>2</sub> = 8.09 Hz, 4H, Ar-*H*), 7.53 (d, *J* = 8.36 Hz, 2H, Ar-*H*), 6.99 (d, *J* = 8.27 Hz, 2H, Ar-*H*), 4.02 (t, *J* = 6.17 Hz, 2H, CH<sub>2</sub>-O), 3.44 (t, *J* = 6.59 Hz, 2H, CH<sub>2</sub>-Br), 1.95 (m, 2H, CH<sub>2</sub>), 1.85 (m, 2H, CH<sub>2</sub>), 1.65 (m, 2H, CH<sub>2</sub>).

<sup>13</sup>C NMR (CDCl<sub>3</sub>, ppm) δ 159.6 (C<sub>Ar</sub>-O), 145.2 (C<sub>Ar</sub>-Ar), 132.5 (C<sub>Ar</sub>), 131.4 (C<sub>Ar</sub>-Ar), 128.3 (C<sub>Ar</sub>), 119.1 (CN), 115.1 (C<sub>Ar</sub>), 110.1 (C<sub>Ar</sub>-CN), 67.7 (CH<sub>2</sub>-O), 33.6 (CH<sub>2</sub>-Br), 32.4 (CH<sub>2</sub>), 28.4 (CH<sub>2</sub>), 24.8 (CH<sub>2</sub>).

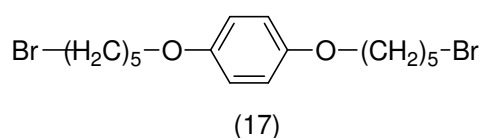
FTIR (NaCl, cm<sup>-1</sup>): ν 2226 (NC), ν 1604 and 1494 (aromatic C=C), ν 1472 (CH<sub>2</sub>), ν 1265 (C-O), ν 1179 (CH<sub>2</sub>-Br).

m.p. 81-84 °C.

Analysis calculated for: C<sub>18</sub>H<sub>18</sub>BrNO: C, 62.80; H, 5.27; Br 23.21; N, 4.07. Found: C, 62.78; H, 5.37; Br 23.29; N, 3.97.

## 3.4.4 Aromatic compounds bearing an alkyl dibromide chain (precursors)

## 1, 4-Bis (5-bromopentyloxy)benzene (17)



According to the experimental method, the starting material 9' (1 g, 9.08 mmol) and 1,5-dibromopentane (2 equiv., 4.14 g, 18.17 mmol) were reacted to afford compound 17 (1.85 g, 50 % yield), as a white solid.

$^1\text{H NMR}$  ( $\text{CDCl}_3$ , ppm)  $\delta$  6.82 (s, 4H, Ar-H), 3.92 (t,  $J=6.2$  Hz, 4H,  $\text{CH}_2\text{-O}$ ), 3.43 (t,  $J=6.8$  Hz, 4H,  $\text{CH}_2\text{-Br}$ ), 1.94 (m, 4H,  $\text{CH}_2$ ), 1.79 (m, 4H,  $\text{CH}_2$ ), 1.62 (m, 4H,  $\text{CH}_2$ ).

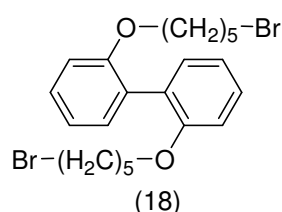
$^{13}\text{C NMR}$  ( $\text{CDCl}_3$ , ppm)  $\delta$  153.1 ( $\text{C}_{\text{Ar-O}}$ ), 115.4 ( $\text{C}_{\text{Ar}}$ ), 68.2 ( $\text{CH}_2\text{-O}$ ), 33.6 ( $\text{CH}_2\text{-Br}$ ), 32.5 ( $\text{CH}_2$ ), 28.6 ( $\text{CH}_2$ ), 24.9 ( $\text{CH}_2$ ).

**FTIR** ( $\text{NaCl}$ ,  $\text{cm}^{-1}$ )  $\nu$  1637 and 1508 (aromatic  $\text{C}=\text{C}$ ),  $\nu$  1420 ( $\text{CH}_2$ ),  $\nu$  1265 ( $\text{C-O}$ ),  $\nu$  1170 ( $\text{CH}_2\text{-Br}$ ).

**m.p.** 95-99 °C

**Analysis calculated for:**  $\text{C}_{16}\text{H}_{24}\text{Br}_2\text{O}_2$ : C, 47.08; H, 5.93; Br, 39.15; Found: C, 46.99; H, 6.00; Br, 39.19.

## 2, 2'-Bis(5-bromopentyloxy)biphenyl (18)



According to the experimental method, the starting material 11' (1 g, 5.37 mmol) and 1,5-dibromopentano (2 equiv., 2.54 g, 10.75 mmol) were reacted to afford compound 18 (1.61 g, 62 %yield), as a colourless oil.

$^1\text{H NMR}$  ( $\text{CDCl}_3$ , ppm)  $\delta$  7.3 (m, 4H, Ar-H), 7.0 (m, 4H, Ar-H), 3.90 (t,  $J = 6.12$  Hz, 4H,  $\text{CH}_2\text{-O}$ ), 3.27 (t,  $J = 6.72$  Hz, 4H,  $\text{CH}_2\text{-Br}$ ), 1.7 (m, 4H,  $\text{CH}_2$ ), 1.6 (m, 4H,  $\text{CH}_2$ ), 1.41 (m, 4H,  $\text{CH}_2$ ).

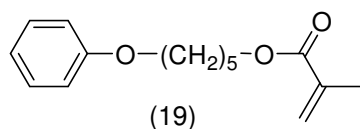
$^{13}\text{C NMR}$  ( $\text{CDCl}_3$ , ppm)  $\delta$  156.4 ( $\text{C}_{\text{Ar-O}}$ ), 131.4 ( $\text{C}_{\text{Ar-Ar}}$ ,  $\text{C}_{\text{Ar}}$ ), 128.3 ( $\text{C}_{\text{Ar}}$ ), 120.2 ( $\text{C}_{\text{Ar}}$ ), 112.2 ( $\text{C}_{\text{Ar}}$ ), 68.1 ( $\text{CH}_2\text{-O}$ ), 33.8 ( $\text{CH}_2\text{-Br}$ ), 32.2 ( $\text{CH}_2$ ), 28.3 ( $\text{CH}_2$ ), 24.8 ( $\text{CH}_2$ ).

**FTIR** ( $\text{NaCl}$ ,  $\text{cm}^{-1}$ )  $\nu$  1637 and 1498 (aromatic  $\text{C}=\text{C}$ ),  $\nu$  1443 ( $\text{CH}_2$ ),  $\nu$  1266 ( $\text{C-O}$ ),  $\nu$  1127 ( $\text{CH}_2\text{-Br}$ ).

**Analysis calculated for:**  $\text{C}_{22}\text{H}_{28}\text{Br}_2\text{O}_2$ : C, 54.56; H, 5.83; Br, 33.00; Found: C, 54.50; H, 5.49; Br, 33.04.

### 3.4.5 Monomethacrylate monomers bearing a linear chain spacer with five methylene units

#### 5-Phenoxy-pentyl methacrylate (19)



According to the experimental method, the starting material 13 (1 g, 4.13 mmol) and methacrylic acid (0.35 g, 4.13 mmol) were reacted to afford monomer 19 (0.71 g, 70 % yield), as a colourless oil.

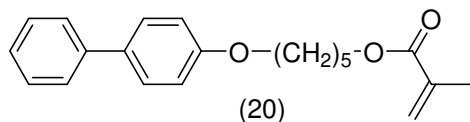
$^1\text{H NMR}$  ( $\text{CDCl}_3$ , ppm)  $\delta$  7.3 (m, 2H, Ar-*H*), 6.9 (m, 3H, Ar-*H*), 6.10 (s, 1H,  $\text{CH}_2$ ), 5.55 (s, 1H,  $\text{CH}_2$ ), 4.21 (t,  $J = 6.55$  Hz, 2H,  $\text{CH}_2\text{-OCO}$ ), 4.0 (t, 2H,  $J = 6.34$  Hz  $\text{CH}_2\text{-OAr}$ ), 1.90 (s, 3H,  $\text{CH}_3$ ), 1.8 (m, 2H,  $\text{CH}_2$ ), 1.7 (m, 2H,  $\text{CH}_2$ ), 1.6 (m, 2H,  $\text{CH}_2$ ).

$^{13}\text{C NMR}$  ( $\text{CDCl}_3$ , ppm)  $\delta$  167.4 ( $\text{C=O}$ ), 159.0 ( $\text{C}_{\text{Ar-O}}$ ), 136.4 ( $\text{C=}$ ); 129.4 ( $\text{C}_{\text{Ar}}$ ), 125.2 ( $=\text{CH}_2$ ), 120.5 ( $\text{C}_{\text{Ar}}$ ), 114 ( $\text{C}_{\text{Ar}}$ ), 67.4 ( $\text{CH}_2\text{-O}$ ), 64.5 ( $\text{CH}_2\text{-OOC}$ ), 29.0 ( $\text{CH}_2$ ), 28.3 ( $\text{CH}_2$ ), 22.6 ( $\text{CH}_2$ ), 18.3 ( $\text{CH}_3$ ).

**FTIR** ( $\text{NaCl, cm}^{-1}$ ):  $\nu$  1637 ( $\text{C=O}$ ),  $\nu$  1599 and 1454 (aromatic  $\text{C=C}$ ),  $\nu$  1401 ( $\text{CH}_2$ ),  $\nu$  1168 ( $\text{C-O}$ ).

**Analysis calculated for:** C, 72.55; H, 8.12; Found: C, 72.50; H, 8.04.

#### 5-(Biphenyl-4-yloxy)pentyl methacrylate (20)



According to the experimental method, the starting material 14 (1 g, 3.13 mmol) and methacrylic acid (0.26 g, 3.13 mmol) were reacted to afford monomer 20 (0.76 g, 75 %), as a white solid.

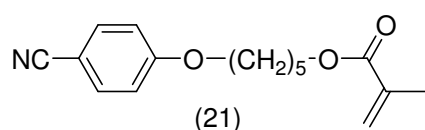
$^1\text{H NMR}$  ( $\text{CDCl}_3$ , ppm)  $\delta$  7.53 (dd,  $J_1 = 13.46$ ,  $J_2 = 8.05$  Hz, 4H, Ar-*H*), 7.41 (t,  $J = 7.57$  Hz, 2H, Ar-*H*), 7.29 (t,  $J = 7.24$  Hz, 1H, Ar-*H*), 6.96 (d,  $J = 8.52$  Hz, 2H, Ar-*H*), 6.11 (s, 1H,  $=\text{CH}_2$ ), 5.55 (s, 1H,  $=\text{CH}_2$ ), 4.19 (t,  $J = 6.49$  Hz, 2H,  $\text{CH}_2\text{-OCO}$ ), 4.01 (t,  $J = 6.29$  Hz, 2H,  $\text{CH}_2\text{-OAr}$ ), 1.95 (s, 3H,  $\text{CH}_3$ ), 1.9 (m, 2H,  $\text{CH}_2$ ), 1.8 (m, 2H,  $\text{CH}_2$ ), 1.6 (m, 2H,  $\text{CH}_2$ ).

$^{13}\text{C NMR}$  ( $\text{CDCl}_3$ , ppm)  $\delta$  167.5 ( $\text{C=O}$ ), 158.6 ( $\text{C}_{\text{Ar-O}}$ ), 140.8 ( $\text{C}_{\text{Ar-Ar}}$ ), 136.4 ( $\text{C=}$ ), 133.6 ( $\text{C}_{\text{Ar-Ar}}$ ), 129.4 ( $\text{C}_{\text{Ar}}$ ), 128.8 ( $\text{C}_{\text{Ar}}$ ), 128.0 ( $\text{C}_{\text{Ar}}$ ), 127.4 ( $\text{C}_{\text{Ar}}$ ), 125.9 ( $=\text{CH}_2$ ), 115.4 ( $\text{C}_{\text{Ar}}$ ), 114.1 ( $\text{C}_{\text{Ar}}$ ), 67.7 ( $\text{CH}_2\text{-O}$ ), 64.5 ( $\text{CH}_2\text{-OCO}$ ), 28.9 ( $\text{CH}_2$ ), 28.4 ( $\text{CH}_2$ ), 22.6 ( $\text{CH}_2$ ), 17.8 ( $\text{CH}_3$ ).

**FTIR** ( $\text{NaCl, cm}^{-1}$ ):  $\nu$  1710 ( $\text{C=O}$ ),  $\nu$  1654 ( $=\text{CH}_2$ ),  $\nu$  1638 and 1518 (aromatic  $\text{C=C}$ ),  $\nu$  1420 ( $\text{CH}_2$ ),  $\nu$  1321 ( $\text{CH}_3$ ),  $\nu$  1265 ( $\text{C-O}$ ).

**m.p.** 30-34 °C.

**Analysis calculated for:**  $\text{C}_{21}\text{H}_{24}\text{O}_3$ : C, 77.75; H, 7.46. Found: C, 77.86; H, 7.56.

**5-(4-Cyanophenoxy)pentyl methacrylate (21)**

According to the experimental method, the starting material 15 (1 g, 3.66 mmol) and methacrylic acid (0.31 g, 3.66 mmol) were reacted to afford the monomer 21 (0.66 g, 65 %), as white solid.

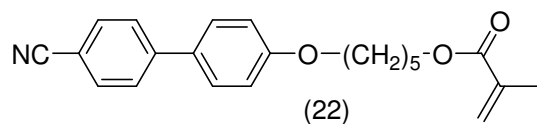
<sup>1</sup>H NMR (CDCl<sub>3</sub>, ppm) δ 7.57 (d, *J* = 8.75 Hz, 2H, Ar-*H*), 6.94 (d, *J* = 8.75 Hz, 2H, Ar-*H*), 6.10 (s, 1H, =CH<sub>2</sub>), 5.56 (s, 1H, =CH<sub>2</sub>), 4.19 (t, *J* = 6.50 Hz, 2H, CH<sub>2</sub>-OCO), 4.02 (t, *J* = 6.30 Hz, 2H, CH<sub>2</sub>-O), 1.95 (s, 3H, CH<sub>3</sub>), 1.9 (m, 2H, CH<sub>2</sub>), 1.8 (m, 2H, CH<sub>2</sub>), 1.6 (m, 2H, CH<sub>2</sub>).

<sup>13</sup>C NMR (CDCl<sub>3</sub>, ppm) δ 167.3 (C=O), 162.1 (C<sub>Ar</sub>-O), 136.3 (C=), 133.3 (C<sub>Ar</sub>), 125.2 (=CH<sub>2</sub>), 119.2 (CN), 115.0 (C<sub>Ar</sub>), 109.9 (C<sub>Ar</sub>-CN), 67.9 (CH<sub>2</sub>-O), 64.3 (CH<sub>2</sub>-OCO), 28.5 (CH<sub>2</sub>), 28.2 (CH<sub>2</sub>), 22.4 (CH<sub>2</sub>), 18.8 (CH<sub>3</sub>).

FTIR (NaCl, cm<sup>-1</sup>): ν 2226 (NC), ν 1712 (C=O), ν 1607 and 1508 (aromatic C=C), ν 1421 (CH<sub>2</sub>), ν 1321 (CH<sub>3</sub>), ν 1266 (C-O).

m.p. 46-50 °C.

Analysis calculated for: C<sub>16</sub>H<sub>19</sub>NO<sub>3</sub>: C, 70.31; H, 7.01; N, 5.12. Found: C, 70.41; H, 7.06; N, 5.14.

**5-(4'-Cyanobiphenyl-4-yloxy)pentyl methacrylate (22)**

According to the experimental method, the starting material 16 (1 g, 2.91 mmol) and methacrylic acid (0.24 g, 2.91 mmol) were reacted to afford the monomer 22 (0.66 g, 65 %), as a white solid.

<sup>1</sup>H NMR (CDCl<sub>3</sub>, ppm) δ 7.65 (dd, *J* = 19.01, 8.16 Hz, 4H, Ar-*H*), 7.52 (d, *J* = 8.43 Hz, 2H, Ar-*H*), 6.98 (d, *J* = 8.44 Hz, 2H, Ar-*H*), 6.11 (s, 1H, =CH<sub>2</sub>), 5.56 (s, 1H, =CH<sub>2</sub>), 4.19 (t, *J* = 6.48 Hz, 2H, CH<sub>2</sub>-OCO), 4.02 (t, *J* = 6.25 Hz, 2H, CH<sub>2</sub>-O), 1.95 (s, 3H, CH<sub>3</sub>), 1.9 (m, 2H, CH<sub>2</sub>), 1.8 (m, 2H, CH<sub>2</sub>), 1.59 (m, 2H, CH<sub>2</sub>).

<sup>13</sup>C NMR (CDCl<sub>3</sub>, ppm) δ 167.4 (C=O), 159.6 (C<sub>Ar</sub>-O), 145.1 (C<sub>Ar</sub>-Ar), 136.4 (C=), 132.44 (C<sub>Ar</sub>-Ar, C<sub>Ar</sub>), 131.2 (C<sub>Ar</sub>), 128.2 (C<sub>Ar</sub>), 127.0 (C<sub>Ar</sub>), 125.2 (=CH<sub>2</sub>), 119.0 (CN), 115.0 (C<sub>Ar</sub>), 109.9 (C<sub>Ar</sub>-CN), 67.7 (CH<sub>2</sub>-O), 64.4 (CH<sub>2</sub>-OCO), 28.7 (CH<sub>2</sub>), 28.3 (CH<sub>2</sub>), 22.5 (CH<sub>2</sub>), 18.2 (CH<sub>3</sub>).

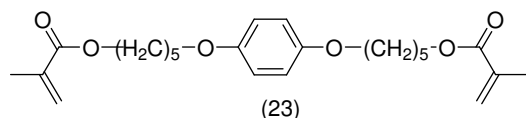
FTIR (NaCl, cm<sup>-1</sup>) ν 2227 (NC), ν 1711 (C=O), ν 1604 and 1494 (aromatic C=C), ν 1471 (CH<sub>2</sub>), ν 1265 (C-O).

m.p. 74-78 °C.

Analysis calculated for: C<sub>22</sub>H<sub>23</sub>NO<sub>3</sub>: C, 75.62; H, 6.63; N, 4.01. Found: C, 75.63; H, 6.62; N, 4.05.

### 3.4.6 Dimethacrylate monomers bearing a linear chain spacer with five methylene units

#### 5, 5'-(1, 4-Phenylenebis(oxy))bis(pentane-5,1-diyl) bis(2-methylacrylate) (23)



According to the experimental method, the starting material 17 (1 g, 2.46 mmol) and methacrylic acid (2 equiv., 0.69 g, 4.92 mmol) were reacted to afford

monomer 23 (0.87 g, 85 % yield), as a colourless liquid.

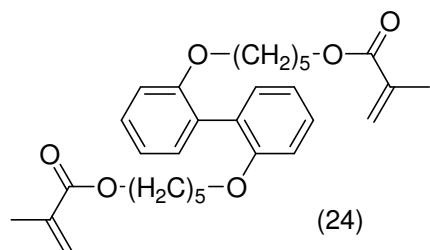
$^1\text{H NMR}$  ( $\text{CDCl}_3$ , ppm)  $\delta$  6.81 (s, 4H, Ar-*H*), 6.10 (s, 2H, = $\text{CH}_2$ ), 5.55 (s, 2H, = $\text{CH}_2$ ), 4.11 (t,  $J=6.3$ , 4H,  $\text{CH}_2\text{-OCO}$ ), 3.87 (t,  $J=6.3$ , 4H,  $\text{CH}_2\text{-O}$ ), 1.94 (s, 6H,  $\text{CH}_3$ ), 1.84 (m, 8H,  $\text{CH}_2$ ), 1.60 (m, 4H,  $\text{CH}_2$ ).

$^{13}\text{C-RMN}$  ( $\text{CDCl}_3$ , ppm)  $\delta$  167.4 ( $\text{C=O}$ ), 153.1 ( $\text{C}_{\text{qAr-O}}$ ), 136.5 ( $\text{C=}$ ), 125.2 (=CH<sub>2</sub>), 115.4 ( $\text{C-Ar}$ ), 68.3 ( $\text{CH}_2\text{-O}$ ), 64.5 ( $\text{CH}_2\text{-OCO}$ ), 29.0 ( $\text{CH}_2$ ), 28.4 ( $\text{CH}_2$ ), 22.6 ( $\text{CH}_2$ ), 18.3 ( $\text{CH}_3$ ).

**FTIR** ( $\text{NaCl}$ ,  $\text{cm}^{-1}$ ):  $\nu$  1716 ( $\text{C=O}$ ),  $\nu$  1636 and 1508 (aromatic  $\text{C=C}$ ),  $\nu$  1406 ( $\text{CH}_2$ ),  $\nu$  1165 ( $\text{C-O}$ ).

**Analysis calculated for:**  $\text{C}_{23}\text{H}_{32}\text{O}_7$ : C, 68.87; H, 8.19. Found: C, 68.80; H, 8.13.

#### 5,5'-(Biphenyl-2,2'-diylbis(oxy))bis(pentane-5,1-diyl) bis(2-methylacrylate) (24)



According to the general method, the starting material 18 (1 g, 2.07 mmol) and methacrylic acid (2 equiv., 0.36g, 4.15 mmol) were reacted to afford monomer 24 (0.70 g, 68 % yield), as a colourless oil.

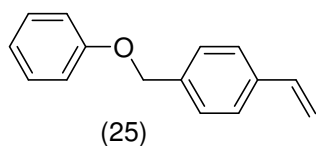
$^1\text{H NMR}$  ( $\text{CDCl}_3$ , ppm)  $\delta$  7.25 (m, 4H, Ar-*H*), 7.00-6.88 (m, 4H, Ar-*H*), 6.06 (s, 2H, = $\text{CH}_2$ ), 5.53 (s, 2H, = $\text{CH}_2$ ), 4.04 (t,  $J = 6.59$  4H,  $\text{CH}_2\text{-OCO}$ ), 3.90 (t,  $J = 6.21$  Hz, 4H,  $\text{CH}_2\text{-O}$ ), 1.92 (s, 6H,  $\text{CH}_3$ ), 1.65 (m, 4H,  $\text{CH}_2$ ), 1.57 (m, 4H,  $\text{CH}_2$ ), 1.35 (m, 4H,  $\text{CH}_2$ ).

$^{13}\text{C NMR}$  ( $\text{CDCl}_3$ , ppm)  $\delta$  167.3 ( $\text{C=O}$ ), 156.4 ( $\text{C}_{\text{qAr-O}}$ ), 136.4 ( $\text{C=}$ ), 131.4 ( $\text{C}_{\text{Ar-Ar}}$ ,  $\text{C}_{\text{Ar}}$ ), 128.3 ( $\text{C}_{\text{Ar}}$ ), 125.1 ( $\text{CH}_2=$ ), 120.1 ( $\text{C}_{\text{Ar}}$ ), 112.2 ( $\text{C}_{\text{Ar}}$ ), 68.1 ( $\text{CH}_2\text{-O}$ ), 64.5 ( $\text{CH}_2\text{-OCO}$ ), 28.8 ( $\text{CH}_2$ ), 28.2 ( $\text{CH}_2$ ), 22.6 ( $\text{CH}_2$ ), 18.2 ( $\text{CH}_3$ ).

**FTIR** ( $\text{NaCl}$ ,  $\text{cm}^{-1}$ ):  $\nu$  1720 ( $\text{C=O}$ ),  $\nu$  1600 and 1503 (aromatic  $\text{C=C}$ ),  $\nu$  1636 (=CH<sub>2</sub>),  $\nu$  1443 ( $\text{CH}_2$ ),  $\nu$  1359 ( $\text{CH}_3$ ),  $\nu$  1296 ( $\text{C-O}$ ).

**Analysis calculated for:**  $\text{C}_{30}\text{H}_{38}\text{O}_6$ : C, 72.85; H, 7.74. Found: C, 72.80; H, 7.70.

## 3.4.7 Vinylic monomers (25-26)

1-(Phenoxymethyl)-4-vinylbenzene (25) <sup>56</sup>

According to the experimental method, the starting material 1 (1 g, 10.63 mmol) and 1-(chloromethyl)-4-vinylbenzene (2 equiv., 3.23 g, 21.27 mmol) were reacted to afford monomer 25 (1.41 g, 63 %), as a white solid.

<sup>1</sup>H RMN (CDCl<sub>3</sub>, ppm) δ 7.41 (dd,  $J_1 = 8.21$ ,  $J_2 = 8.18$  Hz, 4H, Ar-H), 7.29 (dd,  $J_1 = 8.37$ ,  $J_2 = 7.50$  Hz, 2H, Ar-H), 7.0 (m, 3H, Ar-H), 6.72 (dd,  $J_1 = 17.58$ ,  $J_2 = 10.90$  Hz, 1H, =CH), 5.76 (d,  $J = 17.57$  Hz, 1H, =CH<sub>2</sub>), 5.25 (d,  $J = 10.87$  Hz, 1H, =CH<sub>2</sub>), 5.05 (s, 2H, CH<sub>2</sub>).

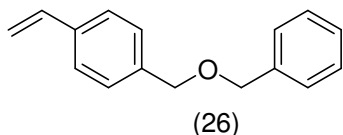
<sup>13</sup>C RMN (CDCl<sub>3</sub>, ppm) δ 158.7 (C<sub>qAr</sub>-O), 136.5 (C<sub>Ar</sub>-C=), 136.4 (C<sub>Ar</sub>-CH<sub>2</sub>, CH=), 129.5 (C<sub>Ar</sub>), 127.7 (C<sub>Ar</sub>), 126.4 (C<sub>Ar</sub>), 121.7 (C<sub>Ar</sub>), 114.8 (C<sub>Ar</sub>), 114.0 (=CH<sub>2</sub>), 69.6 (CH<sub>2</sub>).

FTIR (NaCl, cm<sup>-1</sup>): ν 1630 (CH<sub>2</sub>=C), ν 1600 and 1495 (aromatic C=C), ν 1421 (CH<sub>2</sub>), ν 1379 (CH<sub>3</sub>), ν 1266 (C-O).

m.p 110-114 °C.

Analysis calculated for: C<sub>15</sub>H<sub>14</sub>O: C, 85.68; H, 6.71. Found: C, 85.66; H, 6.78.

## 1-(Benzyloxymethyl)-4-vinylbenzene (26)



According to the experimental method, the starting material 3 (1 g, 9.25 mmol) and 1-(chloromethyl)-4-vinylbenzene (2 equiv., 2.81 g, 18.51 mmol) were reacted to afford monomer 26 (1.33 g, 64%), as a

colourless oil.

<sup>1</sup>H NMR (CDCl<sub>3</sub>, ppm) δ 7.3 (m, 9H, Ar-H), 6.70 (dd,  $J_1 = 17.59$ ,  $J_2 = 10.88$  Hz, 1H, =CH), 5.74 (d,  $J = 17.59$  Hz, 1H, =CH<sub>2</sub>), 5.23 (d,  $J = 10.88$  Hz, 1H, =CH<sub>2</sub>), 4.5 (s, 4H, CH<sub>2</sub>).

<sup>13</sup>C-RMN (CDCl<sub>3</sub>, ppm) δ 137.3 (C<sub>qAr</sub>-C), 136.1 (C<sub>qAr</sub>-C), 135.8 (C<sub>qAr</sub>-C), 135.3 (=CH), 128.3 (C<sub>Ar</sub>), 128.0 (C<sub>Ar</sub>), 126.1 (C<sub>Ar</sub>), 114.0 (=CH<sub>2</sub>), 66.0 (CH<sub>2</sub>), 65.7 (CH<sub>2</sub>).

FTIR (NaCl, cm<sup>-1</sup>) ν 1631 and 1513 (aromatic C=C), ν 1454 (CH<sub>2</sub>), ν 1361 (C-O).

Analysis calculated for: C<sub>16</sub>H<sub>16</sub>O: C, 85.68; H, 7.19. Found: C, 85.60; H, 7.26.



### 3.5 Results obtained under classical synthetic versus microwave irradiation methodologies.

In order to analyse and compare the efficiency between the synthetic methods using classical conditions versus under microwave irradiation, some results were summarised in table 3.8. Comparing the results indicated in the entries 1-4, it is possible to accept the great advantage of microwave conditions over the traditional conditions. In fact although the obtained yields to be similar, there are two remarkable advantages for this last methodology, mainly concerning in time reaction and the solvent amount used. In fact the power supplied (200W) was enough to promote the described chemical reactions with a large reduction in reaction time from hours to minutes. Other way, for these examples, this methodology allows to use very small amounts of solvent or even no solvent, what is not possible under conventional conditions. The synthesis of the compound 14 (entry 5) was much more efficient under microwave conditions, with improved yield (79% versus 37%) and a short reaction time (3 minutes versus 20 hours). In summary, these results suggest that microwave irradiation besides being a cleaner sustainable technology is a simple and effective method for the synthesis of these compounds.

**Table 3.8 – Results obtained by using microwave irradiation or conventional conditions described in the literature**

Entry	Molecular structure of compounds	Microwave conditions	Yield (%)	Conventional conditions	Yield (%)
1	(2)	200W, 5 min (without solvent)	70	At 0 °C for 1h, at room temperature for 4h (butanone) <sup>46</sup> .	70
2	(5)	200W, 1 min (without solvent)	76	At 0 °C for 2h, at room temperature for 1h (butanone) <sup>48</sup> .	70
3	(6)	200W, 5 min (without solvent)	49	At room temperature over night (diethyl ether) <sup>49</sup> .	50
4	(7)	200W, 2 min (without solvent)	70	At 0 °C for 2h, at room temperature for 1h (butanone) <sup>48</sup> .	75
5	(14)	200W, 3 min (DMF)	79	Reflux for 20h (butanone) <sup>53</sup> .	37

### 3.6 Selected monomers

Among all the synthesised monomers, the monomers containing cyano and/or spacer chain group (figure 3.6) were fully characterised due to higher chemical structural compatibility with E7 liquid crystal molecules. The monomers (with cyano and/or with spacer chains groups) properties will be compared to the analogous monomers without cyano group and/or spacer chain and the results will be presented in chapters IV and V.

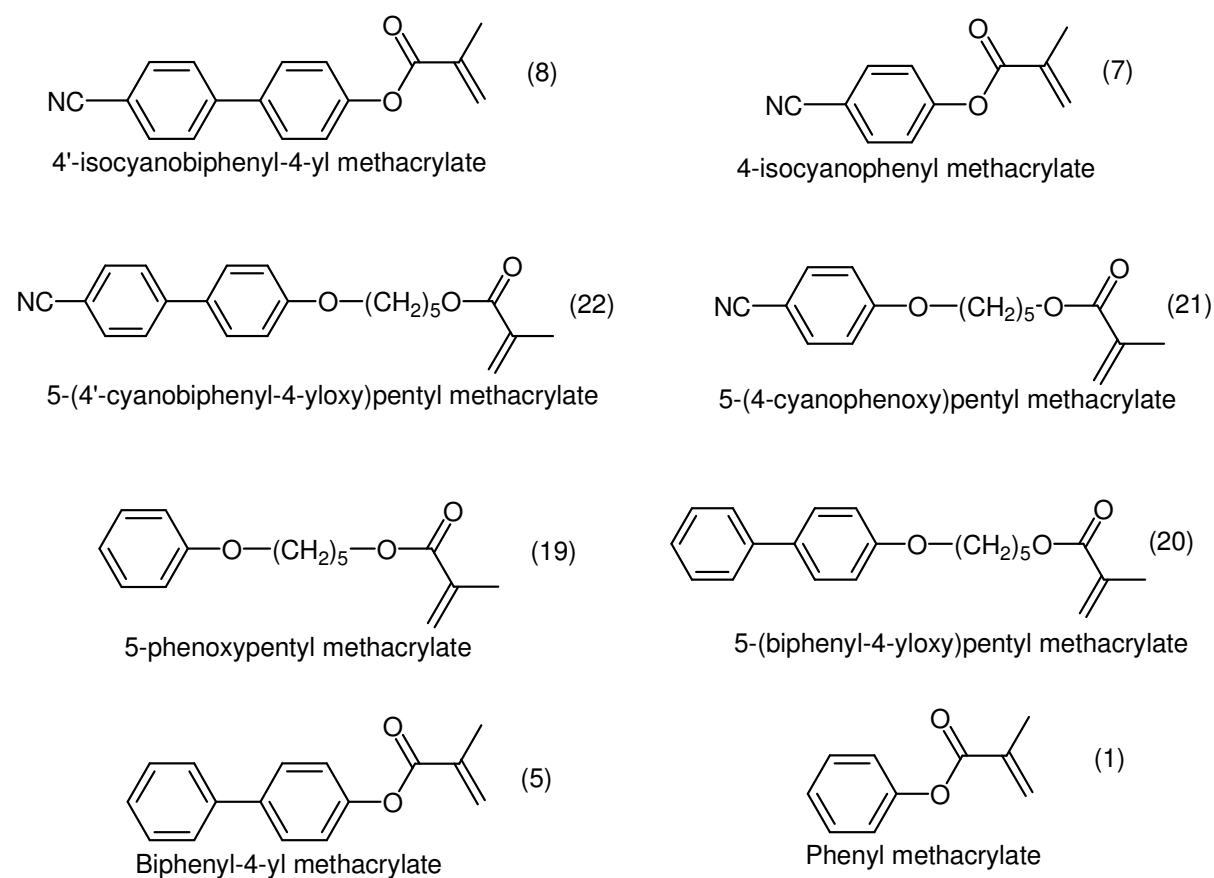


Figure 3.6 – Molecular structure of synthesised monomers with and without cyano and spacer chain group.

## 4 Thermal Characterisation

### 4.1 Outline

The thermal characterisation of the monomers previously synthesised (chapter III, figure 3.6) will be analysed in this chapter. The thermal transitions of monomers were investigated by differential scanning calorimetry (DSC) and complemented using polarised optical microscopy (POM) equipped with a thermal control hot stage. Part of results presented in this chapter and in chapter V have been published<sup>62</sup>.

### 4.2 Calorimetric characterisation

In order to determine the transition temperatures and their associated enthalpies differential scanning calorimetry (DSC) was employed. Figures 4.1-4.8 present the DSC thermograms collected on heating the and on cooling run of cycle I. This cycle, corresponds to the first heating and cooling runs and the cycle II to the second heating and cooling runs.

As mentioned before, the melting temperature ( $T_m$ ) was obtained at the peak of the melting endothermic transition, and in an analogues way the crystallisation temperature either for cold- ( $T_{cc}$ ) or for melt- ( $T_c$ ) crystallisation was obtained at the peak of the respective exothermic transition peak. The glass transition temperature ( $T_g$ ) was taken at the point inflection of the specific heat capacity variation in the transition. The melting and crystallisation enthalpies ( $\Delta H_m$ ) and ( $\Delta H_{cr}$ ), respectively, were determined from the areas under the curve that represents the respective transitions. The information obtained on temperatures and enthalpies is summarised in table 4.1.

Figure 4.1 presents the DSC thermogram collected on cycle I for liquid monomer 19. The heat flux presents a discontinuity characteristic of the glass transition at  $T_g = -86.01^\circ\text{C}$ . At higher temperatures an exothermic peaks characteristic of cold crystallisation emerges at  $-40.19^\circ\text{C}$  with an enthalpy of  $-97.45 \text{ Jg}^{-1}$  followed by a endothermic peak due to melting at  $T_m = -3.62^\circ\text{C}$  with an enthalpy of  $115.52 \text{ Jg}^{-1}$ . During the first cooling rate no transitions were detected, so it is possible that the liquid remained in a supercooled state. During cycle II the same calorimetric behaviour as that obtained for cycle I was observed (not shown).

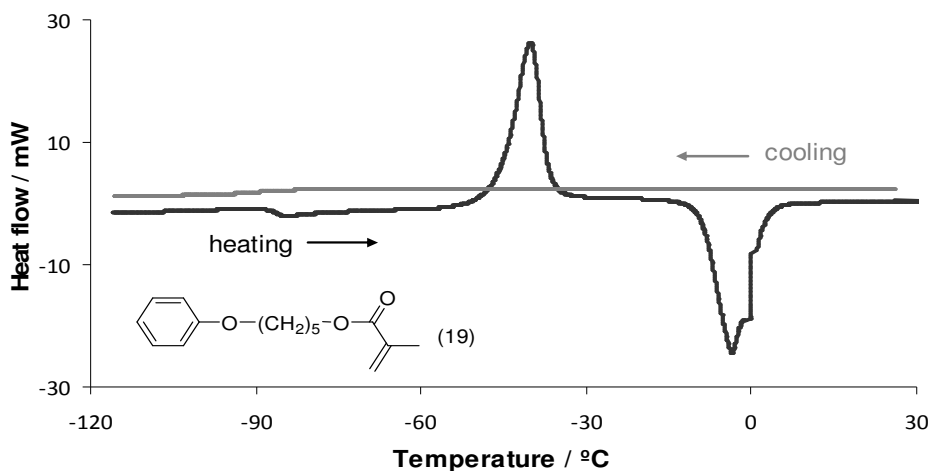


Figure 4.1 – DSC measurement obtained for monomer 19 during cycle I at  $10^{\circ}\text{C min}^{-1}$ .

During cycle I for liquid monomer 1 (figure 4.2) the thermogram shows an endothermic peak at  $18.86^{\circ}\text{C}$  with an enthalpy of  $108.97 \text{ Jg}^{-1}$  due to the melting of the crystalline form and on cooling rate no transitions were detected, thus the liquid could remain in a supercooled state. However during the cycle II the thermograms show endothermic transitions assigned to a glass transitions at  $T_g = -89.02^{\circ}\text{C}$  and melting temperature at  $T_m = 18.86^{\circ}\text{C}$  with an enthalpy of  $107.67 \text{ Jg}^{-1}$ . Cold crystallisation was also observed at  $T_{cc} = -55.13^{\circ}\text{C}$  with an enthalpy of  $-71.0 \text{ Jg}^{-1}$  (not shown). These thermal transitions are very similar to those observed in the thermogram collected for liquid monomer 19.

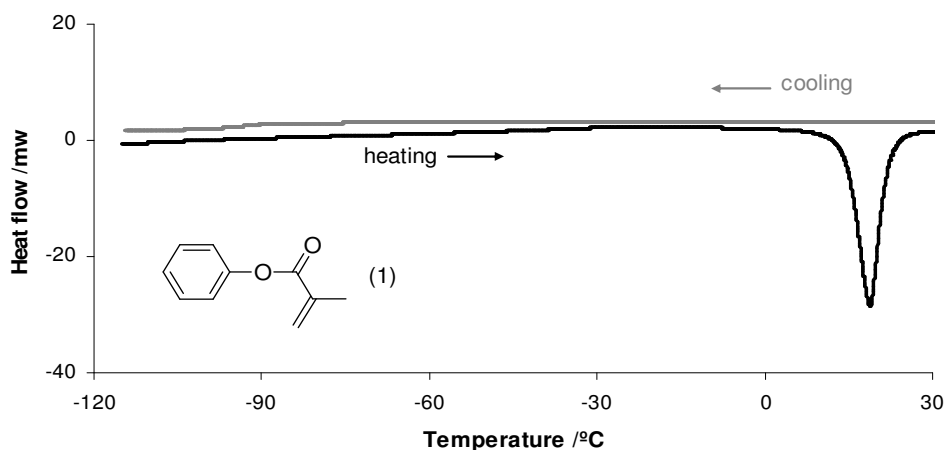


Figure 4.2 – DSC measurement obtained for monomer 1 during cycle I at  $10^{\circ}\text{C min}^{-1}$ .

The solid monomers, 7, 5, 22, 21 and 20 have a different thermal behaviour compared with the liquid monomers (19 and 1) described above. The thermograms for monomers 7, 5, 22, 21 in figures 4.3-4.7, respectively, show reversible systems that on heating give an endothermic peak characteristic of a melting transition and on cooling rate an exothermic peak of crystallisation are observed. The second heating and cooling rates (not shown) were characterised by the same thermal behaviour.

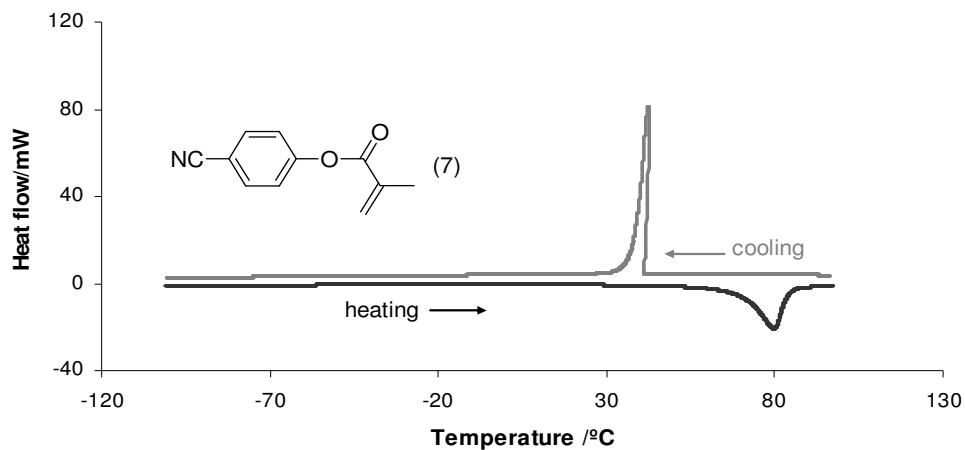


Figure 4.3 – DSC measurement obtained for monomer 7 during cycle I at 10°C min<sup>-1</sup>.

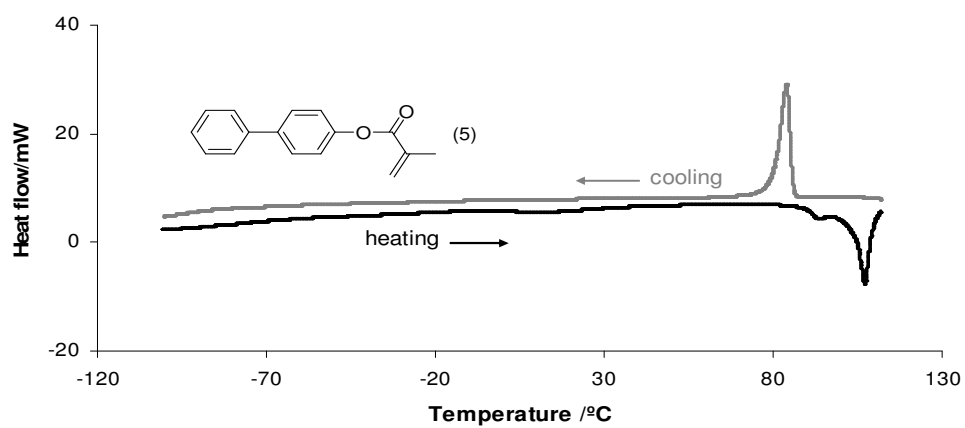


Figure 4.4 – DSC measurement obtained for monomer 5 during cycle I at 10°C min<sup>-1</sup>.

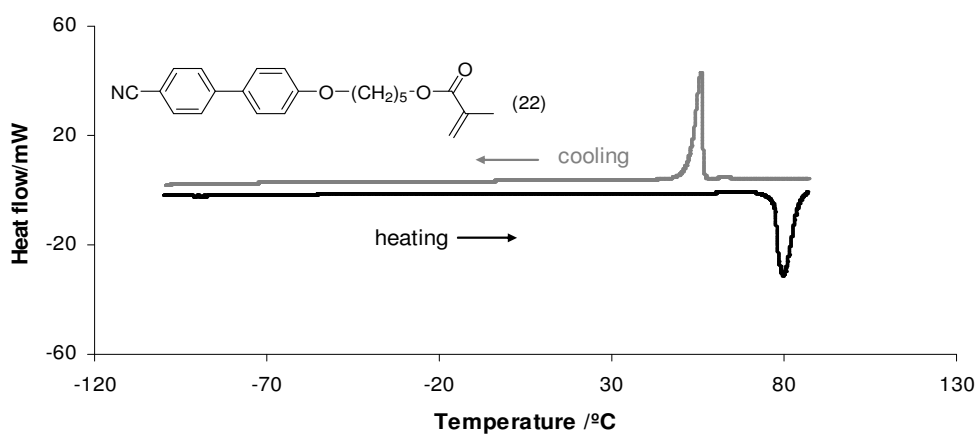


Figure 4.5 – DSC measurement obtained for monomer 22 during cycle I at 10°C min<sup>-1</sup>.

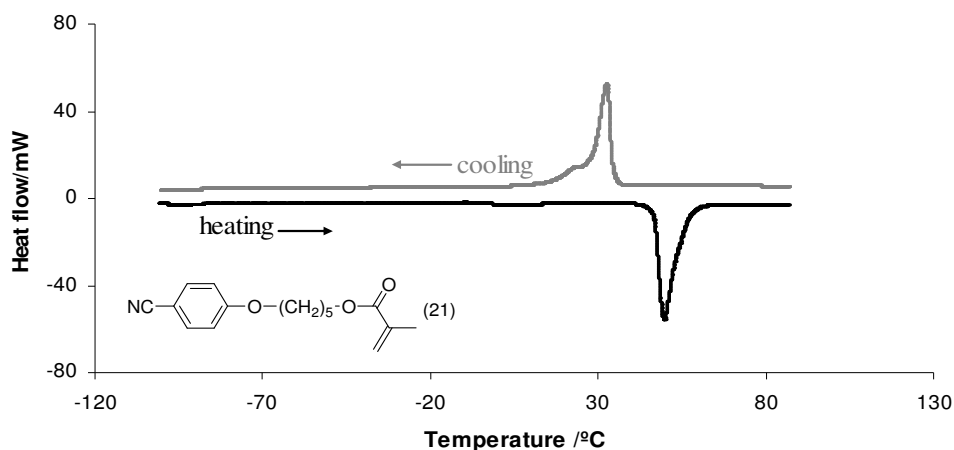


Figure 4.6 – DSC measurement obtained for monomer 21 during cycle I at  $10^{\circ}\text{C min}^{-1}$ .

The monomer 20 (figure 4.7) despite having the same thermal behaviour, this behaviour is not reversible. The thermogram of monomer 20 shows that the crystalline form melts and partially crystallises on cooling. During the first heating rate exhibited an endothermic peak due to a melting transition with  $\Delta H_m=57.84 \text{ Jg}^{-1}$  and during the cooling an exothermic peak due to melt-crystallisation but with  $\Delta H_{cr}= -18.65 \text{ Jg}^{-1}$ . During the second heating this crystalline solid formed melts with  $\Delta H_m=14.93\text{Jg}^{-1}$  and partially crystallises again on cooling but also with a lower value of  $\Delta H_{cr}= -2.86 \text{ Jg}^{-1}$ . The difference between the values of enthalpies associated with endothermic and exothermic transitions suggests that part of the material previously melted could remain in a supercooled state, degraded or polymerised and only a small fraction of the monomer crystallizes during cooling run. This possibility is supported by previous studies of DSC between 25 and  $200^{\circ}\text{C}$  (not shown) which indicate that a temperature of  $100^{\circ}\text{C}$  seems to be enough to initiate the polymerisation of the monomer.

All these monomers reveal a high tendency to have a crystalline form that melts during the heating run followed by melt-crystallisation during the cooling run. The only thermal event during the heating run was the melting transition that showed that until melting the material was in a crystalline phase.

The insertion of a spacer chain, in monomers 20, 21 and 22 decreased the melting temperatures, compared to the analogue monomers without the spacer chain, which make the later structures more rigid.

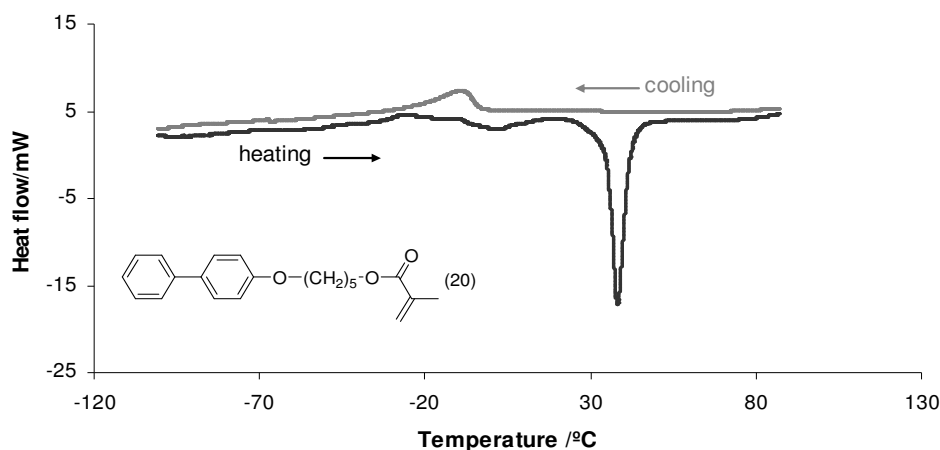


Figure 4.7 – DSC measurement obtained for monomer 20 during cycle I at  $10^{\circ}\text{C min}^{-1}$ .

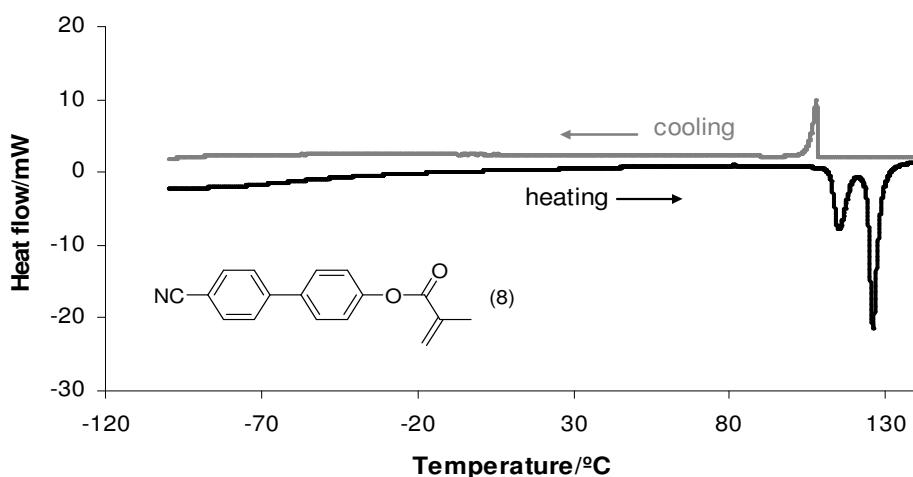


Figure 4.8 – DSC measurement obtained for monomer 8 during cycle I at  $10^{\circ}\text{C min}^{-1}$ .

For monomer 8 it can be seen in figure 4.8 that on the heating run there are two endothermic peaks at  $114.95$  and  $125.90^{\circ}\text{C}$  with enthalpies of  $29.09$  and  $60.40 \text{ J g}^{-1}$ , respectively. However on the cooling run only one exothermic peak emerges at  $107.72^{\circ}\text{C}$  with an enthalpy of  $-14.74 \text{ J g}^{-1}$ . During the second heating run (not shown) part of the amorphous material has a cold crystallisation at  $T_{cc} = 63.61^{\circ}\text{C}$  with an enthalpy of  $-10.43 \text{ J g}^{-1}$  followed by two endothermic transitions at  $109.60$  and  $123.95^{\circ}\text{C}$  with  $7.48$  and  $12.13 \text{ J g}^{-1}$ , respectively. On the second cooling run (not shown) no transitions were detected, so it is possible that liquid remained in a supercooled state or that it polymerised previously. This last possibility is supported by DSC studies between  $25$ - $200^{\circ}\text{C}$  (not shown). POM studies allow a better understanding of the thermal transitions, especially those involved in the thermal behaviour of monomer 8. Thus the data from DSC and POM indicate that crystalline material transitioned to a mesophase state which can be assigned to the first endothermic peak followed by a transition to an isotropic state assigned to the second endothermic peak. The peak at  $114.95^{\circ}\text{C}$  can be assigned to solid

to mesophase transition temperature ( $T_{SM}$ ) and at 125.90°C to mesophase to isotropic transition temperature ( $T_{MI}$ ).

**Table 4.1 - Thermal properties of monomers obtained by DSC during different cooling/heating cycles**

Monomer	Cycle	Heating run at 10°C min <sup>-1</sup>					Cooling run at 10°C min <sup>-1</sup>		
		glass transition	Cold-crystallisation	Melting		Melt-crystallisation	Glass transition		
		$T_g/^\circ\text{C}$	$T_{cc}/^\circ\text{C}$	$\Delta H_{cr}/\text{Jg}^{-1}$	$T_m/^\circ\text{C}$	$\Delta H_m/\text{Jg}^{-1}$	$T_c/^\circ\text{C}$	$\Delta H_{cr}/\text{Jg}^{-1}$	$T_g/^\circ\text{C}$
<b>19</b>	I	-86.01	-40.19	-97.45	-3.62	115.52	-	-	-
	II	-86.01	-39.83	-96.60	-3.58	114.80	-	-	-
<b>1</b>	I	-	-	-	18.86	108.97	-	-	-
	II	-89.02	-55.13	-71.00	18.86	107.67	-	-	-
<b>7</b>	I	-	-	-	81.53	56.03	44.28	91.92	-
	II	-	-	-	79.52	76.00	38.26	-90.85	-
<b>5</b>	I	-	-	-	-	-	83.99	-83.45	-
	II	-	-	-	106.04	71.35	82.72	-82.02	-
<b>8</b>	I	-	-	-	114.95 125.90	29.09 60.40	107.72	-14.74	-
	II	-	63.61	-10.43	109.60 123.95	7.48 12.13	-	-	-
<b>21</b>	I	-	-	-	49.80	115.70	32.53	-105.98	-
	II	-	-	-	49.68	111.52	31.28	-91.19	-
<b>20</b>	I	-	-	-	38.19	57.84	-9.24	-18.65	-
	II	-	-	-	16.27	26.48	-8.13	-2.87	-
<b>22</b>	I	-	-	-	79.77	85.21	55.90	-64.55	-
	II	-	-	-	78.14	69.36	53.71	-24.29	-



### 4.3 Polarised optical microscopy characterisation

The thermal properties of monomers were complemented with polarised optical microscopy (POM) studies. The polarised optical microscope equipped with a hot stage only allows the observation of transitions from 20 to 300°C and therefore for liquid monomers was not possible an analysis by POM with the same conditions used in DSC (-130 to 25°C). Optical observations allow the determination not only temperatures for each transition but also the texture acquired by the sample. Furthermore, polarised optical microscopy can evaluate the possibility of the existence of liquid crystalline phases. As mentioned before an isotropic phase placed between crossed polarizers does not allow polarised light to pass through and what is observed is simply a black uniform image, unlike what is observed for a birefringent phase (optical anisotropy). The values of the thermal properties determined by POM are summarised in table 4.2.

The texture for liquid monomers 19 and 1 which may be analysed in the optical microphotographs presented in figures 4.9 and 4.10, respectively, revealed an isotropic phase on heating and the cooling runs between 30 and 100°C and no birefringent phase was observed. The spheres that appear in the images are spacers of ITO cell.

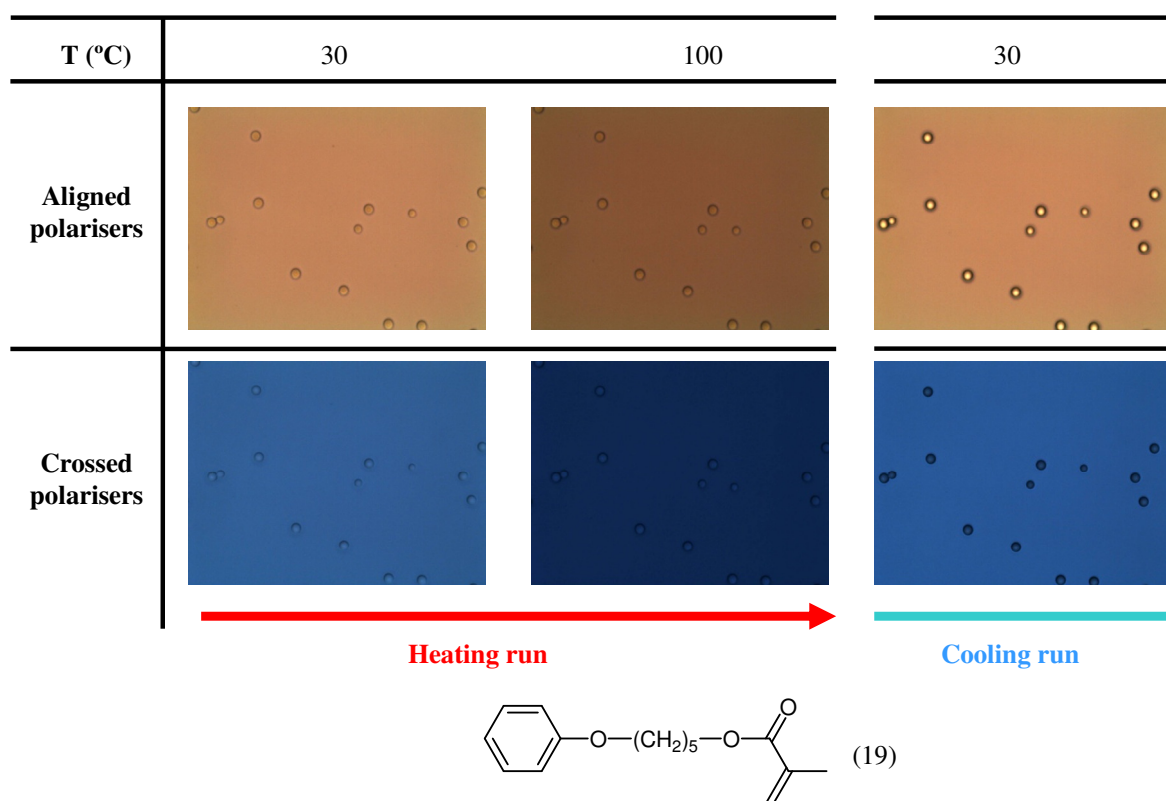
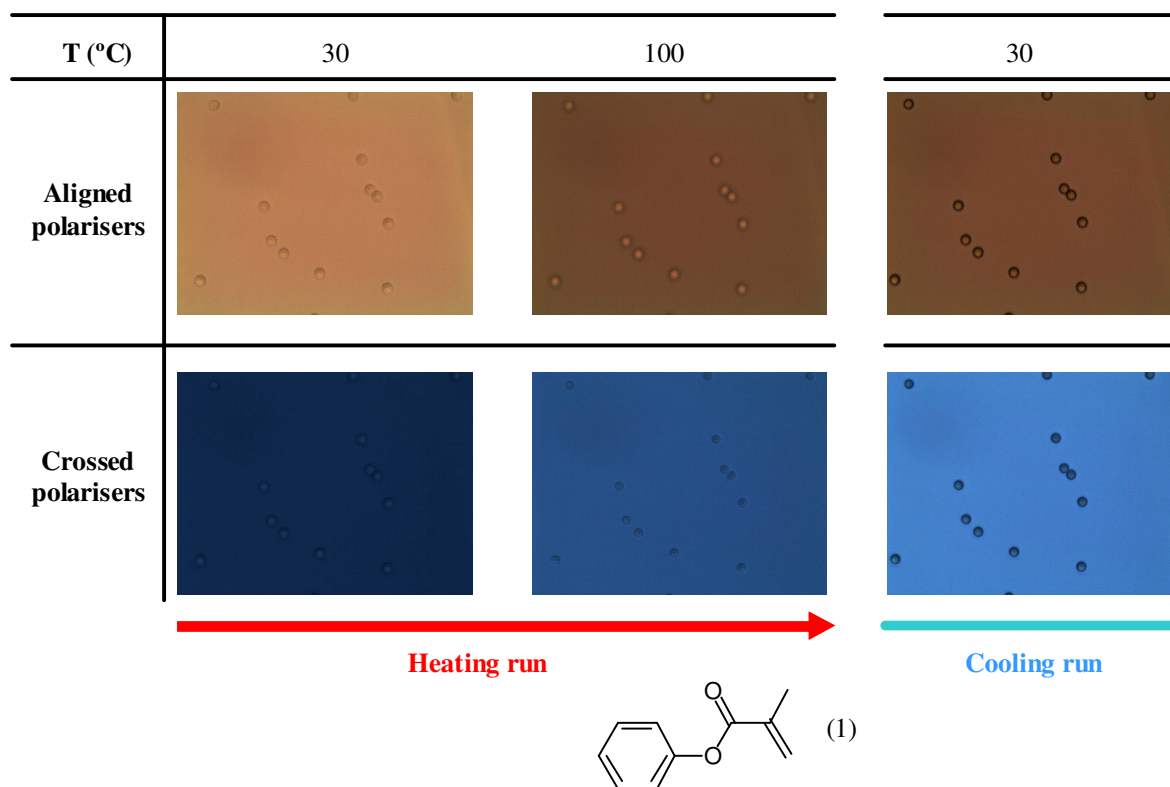


Figure 4.9 – Optical micrographs of monomer 19 at specific temperatures during the heating and cooling runs at 10°C min<sup>-1</sup>.



**Figure 4.10 – Optical micrographs of monomer 1 at specific temperature during the heating and cooling runs at  $10^{\circ}\text{C min}^{-1}$ .**

Optical microscopy pictures of monomers 7, 5, 22, 21 and 20 are present in figures 4.11-4.15 respectively. The analysis of these figures revealed a birefringent texture in the solid state. However, this property was lost with melting transition and the liquid state showed an optic isotropic structure that remained until the crystallisation temperature where again of the monomers acquire a birefringent texture.

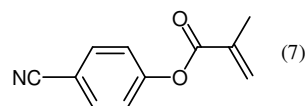
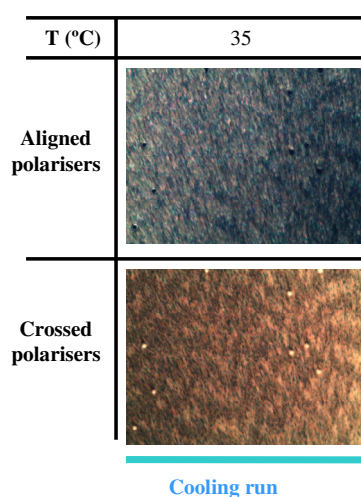
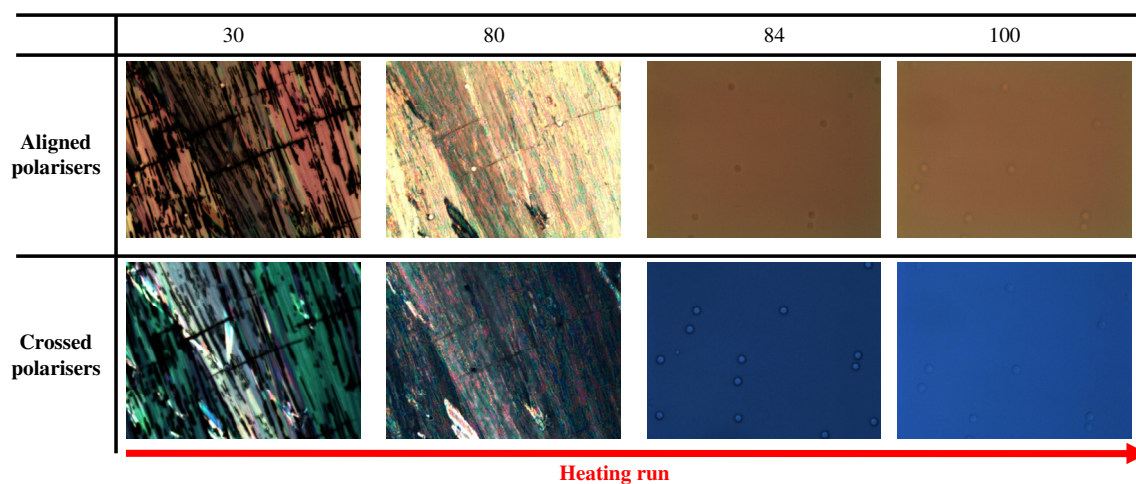


Figure 4.11 – Optical micrographs of monomer 7 at specific temperature during the heating and cooling run at 10°C min<sup>-1</sup>.

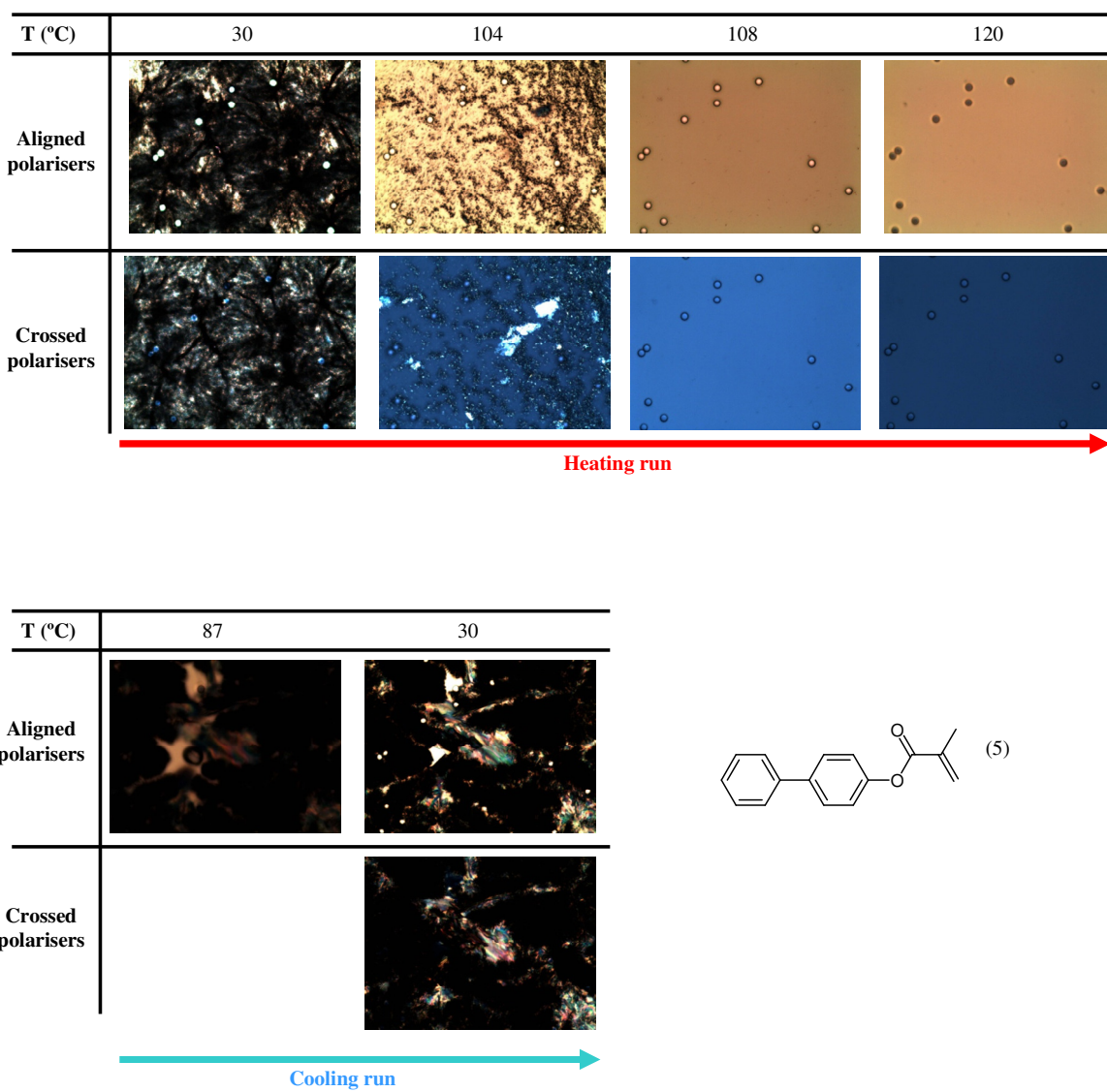
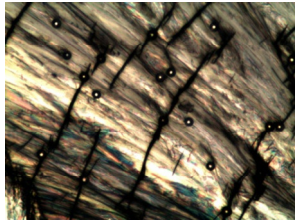
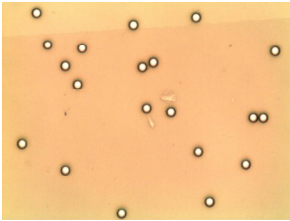
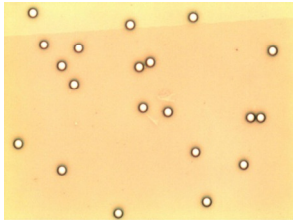
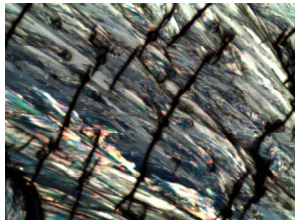
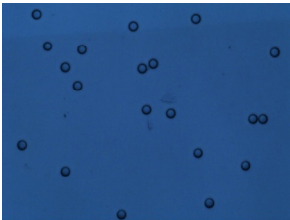


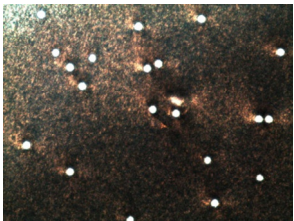
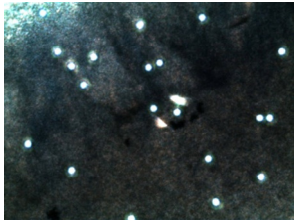



Figure 4.12 – Optical micrographs of monomer 5 at specific temperatures during the heating and cooling runs at  $10^{\circ}\text{C min}^{-1}$ .

T (°C)	30	78	100
Aligned polarisers			
Crossed polarisers			

Heating run 

T (°C)	63
Aligned polarisers	
Crossed polarisers	

Cooling run 

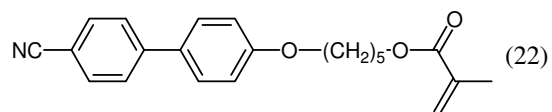


Figure 4.13 – Optical micrographs of monomer 22 at specific temperatures during the heating and cooling runs at  $10^{\circ}\text{C min}^{-1}$ .



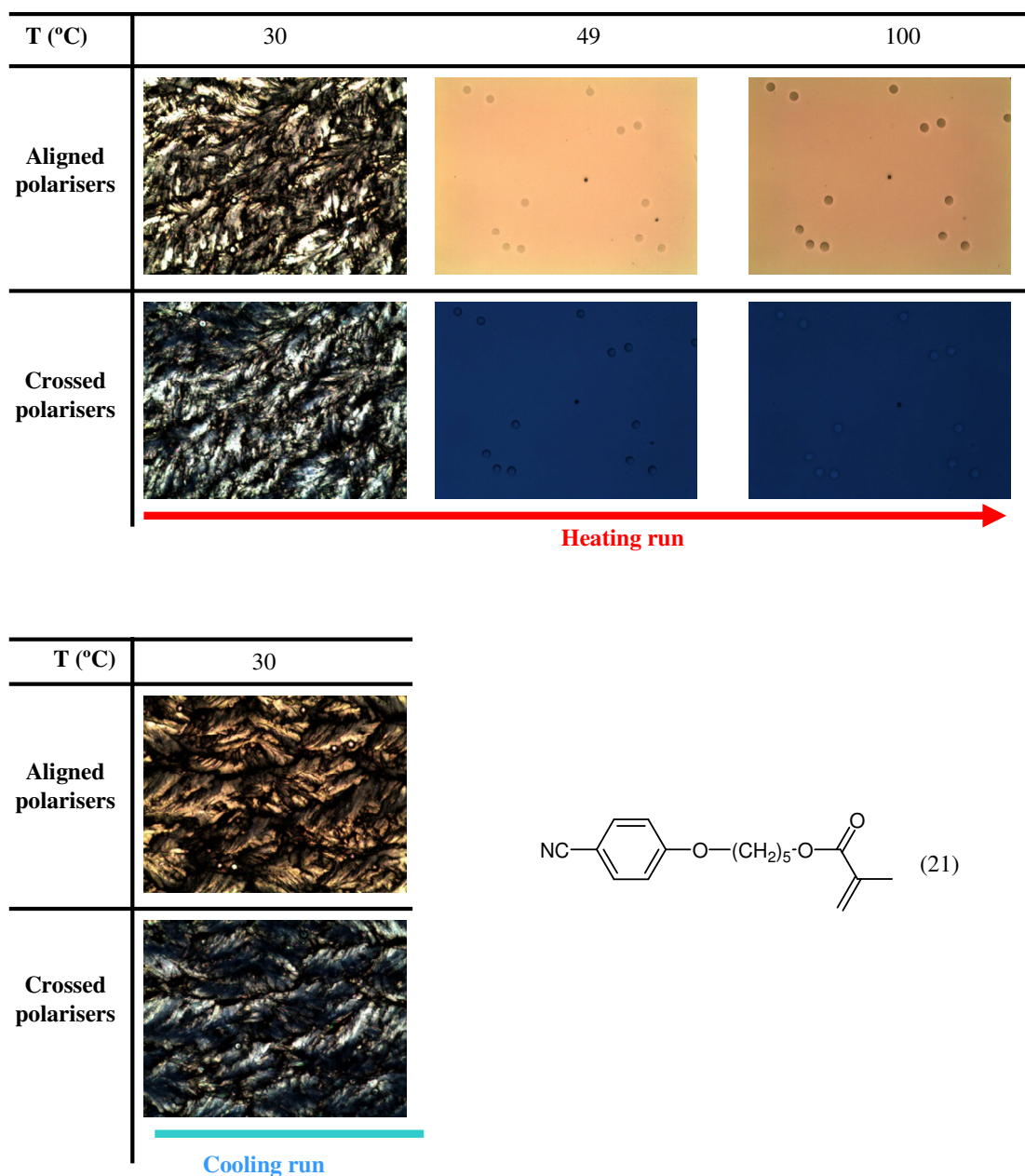
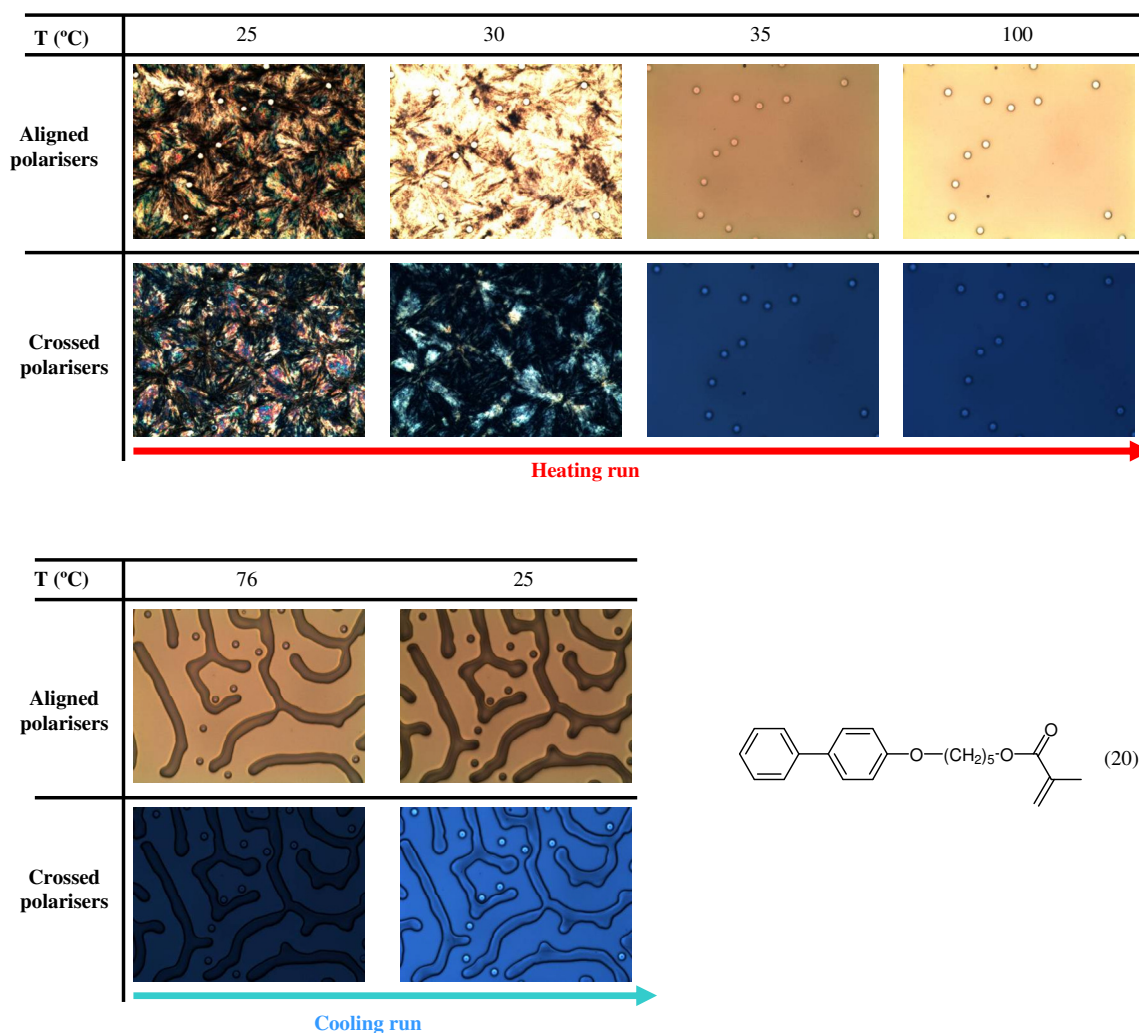
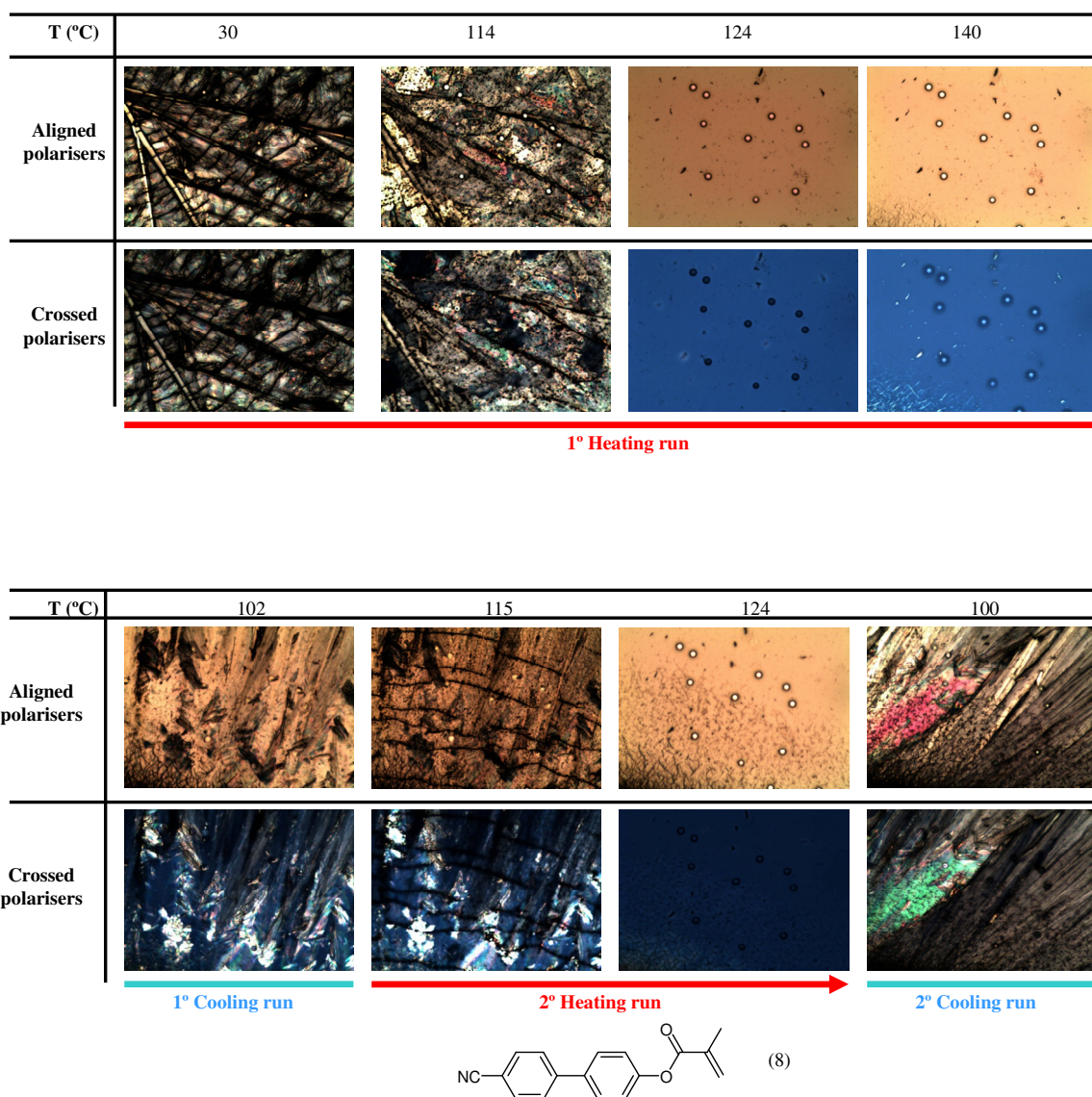


Figure 4.14 – Optical micrographs of monomer 21 at specific temperatures during the heating and cooling run at  $10^{\circ}\text{C min}^{-1}$ .



**Figure 4.15 – Optical micrographs of monomer 20 at specific temperatures during the heating and cooling runs at  $10^{\circ}\text{C min}^{-1}$ .**

As mentioned before, in DSC analysis monomer 8 showed a particular thermal behaviour with two endothermic transitions one after the other in the heating run. The results of combined POM and DSC studies allow a better understanding of the type of transitions involved in all the monomers and in particular in monomer 8. The optical microscopy picture presented in figure 4.16 shows in the heating run that the birefringent solid material first transition to a mesophase at  $114^{\circ}\text{C}$  ( $T_{SM}$ ). This mesophase was assigned based on the observation of birefringence and fluidity. However this phase with the increase of temperature transitioned to an isotropic phase at  $124^{\circ}\text{C}$  ( $T_{MI}$ ). During the cooling run, at  $102^{\circ}\text{C}$  the isotropic phase crystallizes out, so that in the second heating run transition to an isotropic phase at  $124^{\circ}\text{C}$ . This isotropic phase crystallizes at  $100^{\circ}\text{C}$  into a birefringent material. From POM studies it was possible to observe the onset of polymerisation at  $140^{\circ}\text{C}$  which is in agreement with the DSC analysis.



**Figure 4.16 - Optical micrographs of monomer 8 at specific temperatures during the first and second heating at 10°C min<sup>-1</sup>.**

The melting temperature determined by DSC for all monomers analysed seems to be corroborated by the melting temperature determined by capillarity. However, the transition temperatures determined by POM show small differences. Although the programme for the heating and the cooling runs was the same (10°C min<sup>-1</sup>) it was difficult to keep exactly the same ramp throughout the POM analysis. During POM measurements the runs of heating and cooling were stopped momentarily to take optical micrographs.



Table 4.2 – Thermal properties of monomers obtained by POM during heating/cooling runs.

Monomer	Initial optical property	Heating run at 10°C min <sup>-1</sup>		Cooling run at 10°C min <sup>-1</sup>	
		Melting		Melt-crystallisation	
		T/°C	Optical property	T <sub>c</sub> /°C	Optical property
19	Isotropic	-	-	-	-
1	Isotropic	-	-	-	-
7	Birefringent	84(T <sub>m</sub> )	Isotropic	35	Birefringent
5	Birefringent	108(T <sub>m</sub> )	Isotropic	87	Birefringent
22	Birefringent	78(T <sub>m</sub> )	Isotropic	63	Birefringent
21	Birefringent	49(T <sub>m</sub> )	Isotropic	30	Birefringent
20	Birefringent	35(T <sub>m</sub> )	Isotropic	-	-
8	Birefringent	114 (T <sub>SM</sub> )	Birefringent	102	Birefringent
		124 (T <sub>MI</sub> )	Isotropic		



## 5 Structural and electro-optical characterisation

### 5.1 Outline

The structural characterisation of polymers prepared with the monomers previously synthesised (chapter III, figure 3.6) and the electro-optical characterisation of the PDLCs prepared with the same monomers will be analysed. This studied was based on the structural analysis by the evaluation of molecular weights by gel permeation chromatography (GPC), structural characterisation by scanning electronic microscopy (SEM) and determination of the electro-optical properties of the PDLC films by measuring the voltage dependence on the transmitted light.

### 5.2 Molecular weights and polymer structures

The molecular weight of the polymer matrix plays an important role in the morphologies of the matrix and therefore in the liquid crystal domain size and shape. If the polymer chain increases with an increase in molecular weight leading to a higher network density, the size of liquid crystal domains should decrease. This promotes the interaction between polymer and liquid crystal molecules and the opposite is true for smaller chains. As previously mentioned, the size and the shapes of liquid crystal domains are correlated with the anchoring strength on the interface between the liquid crystal molecules and polymer molecules. The anchoring strength determines the electric field needed to achieve the transparent state in the PDLC. Generally, the strength of the field needed is inversely proportional to the liquid crystal domain size. A number of factors influence the electro-optical response of PDLCs and the investigation of these parameters allows control of the performance of these devices. So, it is important understand and establish the effect of the molecular structure of the polymerisable monomers on the molecular weight of the polymer and the effect of molecular weight on the morphology and electro-optical properties.

#### 5.2.1 Characterisation of molecular weights

Gel permeation chromatography (GPC) is a liquid chromatography technique that separates molecules according to sizes and not according to chemical affinities toward the porous substrate<sup>40</sup>. Large polymer molecules with higher molecular weights can move into pores but since there are only a few large pores available to them, they reside, on average, less time in pores than smaller molecules. Therefore, larger molecules are eluted first. On the other hand, smaller polymer molecules with lower molecular weights can fit into the small pores and penetrate into a larger number of pores. So, the

elution time increases with decreasing molecular size<sup>41</sup>. This correlation between elution time and molecular weight was observed for the polymer analysed. The values of average molecular weights ( $M_n$  and  $M_w$ ) and polydispersity index (PDI) for a mixture of monomer/glycidyl methacrylate (50/50 w/w) after thermal and photochemical polymerisation are summarised in Tables 5.1 and 5.2, respectively. It was possible to observe differences between polymer matrixes prepared by thermal polymerisation and prepared by photochemical polymerisation. For the thermal polymerisation, the polymers have a number average molecular weight,  $M_n$ , around  $e^8$  or  $e^{12}$ , and for photochemical polymerisation polydispersities are higher and  $M_n$  is around  $e^{12}$ . Generally, the polymers with lower molecular weight possess a lower polydispersion, indicating that there are chains with more uniform lengths (size), but no correlation is observed with the molecular structure of the respective monomers.

**Table 5.1 – Values of average molecular weights ( $M_n$  and  $M_w$ ) and polydispersity index (PDI) for polymers prepared with a mixture of monomer/glycidyl methacrylate (50/50 w/w) by thermal polymerisation.**

Monomers used in co-polymerisation	PDI	Peak/min	$\ln (M_w/\text{gmol}^{-1})$	$\ln (M_n/\text{gmol}^{-1})$
8	1.91	13.86	12.80	12.15
22	1.40	14.97	12.51	12.16
19	1.44	13.57	13.05	12.69
5	1.04	20.51	8.13	8.09
7	1.04	20.81	8.02	7.99
21	1.04	20.47	8.16	8.12
20	1.05	20.14	8.22	8.17

**Table 5.2 – Values of average molecular weights ( $M_n$  and  $M_w$ ) and polydispersity index (PD) for polymers prepared with a mixture of monomer/glycidyl methacrylate (50/50 w/w) by photochemical polymerisation.**

Monomers used in co-polymerisation	PDI	Peak/min	$\ln (M_w/\text{gmol}^{-1})$	$\ln (M_n/\text{gmol}^{-1})$
8	1.51	14.28	12.80	12.39
22	1.47	14.68	12.36	11.98
19	1.35	15.06	12.04	11.74
5	1.24	15.78	11.67	11.45
7	1.08	14.37	12.30	12.23
21	1.38	15.63	11.72	11.39
20	1.36	22.36	6.99	6.68

### 5.2.2 Microstructure of the polymer matrix

The microscopic images of the microstructure of the polymeric matrix were evaluated by scanning electronic microscopy (SEM). Some microscopic images can be assigned to the swiss cheese (figures 5.3, 5.4 (a) and 5.5) or polymer ball (figures 5.1 (a), 5.7 (a) and 5.8) types of morphology, but for some samples these morphologies are not uniform across the sample. For other samples it was not possible to identify any morphology as is show in figures 5.1 (b), 5.2, 5.4 (b), 5.6 and 5.7 (b). These results can suggest that the chemical affinity of polymerisable monomers with liquid crystal molecules due to their similarities in chemical structure produces a smaller phase separation and therefore the E7 liquid crystal molecules would be highly embedded in the matrix. It is also possible to observe that it cannot be established a correlation between the molecular structure of the polymerisable monomers and polymerisation conditions. Although the samples for analysis by GPC and SEM were not prepared with the same conditions, it is not possible to establish a correlation between the molecular weight of polymers and the microstructure of the polymer matrix.

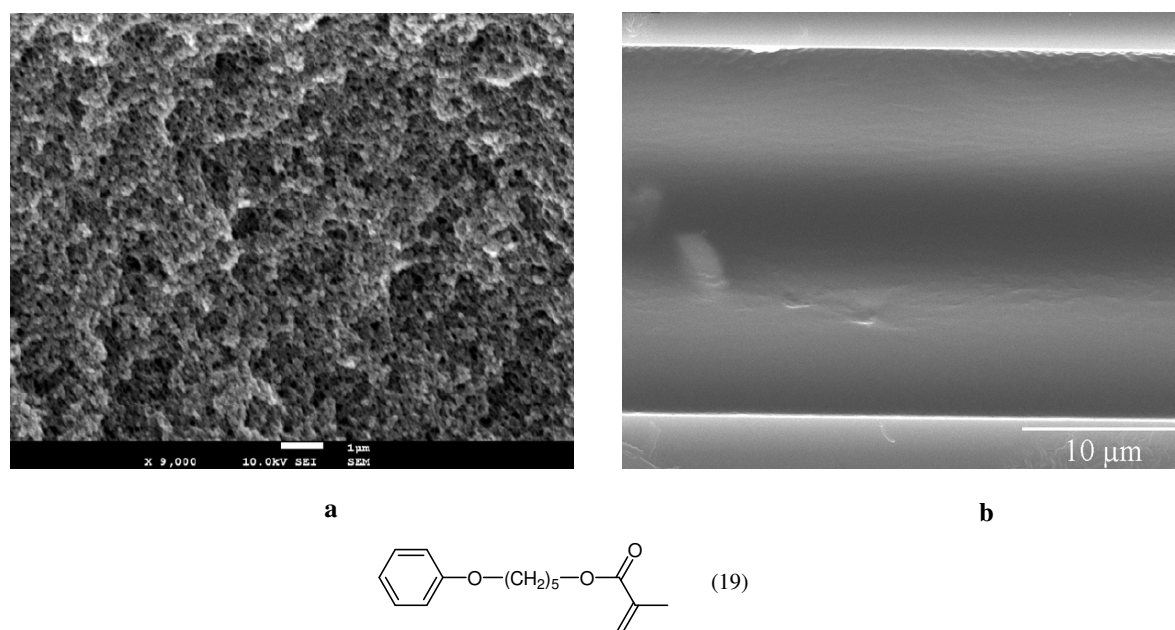


**Figure 5.1 – SEM micrographs for the microstructure of the polymer matrix prepared by (a) thermal and (b) photochemical polymerisation of monomer 19.**

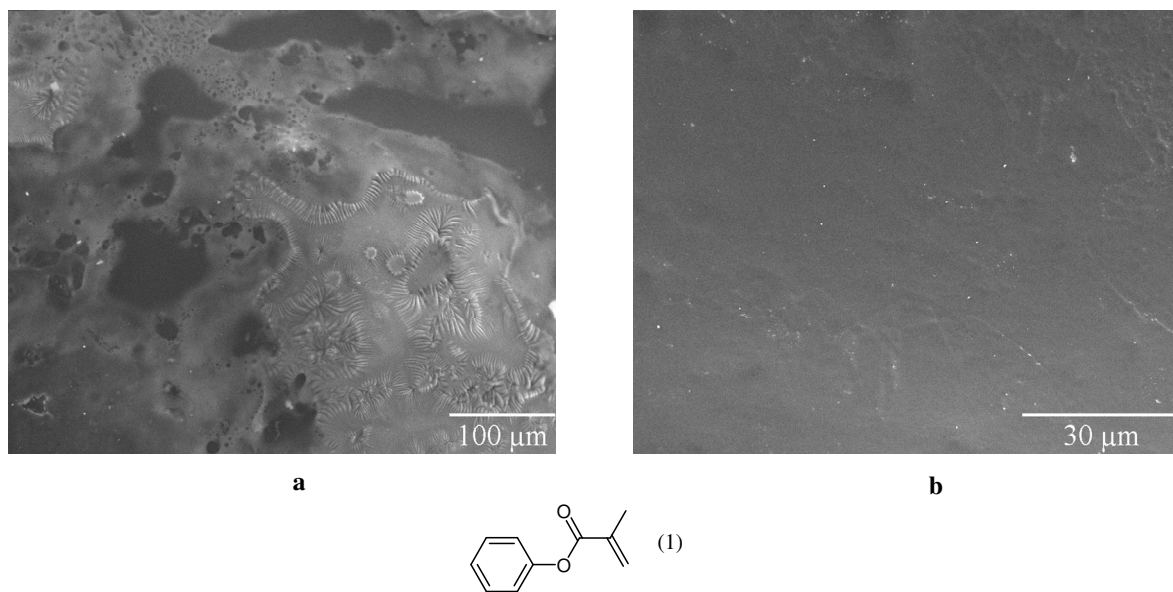


Figure 5.2 – SEM micrographs for the microstructure of the polymer matrix prepared by (a) thermal and (b) photochemical polymerisation of monomer 1.

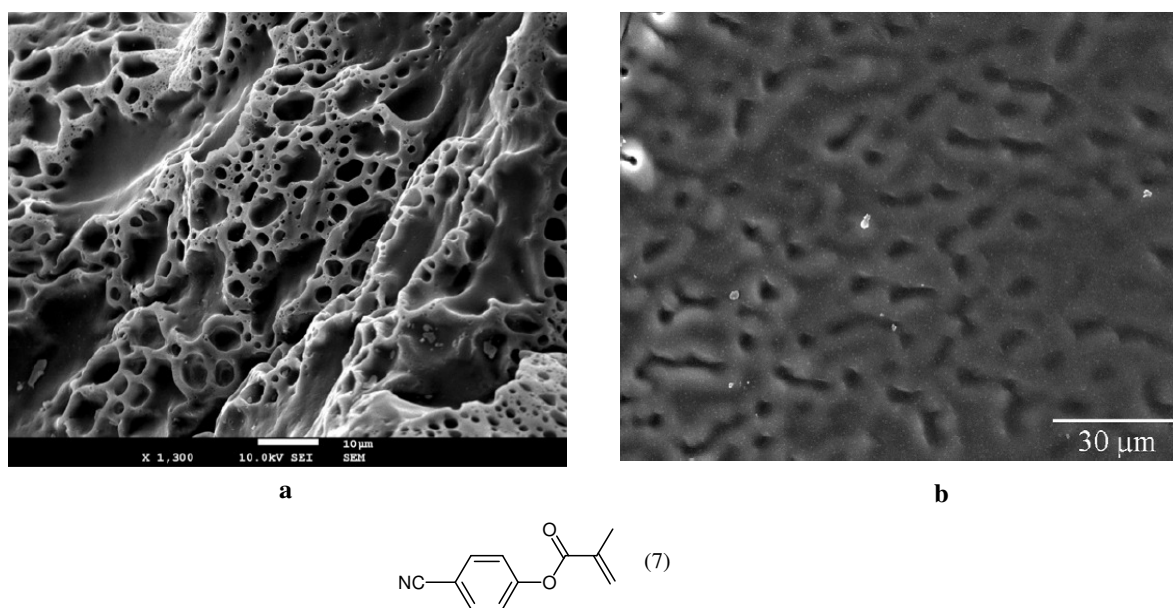


Figure 5.3 – SEM micrographs for the microstructure of the polymer matrix prepared by (a) thermal and (b) photochemical polymerisation of monomer 7.

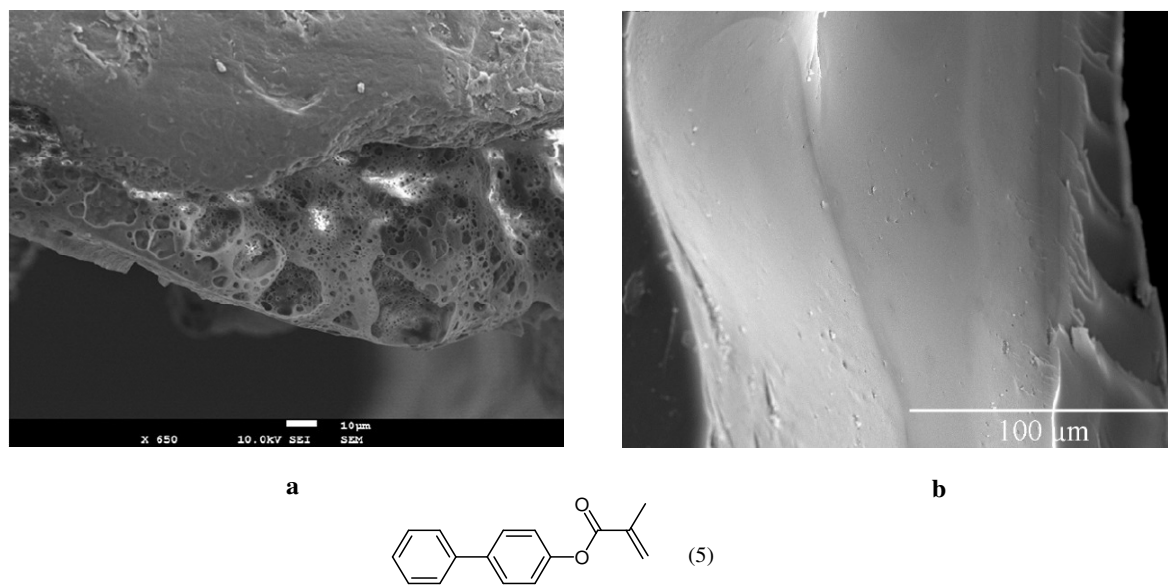


Figure 5.4 – SEM micrographs for the microstructure of the polymer matrix prepared by (a) thermal and (b) photochemical polymerisation of monomer 5.

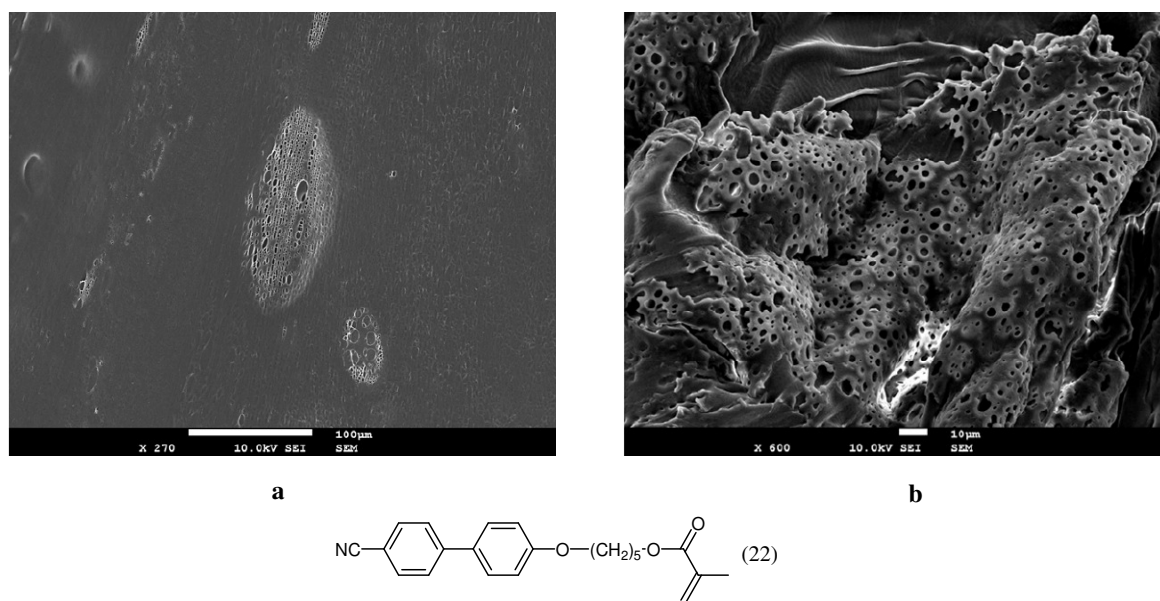


Figure 5.5 – SEM micrographs for the microstructure of the polymer matrix prepared by (a) thermal and (b) photochemical polymerisation of monomer 22.

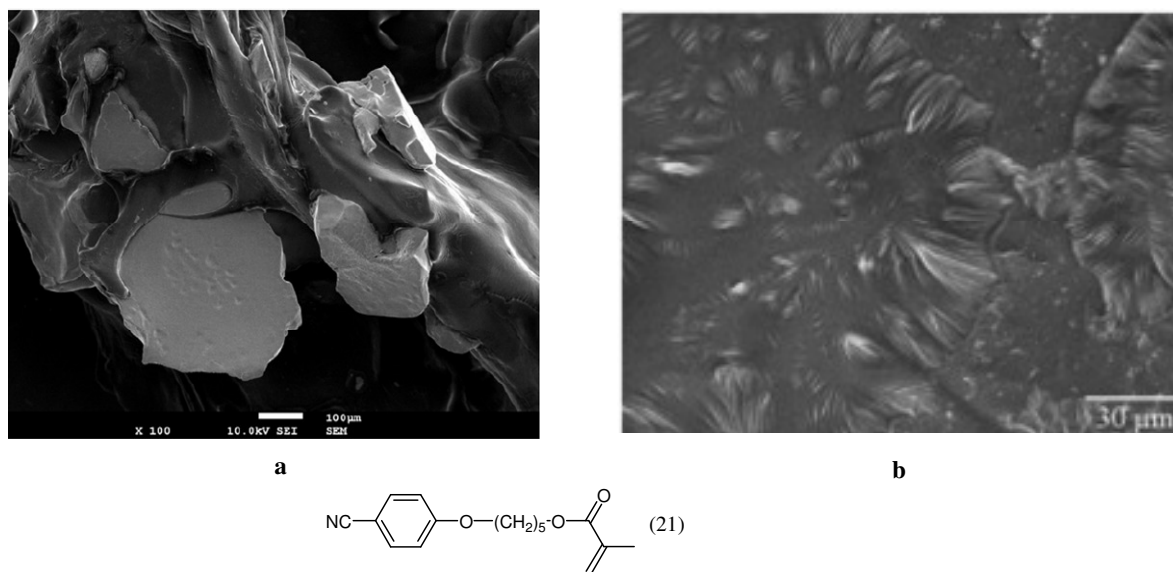


Figure 5.6 – SEM micrograph for the microstructure of the polymer matrix prepared by (a) thermal and (b) photochemical polymerisation of monomer 21.

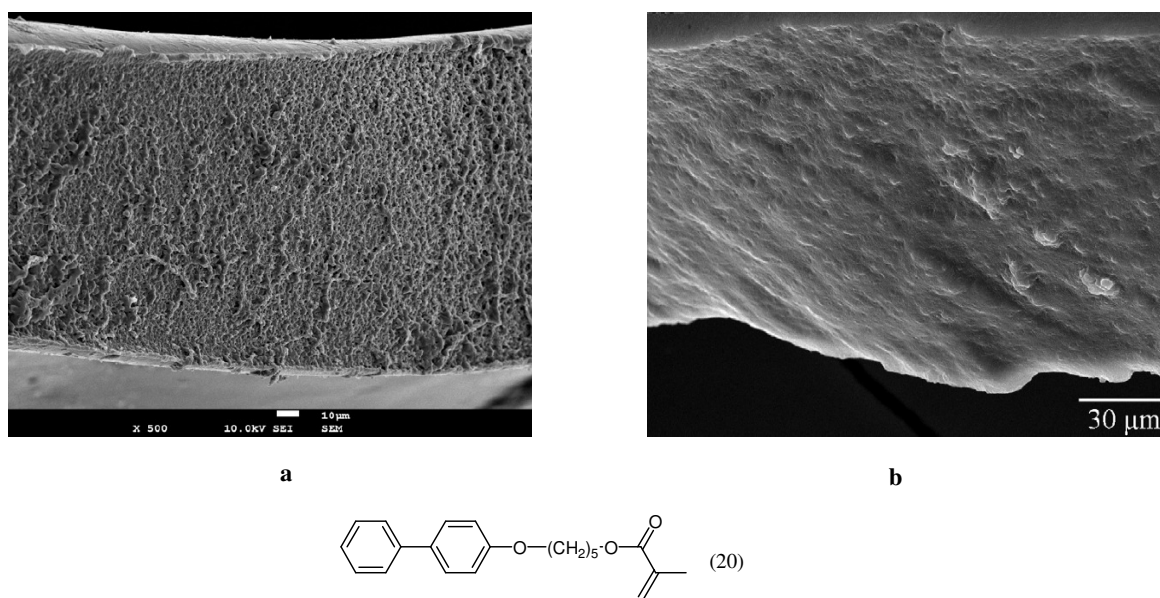


Figure 5.7 – SEM micrograph for the microstructure of the polymer matrix prepared by (a) thermal and (b) photochemical polymerisation of monomer 20.



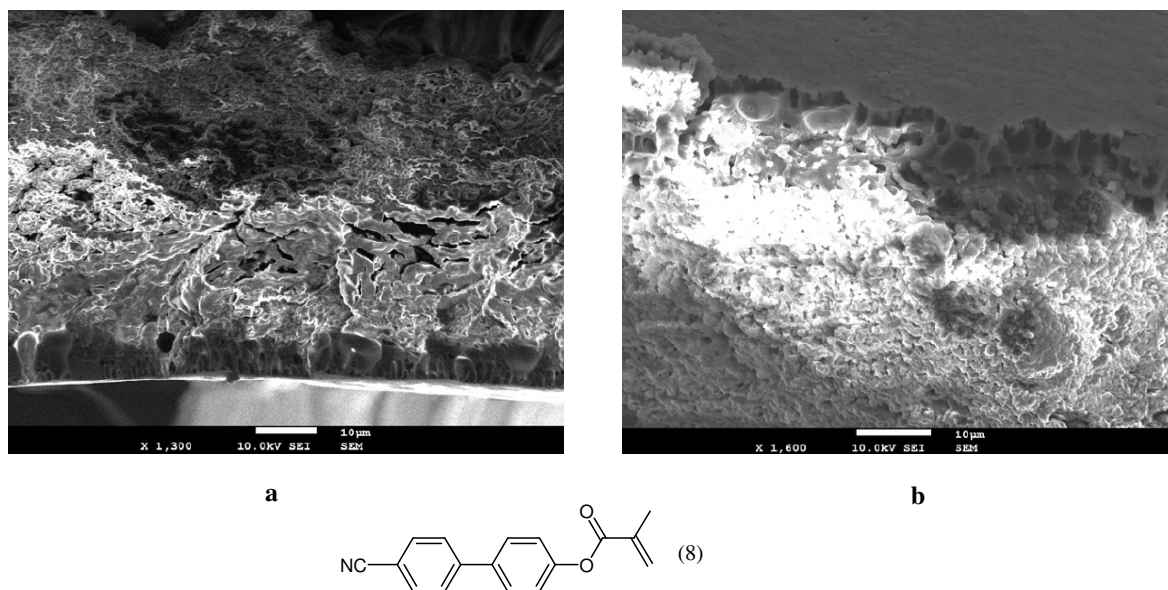


Figure 5.8 – SEM micrograph for the microstructure of the polymer matrix prepared by (a) thermal and (b) photochemical polymerisation of monomer 8.

### 5.2.3 Electro-optical characterisation

The PDLCs prepared with the monomers synthesised show a poor electro-optical response (figure 5.9). In most of the studies the PDLC cells show a good opacity after polymerisation with a transmittance of the initial opaque state,  $T_{\text{OFF}} \approx 0\%$ . However, the electro-optical study did not reveal a significant difference on the transmission of the sample with the application of an electric field up to 400V ( $20\text{V } \mu\text{m}^{-1}$ ) the maximum transmittance,  $T_{\text{MAX}}$  being less than 4%. The reason for this non-ideal behaviour is unclear however it is possible to suggest explanations.

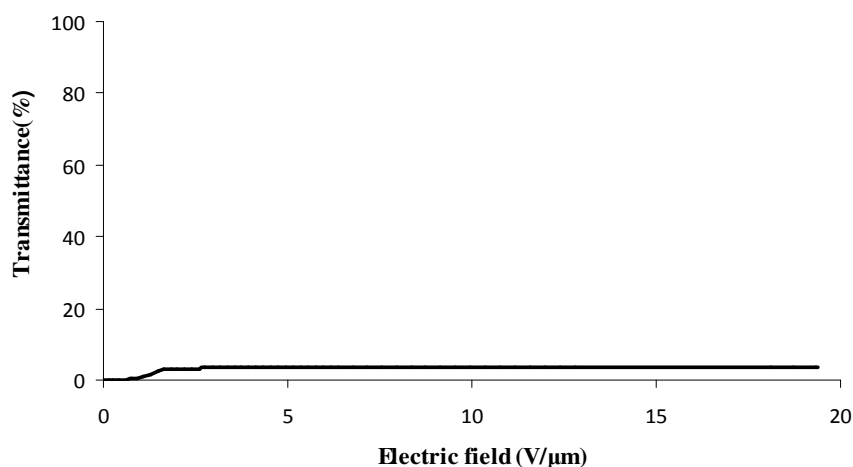


Figure 5.9 – General electro-optical response for PDLC films prepared by the PIPS method with the monomers synthesised + E7 in a ratio of 30/70 (w/w).

As mentioned before, the electro-optical properties of PDLC films depend on numerous parameters, namely, the structure and the molecular weight of the polymeric matrix (size and shape of the liquid crystal domains). These factors control the dynamics between alignment and random distribution when the electric field is applied and after removal of the electric field, respectively. These dynamics are very much dependent on anchoring force. This force is related to the interactions between the liquid crystal molecules and the polymeric matrix at the interface of LC domains and polymer matrix. The electro-optical results for PDLC films studied in this work suggested that a higher molecular affinity between the polymeric matrix and the liquid crystal could increase the anchoring effect.

The similar molecular structure between the molecules of monomer and the LC could have led to a higher affinity between molecules of polymer and molecules of liquid crystal in the interfaces matrix–LC domains. In this way the electric field applied could not overcome the interactions as the interface and the PDLC remained in an opaque state. So, if the liquid crystal molecules do not align themselves along the electric field the PDLC films appear opaque. The higher affinity between molecular structure of polymer matrix and LC molecules caused an increase in anchoring strength, i.e. it hindered the alignment of the liquid crystal molecule and could be the cause of the low electro-optical response of PDLC films.

In conclusion, the chemical affinity between the polymerisable monomers and the liquid crystal molecules can provide better affinity between the two which creates a more homogeneous mixture with a consequent phase separation in which the liquid crystal is uniformly dispersed in the polymer matrix. However, this affinity could be higher enough to increase the anchoring effect not allowing a good electro-optical response.

## 6 Conclusions

A series of new monomers with structurally diverse functionalisation was successfully synthesised under microwave irradiation. These results were compared with those obtained following classical methods. The comparison of these methodologies clearly indicates the considerable reduction in time and the amount of solvent used in the reactions under microwave irradiation. Therefore, two of the advantages, the reduction in time and solvents obtained by the use of microwave irradiation are demonstrated. Beyond that, the majority of monomers were synthesised in one step and in some cases in two steps that provided a simple and effective method of synthesis. The GPC analysis of copolymers (monomers synthesised and glycidyl methacrylate) revealed that it is not possible to establish a correlation between the molecular structure of the polymerisable monomers and the molecular weight of polymers. The microstructure of the polymer matrix was evaluated by SEM. From these studies, was also not possible to establish the effect of molecular structure and molecular weight of respectively monomers. Nevertheless, the absence of a typical morphology on most microscopic images seems to indicate that the liquid crystal remains highly impregnated in the polymer matrix thus their micro-domains can not be visualised. The phase transformations of the monomers were investigated by DSC and complemented by POM. In general, the thermal behaviour seems to be that of a reversible system and the monomers show a high tendency to melting followed by a melt-crystallisation. The spacer chain in the molecular structure of the monomers decreases the melting temperature in comparison with the respective monomers without this chain. The POM analyses confirmed the transition determined by DSC and allowed an observation of the texture acquired by the sample. The analysis of solid monomers showed a birefringent texture in the solid state that where lost in the melting transition where an isotropic phase is acquired. However, monomer 8 revealed a different thermal behaviour with a mesophase between 114-124°C. On the other hand, the liquid monomers showed a isotropic properties in all temperature ranges.

The electro-optical responses of all PDLCs prepared by the PIPS method with the composites of monomers synthesised–E7 exhibit a lower transmittance upon the application of an electric field. This behaviour can be interpreted as the result of a higher anchoring effect. Thus, even the application of a higher electric field could not orient the E7 molecules along the direction of the electric field and they scattered strongly the incident light. The similarity in molecular structure between so that better homogenisation of the mixture can be achieved and a uniform phase separation but it should not be too high to avoid a higher anchoring effect which resulted in a low electro-optical response of the PDLCs.



## 7 Bibliography

1. Collings, P. J.; Hird, M., Introduction To Liquid Crystal. Taylor and Francis: London, 2004.
2. Bisoyi, H. K.; Sandeep, K., Liquid-crystal nanoscience: an emerging avenue of soft self-assembly. *Chem. Soc. Rev* **2011**, 40, 306-319.
3. Collings, P. J., Liquid Crystals:Nature´s Delicate Phase of Matter. 2 ed.; Princeton University Press: New Jersey, 2002.
4. Rizvi, Z. T., Liquid crystalline Biopolymers: A New Arena for Liquid Crystal Research. *J. Mol. Liq.* **2002**, 1, 43-53.
5. Van Doren, H. A.; Smits, E.; Pestman, J. M.; Engberts, J. B. F. N.; Kellogg, R. M., Mesogenic sugars. From aldoses to liquid crystals and surfactants. *Chem. Soc. Rev.* **2000**, 29, 183-199.
6. Martins, A. F., Os cristais líquidos. Fundação Clouste Gulbenkian-Colóquio/Ciências: Lisboa, 1991.
7. Bedjaoui, L.; Gogibus, N.; Ewen, B.; Pakula, T.; Coqueret, X.; Benmouna, M.; Maschke, U., Preferential Solvation of the eutectic mixture of liquid crystal E7 in a polysiloxane. *Polymer* **2004**, 45, 6555-6560.
8. Bradbury, S.; Abramwitz, M.; Davidson, M. W., Microscopy Configuration. <http://www.olympusmicro.com/primer/techniques/polarized/configuration.html> (November 2011)
9. Nomura, H.; Suzuki, S.; Atarashi, Y., Electrooptical Properties of Polymer Films Containing Nematic Liquid Crystal Microdroplets. *Jpn. J. Appl. Phys.* **1990**, 29, 522-528.
10. Almeida, P. L. M. M. Estudo e Optimização de um novo dispositivo electro-optico tipo PDLC. PhD Thesis, Faculdade de Ciências e Tecnologia, Universidade Nova de Lisboa, Lisboa, 2001.
11. Senyuk, B., Liquid crystals: a simple view on a complex matter. <http://dept.kent.edu/spie/liquidcrystals/> (November,2011)
12. Brás, A., R., E.; Henriques, S.; Casimiro, T.; Aguiar-Ricardo, A.; Sotomayor, J.; Caldeira, J.; Santos, C.; Dionísio, M., Characterization of a Nematic Mixture by Reversed-Phase HPLC and UV Spectroscopy: Application to Phase Behavior Studies in Liquid Crystal-CO<sub>2</sub> Systems. *Liq. Cryst.* **2007**, 34, 591-597.
13. Benkhald, L.; Coqueret, X.; Traisnel, A.; Maschke, U.; Mechernene, L.; Benmouna, M., A Comparative Study of UV and EB-Cured PDLC Films via Electro-Optical Properties. *Mol.Cryst.liq.Cryst.* **2004**, 412, 477/[2087]-483/[2093].
14. Drazaic, P. S., Liquid Crystal Dispersions World Scientific Publishing: Singapore, 1995.
15. Park, S.; Hong, W. J., Polymer dispersed liquid crystal film for variable-transparency glazing. *Thin Solid Films* **2009**, 517, 3183-3186.
16. Devdatt, L. K.; Nikolaos, A. P., Method of Determination of Initiator Efficiency: Application to UV Polymerizations Using 2,2-Dimethoxy-2-phenylacetophenone. *Macromolecules* **1994**, 27, 733-738.
17. Ates, S.; Aydogan, B.; Torun, L.; Yagci, Y., Synthesis and characterization of triptycene type cross-linker and its use in photoinduced curing applications. *Polymer* **2010**, 51, 825-831.
18. Li, W.; Cao, Y.; Kashima, M.; Kong, L.; Yang, H., Control of the Microstructure of Polymer Network and Effects of the Structures of Polymerizable Monomers On the Electro-optical properties of UV- Cured Polymer Dispersed Liquid Crystal Films. *J. Polym. Sci., Part B: Polym. Phys.* **2008**, 46, 1369-1375.
19. Vaz, N. A.; Montgomery, G. P., Refractive indices of polymer-dispersed liquid crystal film materials: Epoxy based systems. *J. Appl. Phys.* **1987**, 62, 3161-3172.
20. Bulgakova, S. A.; Mashin, A. I.; Kazantseva, I. A.; Kashtanov, D. E.; Jones, M. M.; Tsepkov, G. S.; Korobkov, A. V.; Nezhdanov, A. V., Influence of the Composition of the Polymer Matrix on the Electrooptical Properties of Films with a Dispersed Liquid Crystal. *Russ. J. Appl. Chem.* **2008**, 81 1446-1451

21. Amundson, K.; Blaaderen, A., V.; Wiltzius, P., Morphology and electro-optical properties of polymer-dispersed liquid crystal films *Am. Phys. Soc.* **1997**, 55, 1646-1654.
22. Han, W. J., Morphological Studies of Polymer Dispersed Liquid Crystal Materials. *Korean J.Phys.Soc.* **2006**, 49, 563-568.
23. Yokoyama, H., Surface Anchoring of Nematic Liquid Crystals. *Mol. Cryst. liq. Cryst.* **1988**, 165, 265-316.
24. Andy, F. Y. G.; Tsung, C. K.; Mo, H. L., Polymer Dispersed Liquid crystal Films with memory characteristics. *J. Appl.Phys.* **1992**, 31, 3366-3369.
25. Rumiko, Y.; Susumu, S., Highly transparent memory states by phase transition with a field in polymer dispersed liquid crystal films. *J. Appl. Phys.* **1992**, 31, 254-256.
26. Yan, B.; He, J.; Bao, R.; Bai, X.; Wang, S.; Zeng, Y.; Wang, Y., Modification of electro-optical properties of polymer dispersed liquid crystal films by iniferter polymerization. *Eur. Polym. J.* **2008**, 44, 952-958.
27. Wonsool, A.; Ha, K., Temperature effects on LC Droplets Formation of PDLC films with thermoplastic Matrix. *Korea Polym. J.* **1999**, 7, 130-135.
28. He, J.; Bin, Y.; Wang, X.; Yu, B.; Wang, Y., A novel Polymer dispersed Liquid Crystal film prepared by reversible addition fragmentation chain transfer polymerization. *Eur. Polym. J.* **2007**, 43, 4037-4042.
29. Ahmad, F.; Jamil, M.; Jeon, Y. J.; Woo, L. J.; Jung, J. E.; Jang, J. E.; Lee, G. H.; Park, J., Comparative study on the electrooptical properties of polymer-dispersed liquid crystal films with different mixtures of monomers and liquid crystals. *J. Appl.Polym. Sci.* **2011**, 121, 1424-1430.
30. Manni, A.; Gobbi, L.; Simoni, F., Novel PDLC Films Based On a Photoactive Polymeric Binder. *Mol. Cryst. Liq. Cryst.* **2003**, 398, 281-291.
31. Orzeszko, B.; Ksyta, M. D.; Orzeszko, A., An Efficient, Facile, and Fast Synthesis of 4-alkoxy-4'-hydroxybiphenyls. *Synth. Commun.* **2002**, 32, 3425-3429.
32. Crawford, G. P.; Zumer, S., Liquid Crystals in Complex Geometries. Taylor and Francis: London, 1996.
33. Vicari, L., Optical Applications of Liquid Crystals. Institute of Physics Publishing: Bristol and Philadelphia, 2003.
34. Kuang, P.; Park, J., M.; Leung, W.; Mahadevapuram, R., C.; Nalwa, K., S.; Kim, T., G.; Chaudhary, S.; Ho, K., M.; Constant, K., A New Architecture for Transparent Electrodes: Relieving the Trade-Off Between Electrical Conductivity and Optical Transmittance. *J. Adv. Mater.* **2011**, 23, 2469-2473.
35. Kappe, O. C., Controlled Microwave Heating in Modern Organic Synthesis. *Angew. Chem. Int. Ed.* **2004**, 43, 6250-6284.
36. Hayes, B. L., Microwave Synthesis: Chemistry at the Speed of Light CEM Publishing: Matthews, NC, 2002.
37. Tierney, J. P.; Lidström, P., Microwave assisted organic synthesis. Black well Publishing Ltd: Oxford, **2005**.
38. Loupy, A.; Perreux, L.; Liagre, M.; Burle, K.; Moneuse, M., Reactivity and selectivity under microwaves in organic chemistry. Relation with medium effects and reaction mechanisms. *Pure Appl. Chem.* **2001**, 73, 161-166.
39. Wiesbrock, F.; Hoogenboom, R.; Schubert, S. U., Single-mode microwave ovens as new reaction devices: Accelerating the living polymerization of 2 ethyl-2-oxazoline. *Macromol. Rapid Commun.* **2004**, 25, 1895-1899.
40. Elias, H.-G., An Introduction to Polymer Science. Wiley-VCH: New York, 1997.
41. Braun, D.; Cherdrón, H.; Rehahn, M.; Ritter, H.; Voit, B., Polymer Synthesis: Theory and practice. 4 ed.; Springer: 2005.
42. Devedjiev, I.; Petrova, K.; Glavchev, I., Preparation of glycidylmethacrylate. *J. Univ. Chem. Technol. Metallurgy* **2000**, 35, 87-90.
43. Plaza, M. T. V. Molecular mobility of n-ethylene glycol dimethacrylate glass formers upon free radical polymerization. PhD Thesis, Faculdade de Ciências e Tecnologia, Universidade Nova de Lisboa, Lisboa, 2007.
44. <http://www.sigmaaldrich.com/> (December,2011)

45. Barros, M. T.; Mouquinho, A.; Petrova, K.; Saavedra, M.; Sotomayor, J., Fast synthesis employing a microwave assisted neat protocol of new monomers potentially useful for the preparation of PDLC films. *Cent.Eur.J.Chem* **2011**, 9, 557-566.
46. Reddy, G. J.; Naidu, S. V.; Reddy, A. V., Synthesis and Characterization of Poly(N-phenyl methacrylamide-co-methyl methacrylate) and Reactivity Ratios Determination. *J. Appl. Polym. Sci.* **2003**, 90, 2179.
47. Casadei, M. A.; Cesa, S.; Inesi, A., Electrochemical Studies on Haloamides. Part XII. Electrosynthesis of Oxazolidine-2,4-diones. *Tetrahedron* **1995**, 51, (20), 5891-5900.
48. Vijayanand, P. S.; Kato, S.; Satokawa, S.; Kojima, T., Copolymerization of 4-cyanophenyl methacrylate with methyl methacrylate: Synthesis, characterization and determination of monomer reactivity ratios. *Polym. Bull* **2007**, 59, 469-480.
49. Chênevert, R.; Pelchat, N.; Morin, P., Lipase-mediated enantioselective acylation of alcohols with functionalized vinyl esters: acyl donor tolerance and applications. *Tetrahedron: Asymmetry* **2009**, 20, 1191-1196.
50. Lal, J.; Green, R., The Preparation of Some Esters of Methacrylic Acid. *J. Org. Chem* **1955**, 20, 1030-1033.
51. Pinazzi, C; Comptes Rendus des Seances de l'Academie des Sciences. *Serie C: Sciences Chimiques* **1972**, 274, (44).
52. Braun, J. V.; Steindorff, A., Ueber einige Verbindungen der Pentamethylenreihe. *Chem. Berichte (In German)* **1905**, 38, 956-966.
53. Slugovc, C.; Demel, S.; Riegler, S.; Hobisch, J.; Stelzer, F., Influence of functional groups on ring opening metathesis polymerisation and polymer properties. *J. Mol. Cat. A: Chem.* **2004**, 213, 107-113.
54. Berg, S.; Newbery, G., The Search for Chemotherapeutic Amidines. Part X. Substituted 4 : 4'-Diamidino-aw-diphenoxyalkanes and -diphenyl Ethers. *J. Chem. Soc.* **1949**, 642-645.
55. Yelamaggad, C. V.; Tamilenth, V. P., Synthesis and thermal properties of liquid crystal trimers comprising cyanobiphenyl and salicylaldehyde anisometric segments. *Tetrahedron* **2009**, 65, 6403-6409.
56. Dneprovskii, A. S.; Tuchkin, A. I., Radical-Anion Nucleophilic Substitution in p-Bromobenzyl Methyl and p-Bromobenzyl Phenyl Ethers. Competing Fragmentations of Radical Anions. *Russ.J. Org. Chem.* **1997**, 33, 1601-1605.
57. Ikeuchi, Y.; Taguchi, T.; Hanzawa, Y., Zirconocene-Mediated and/or Catalyzed Unprecedented Coupling Reactions of Alkoxy-methyl-Substituted Styrene Derivatives. *J. Org. Chem* **2005**, 11, 4354-4359.
58. Barros, M. T.; Petrova, K.; Ramos, A. M., Regioselective Copolymerization of Acryl Sucrose monomers. *J. Org. Chem.* **2004**, 69, 7772-7775.
59. Aileen, A.; Imrie, T. C.; Imirie, C., Effect of spacer length on the thermal properties of side-chain liquid crystal polymethacrylates. *Macromolecules* **1995**, 28, 3617-3624.
60. Crucho, C. C.; Petrova, K. T.; Pinto, R. C.; Barros, M. T., Novel Unsaturated Sucrose Ethers and Their Application as Monomers. *Molecules* **2008**, 13, 762-770.
61. Silverstein, R. M.; Webster, F. X.; Kiemle, D. J., *Spectrometric Identification of Organic Compounds*. John Wiley & Sons, Inc: New York, 2005.
62. Mouquinho, A.; Saavedra, M.; Maiou, A.; Petrova, K.; Barros, M. T.; Figueirinhas, J. L.; Sotomayor, J., Films Based on New Methacrylate Monomers: Synthesis, Characterisation and Electro-optical properties. *Mol. Cryst. liq. Cryst.* **2011**, 542, 132/[654]-140[662].





## 8 Appendix

## 8.1 NMR Spectra

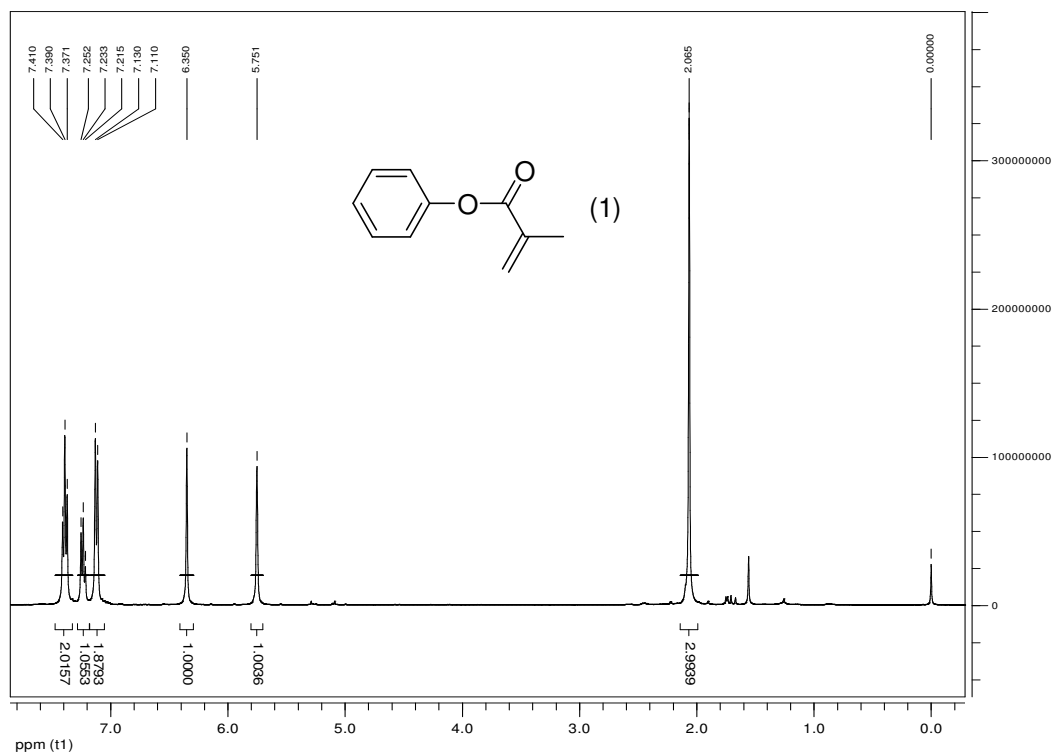


Figure 8.1 – Proton NMR spectrum of monomer 1.

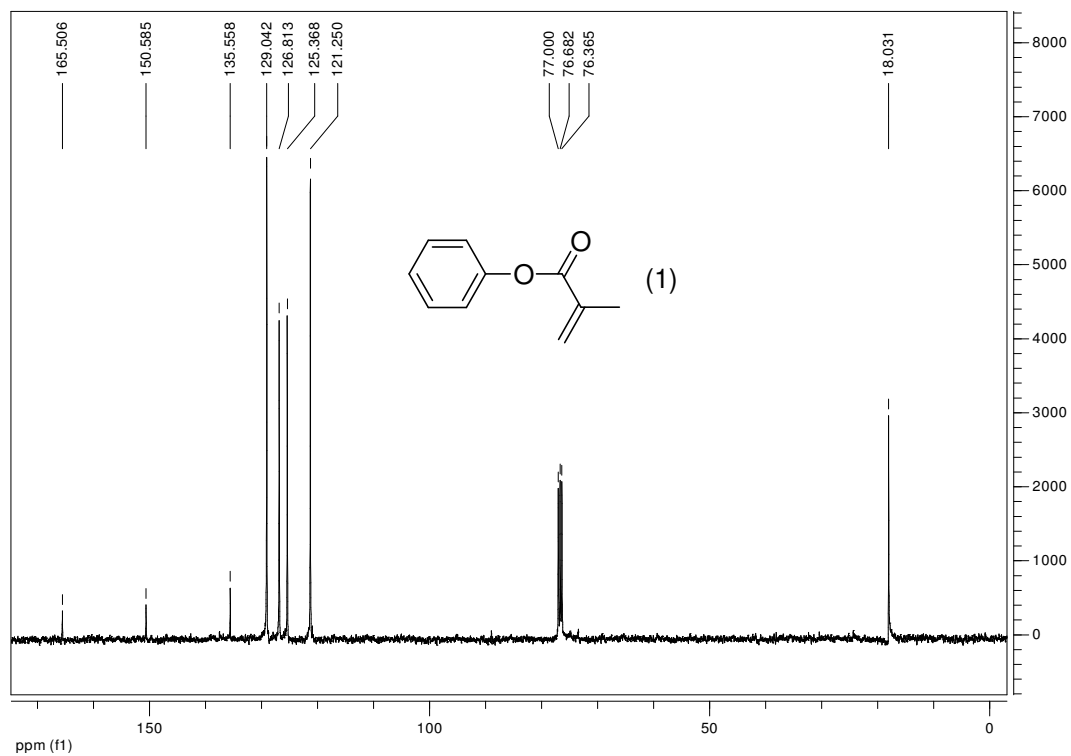


Figure 8.2 – Carbon NMR spectrum of monomer 1.

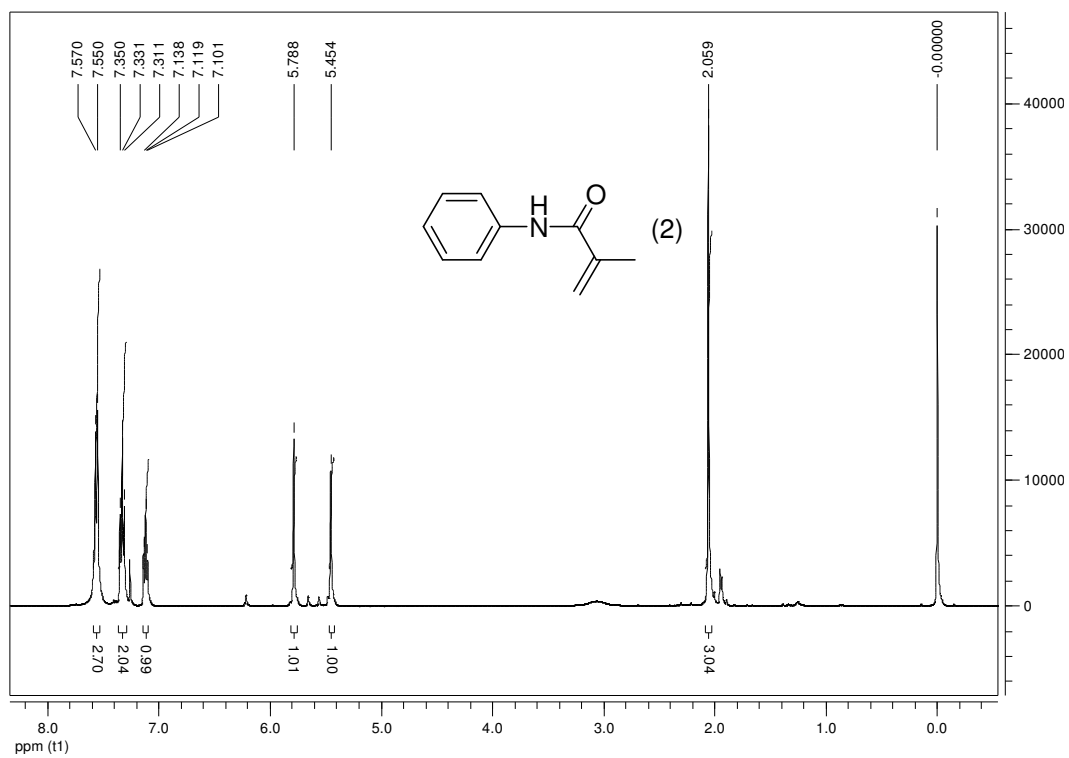


Figure 8.3 – Proton NMR spectrum of monomer 2.

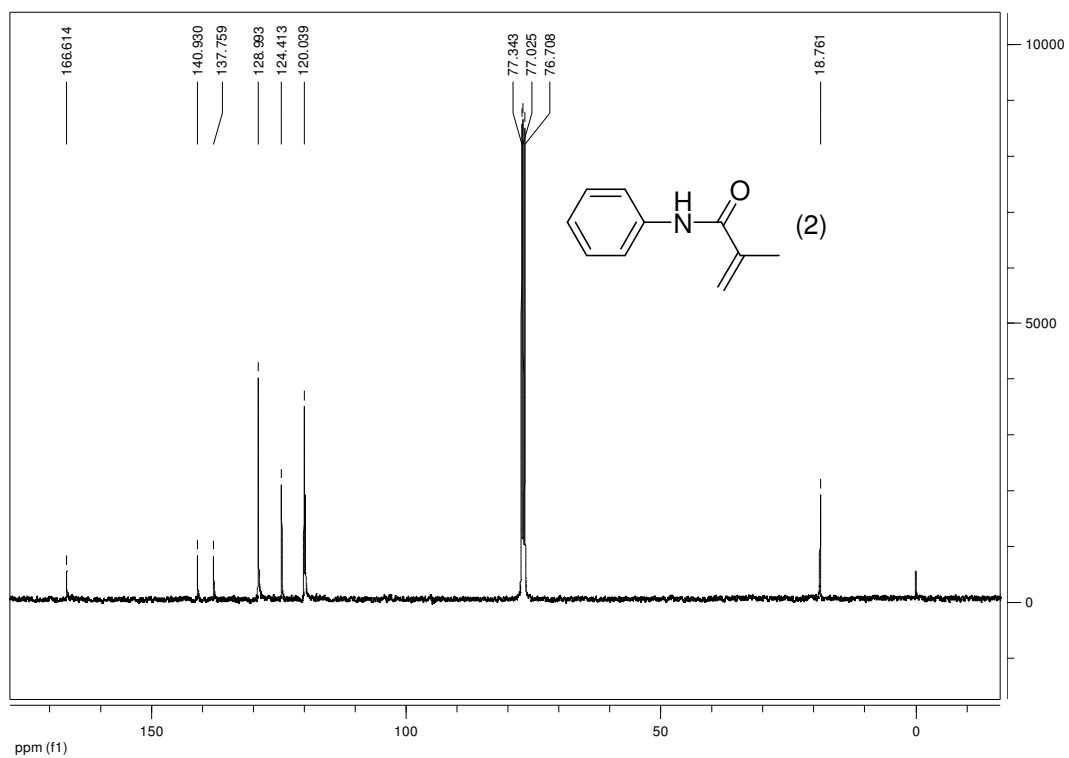


Figure 8.4 – Carbon NMR spectrum of monomer 2.

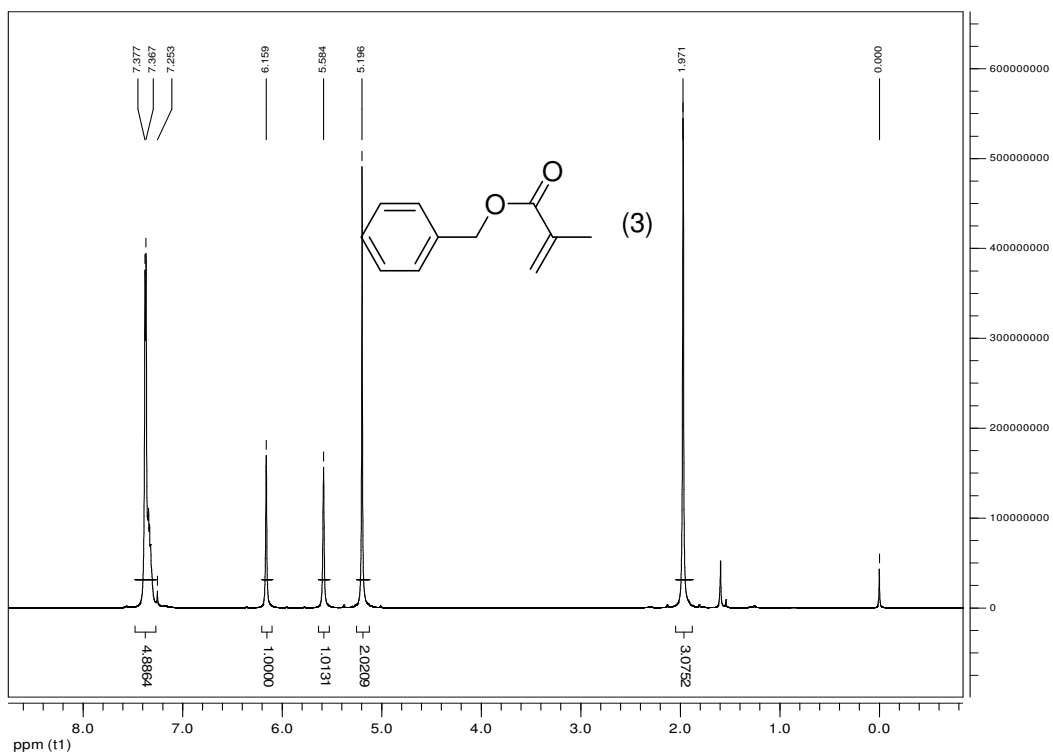


Figure 8.5 – Proton NMR spectrum of monomer 3.

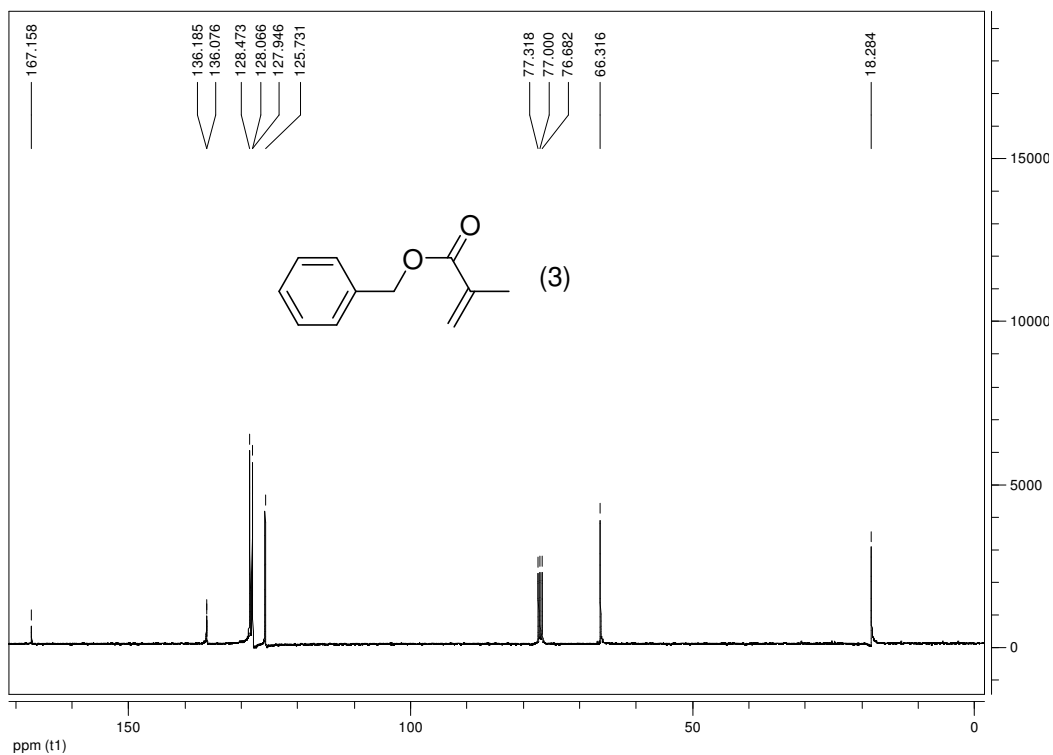


Figure 8.6 – Carbon NMR spectrum of monomer 3.

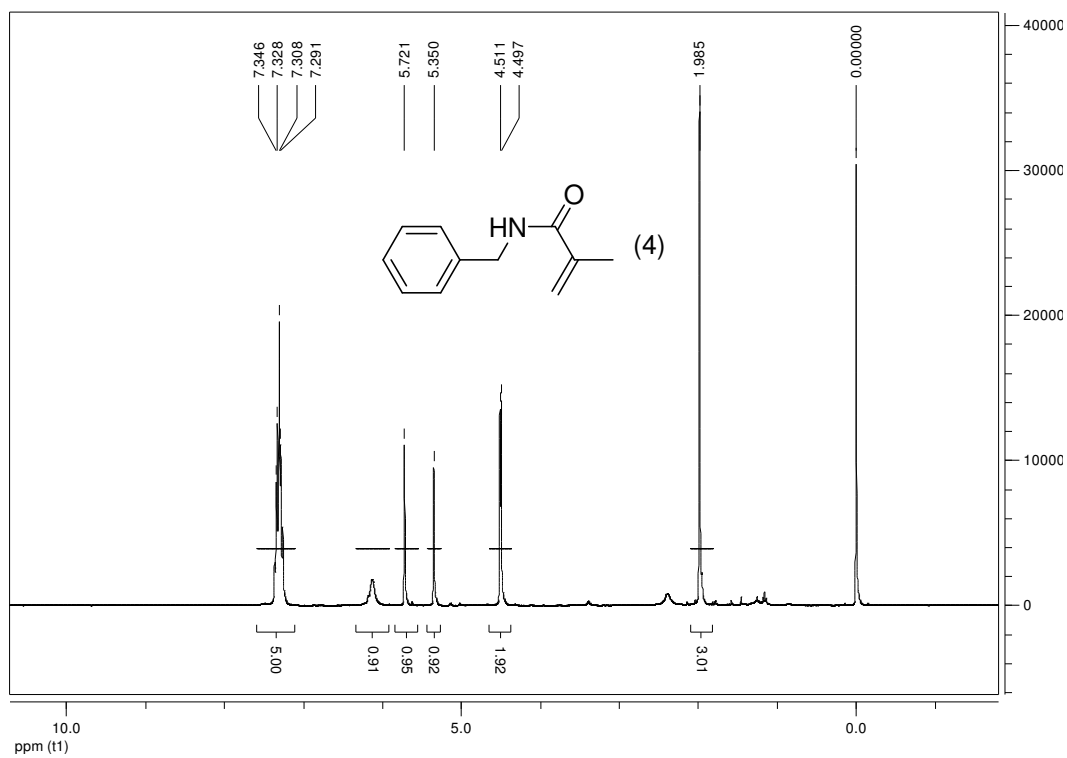


Figure 8.7 – Proton NMR spectrum of monomer 4.

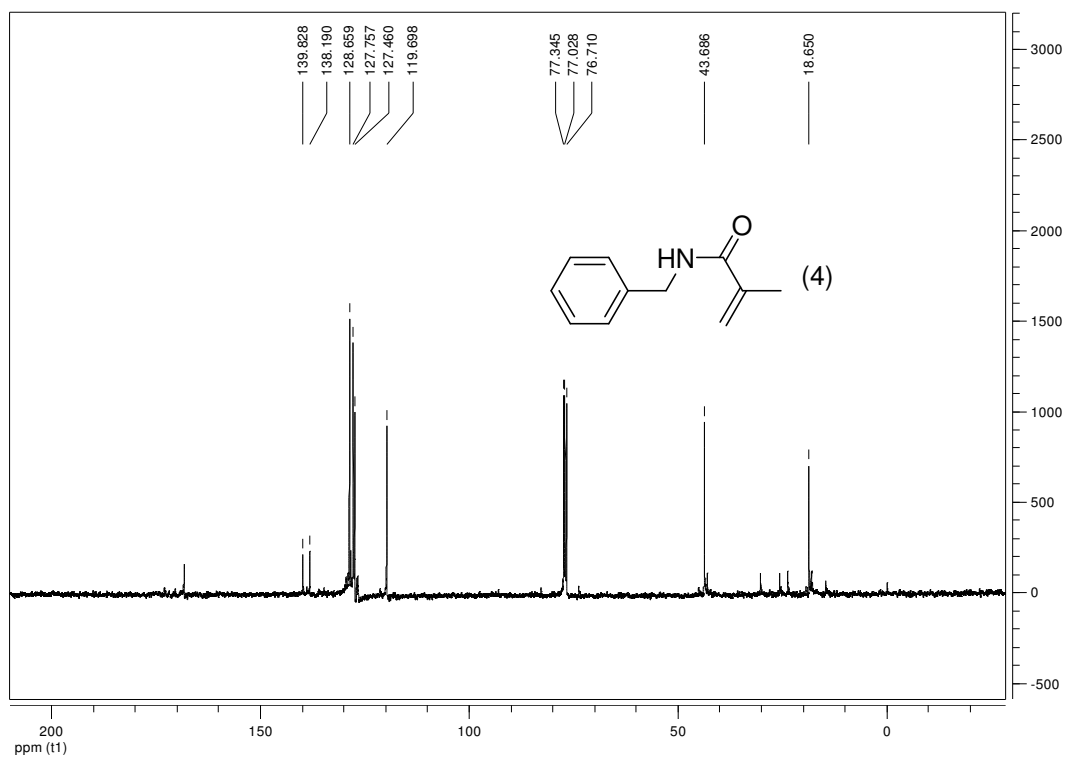


Figure 8.8 – Carbon NMR spectrum of monomer 4.

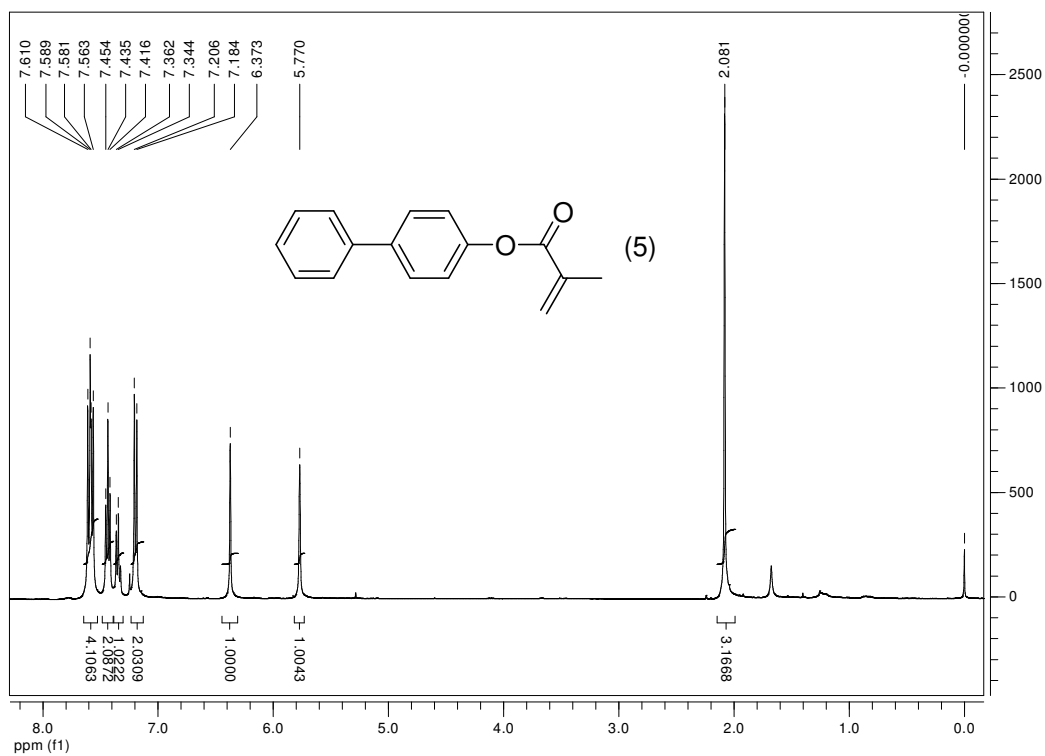


Figure 8.9 – Proton NMR spectrum of monomer 5.

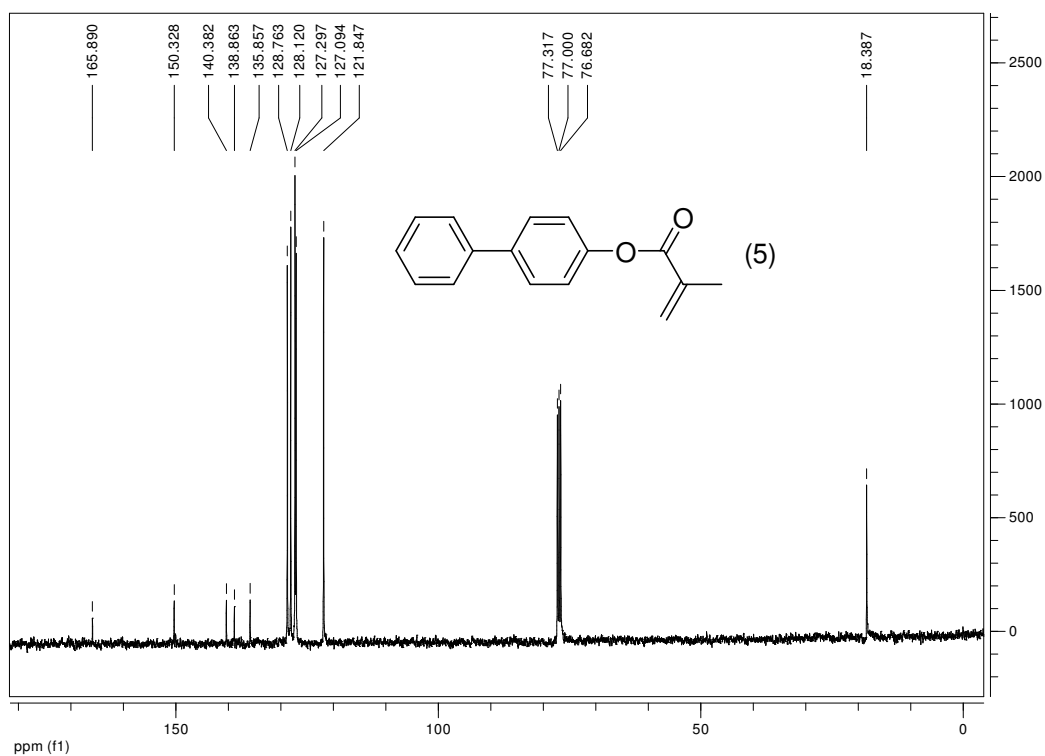


Figure 8.10 – Carbon NMR spectrum of monomer 5.

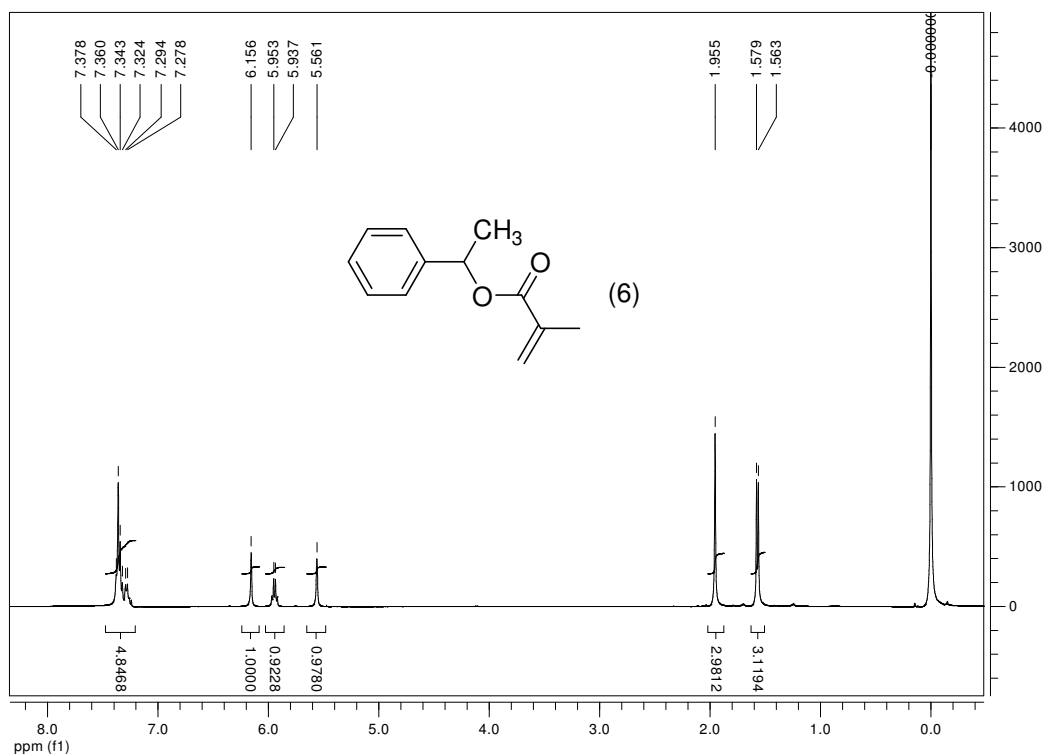


Figure 8.11 – Proton NMR spectrum of monomer 6.

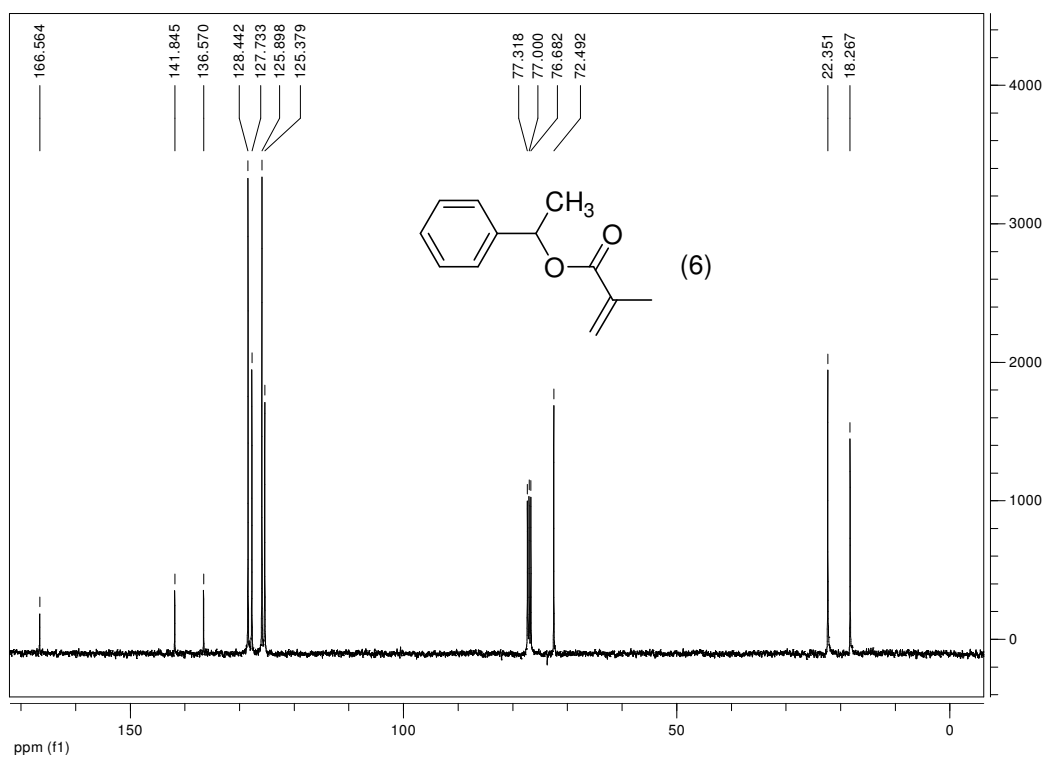


Figure 8.12 – Carbon NMR Spectrum of monomer 6.

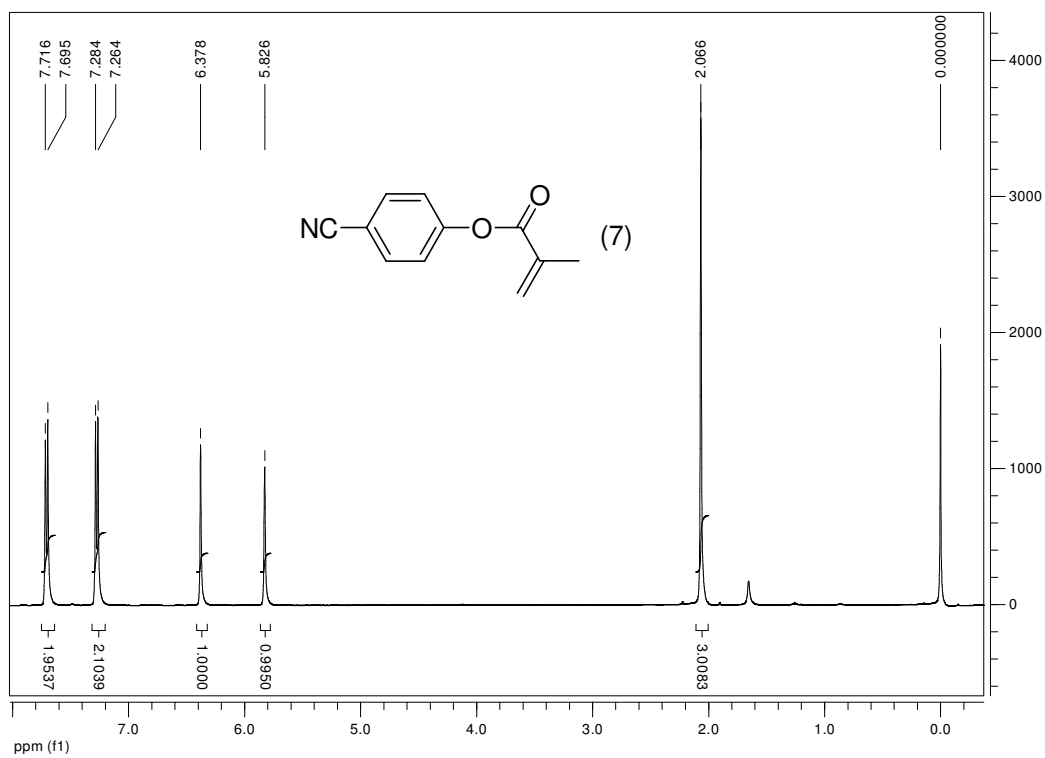


Figure 8.13 – Proton NMR spectrum of monomer 7.

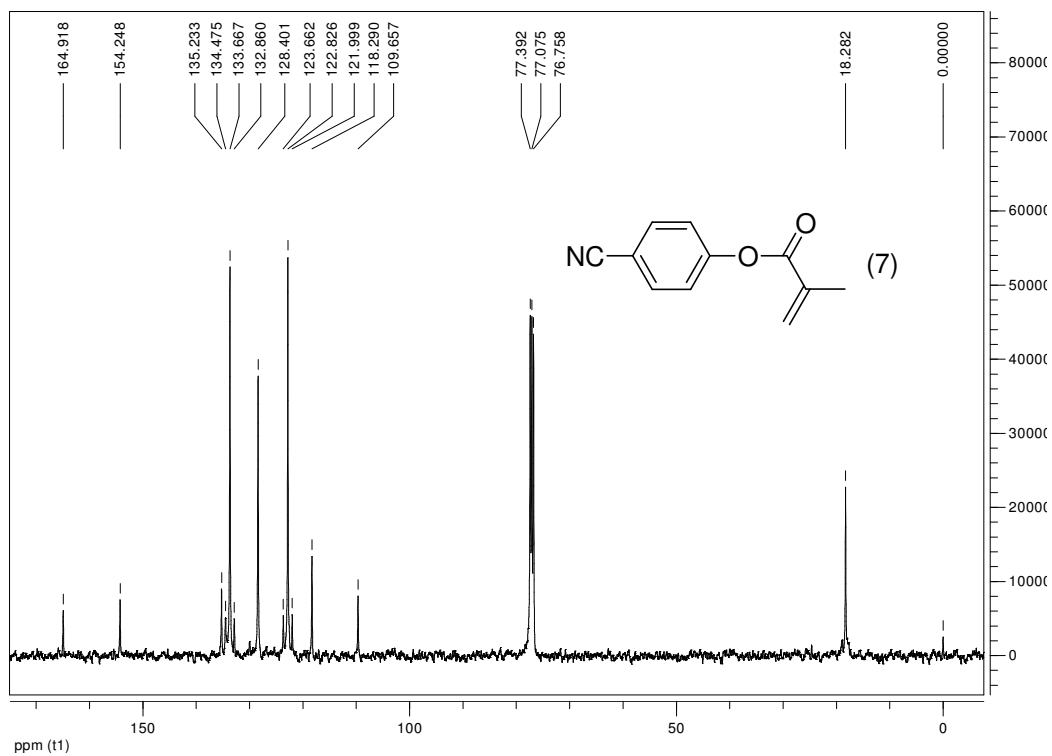


Figure 8.14 – Carbon-13 NMR spectrum of monomer 7.

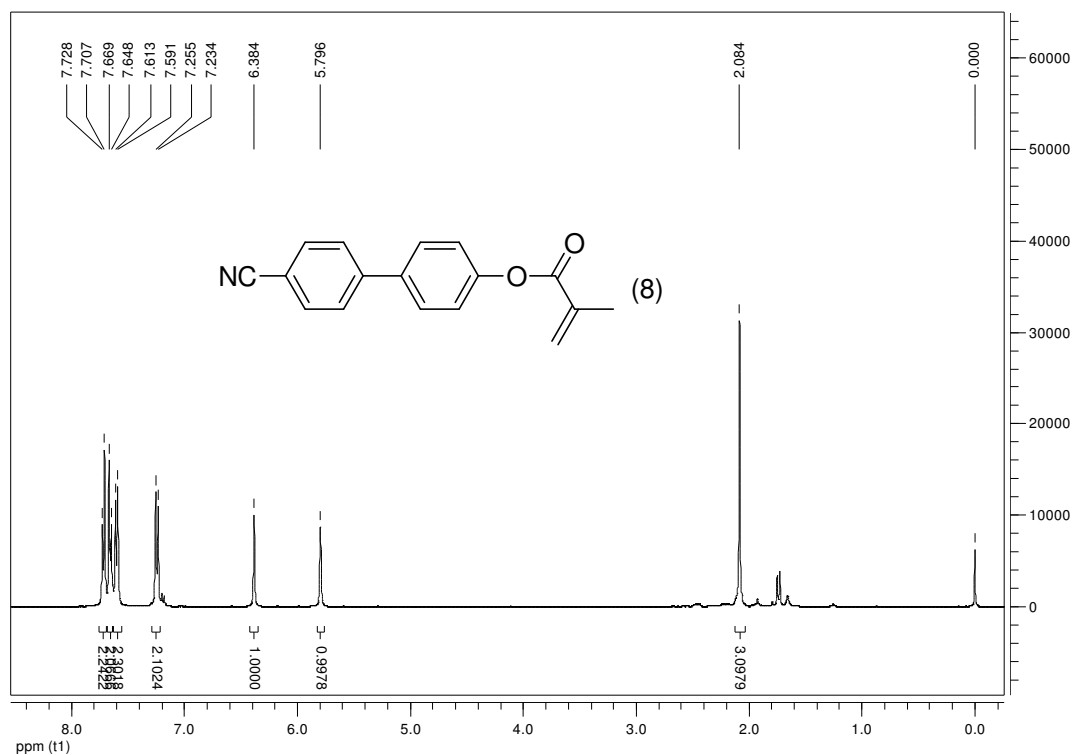


Figure 8.15 – Proton NMR spectrum of monomer 8.

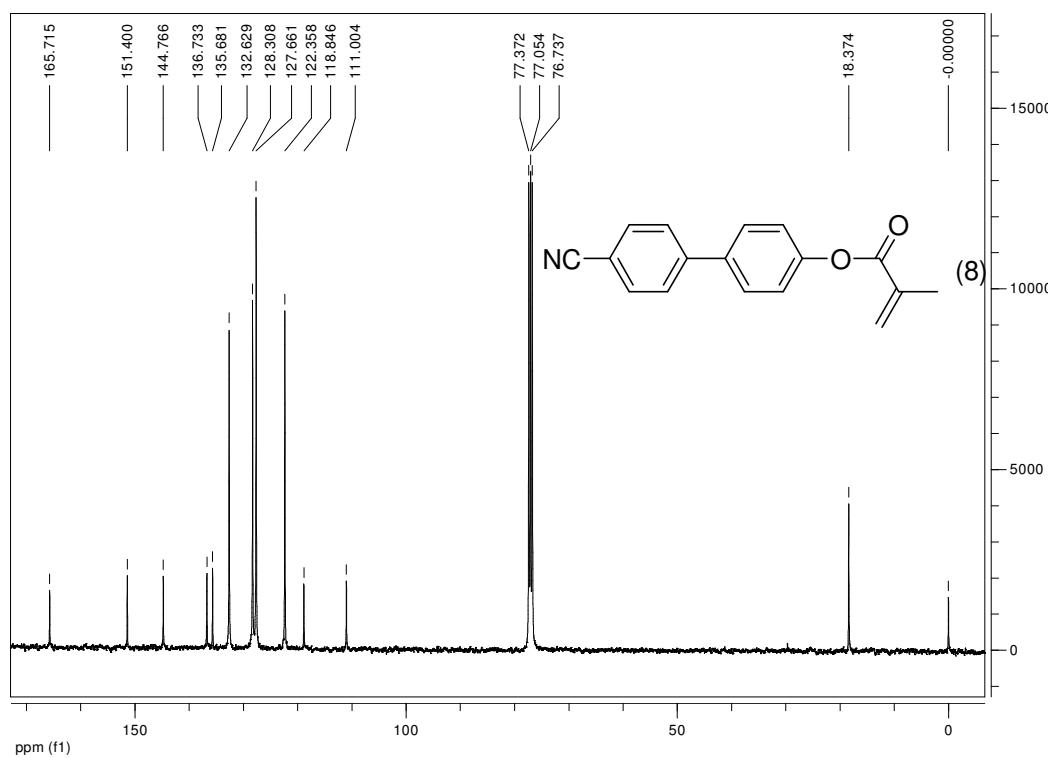
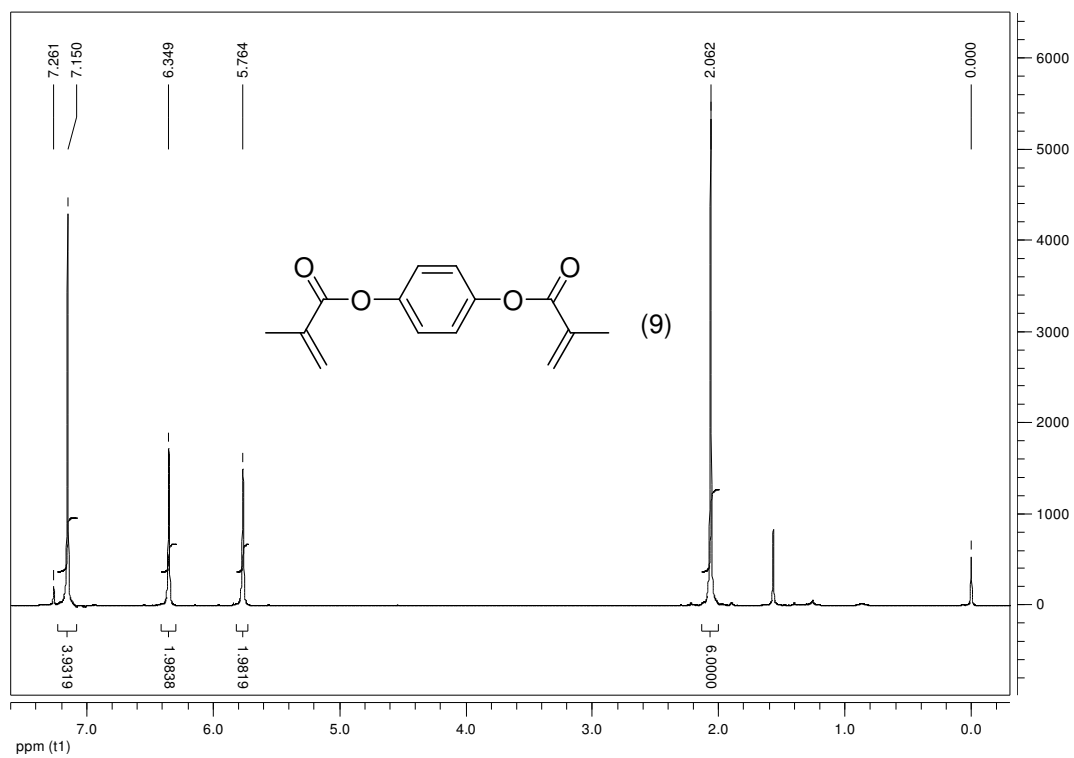
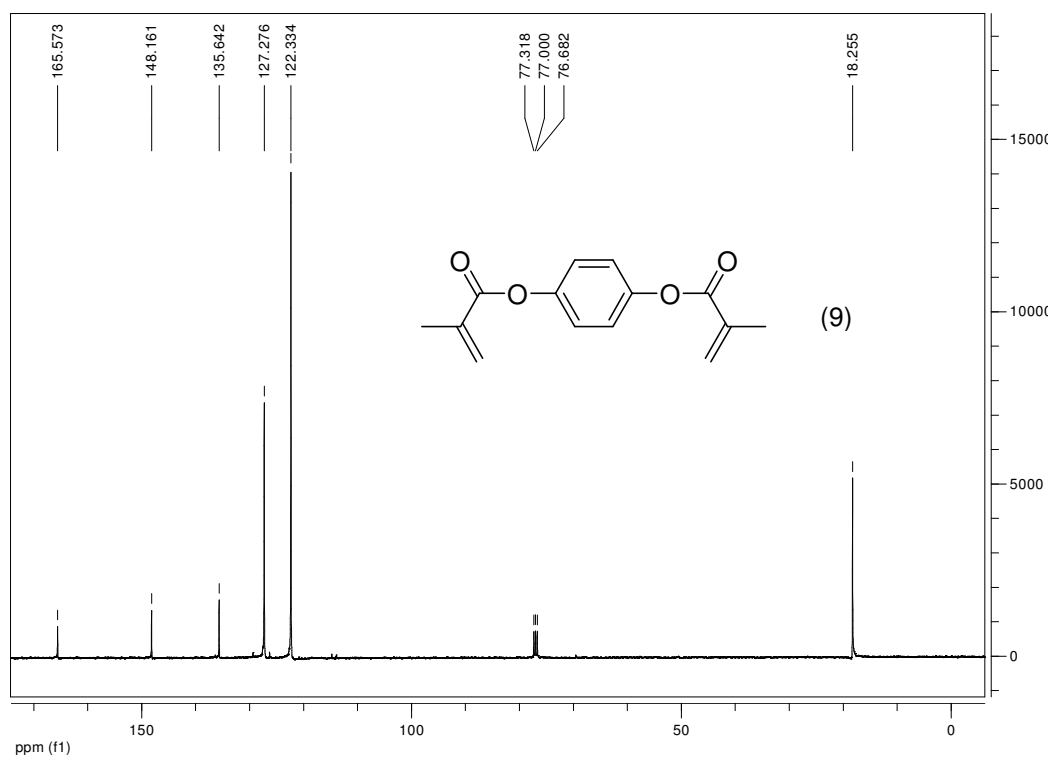


Figure 8.16 – Carbon NMR spectrum of monomer 8.



**Figure 8.17 – Proton NMR spectrum of monomer 9.****Figure 8.18 – Carbon NMR spectrum of monomer 9.**

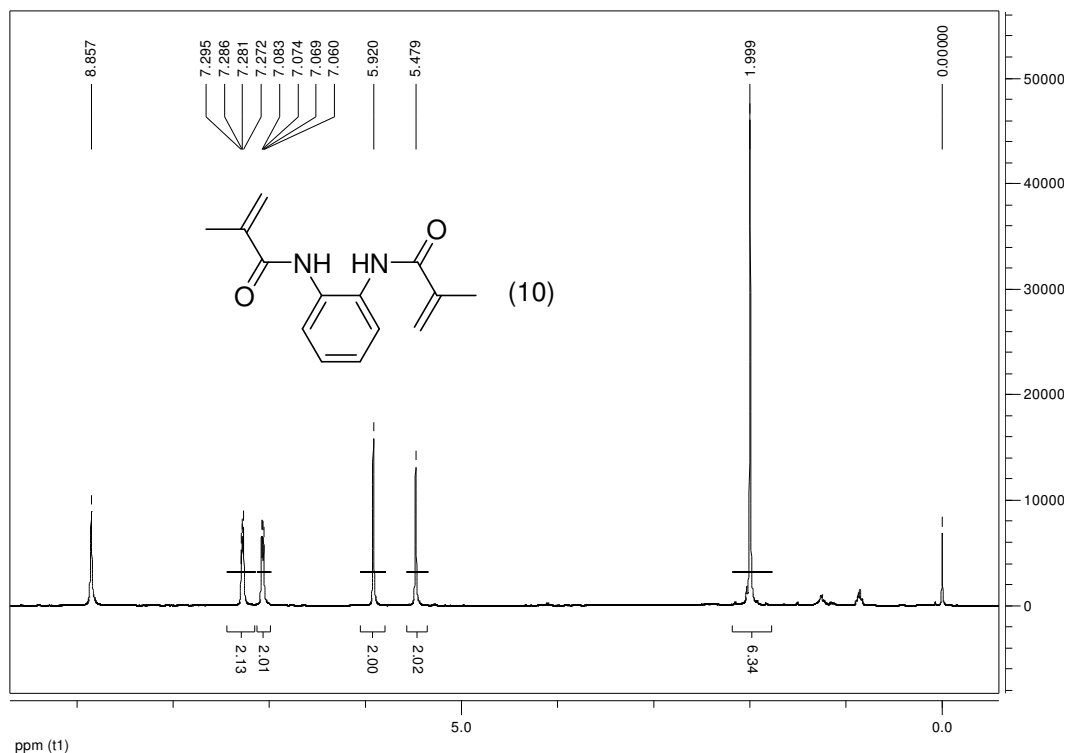


Figure 8.19 – Proton NMR spectrum of monomer 10.

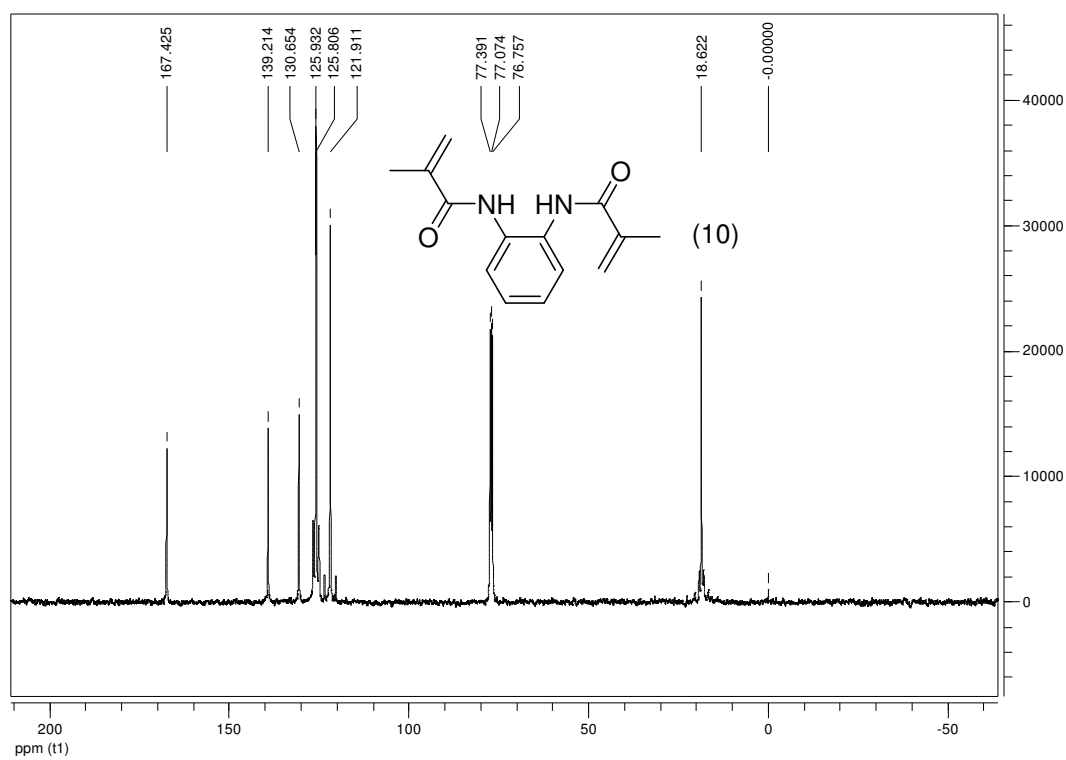


Figure 8.20 – Carbon NMR spectrum of monomer 10.

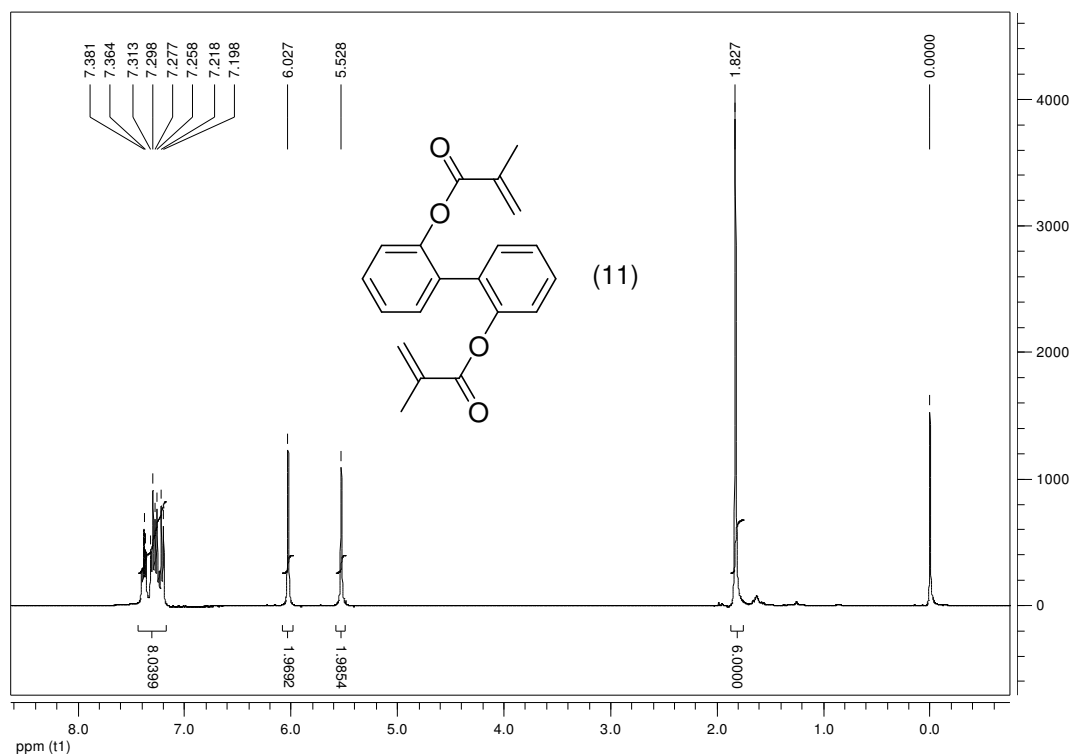


Figure 8.21 – Proton NMR spectrum of monomer 11.

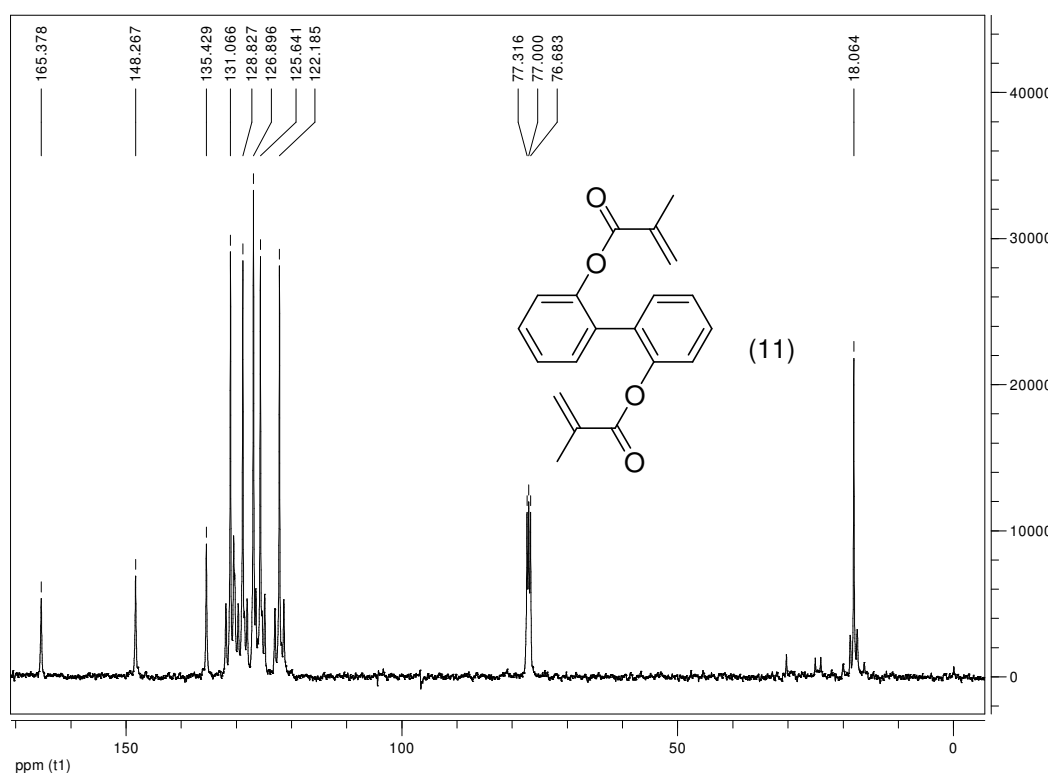


Figure 8.22 – Carbon NMR spectrum of monomer 11.

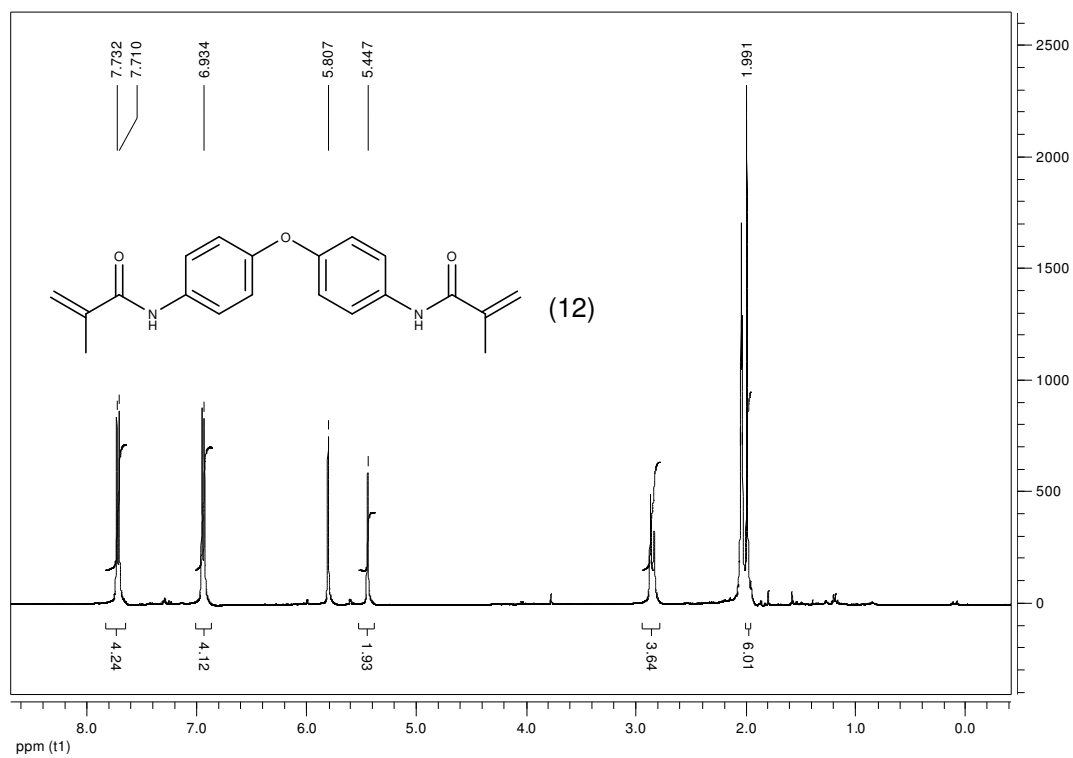


Figure 8.23 – Proton NMR spectrum of monomer 12

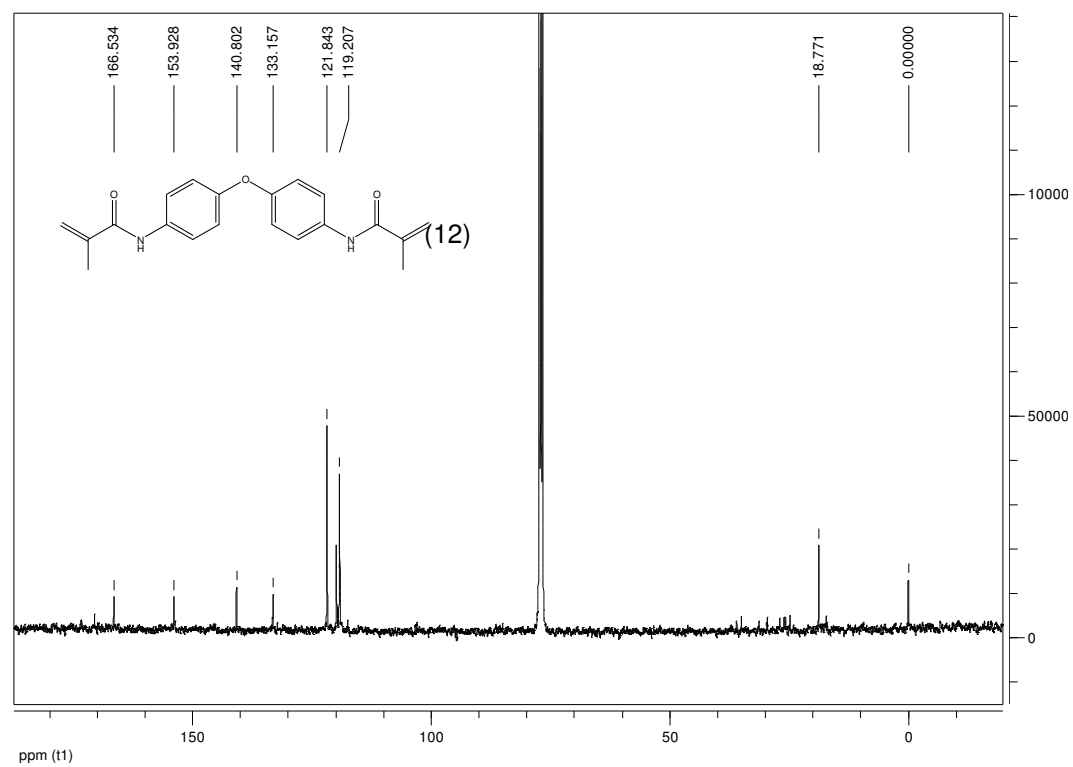


Figure 8.24 – Carbon NMR spectrum of monomer 12.

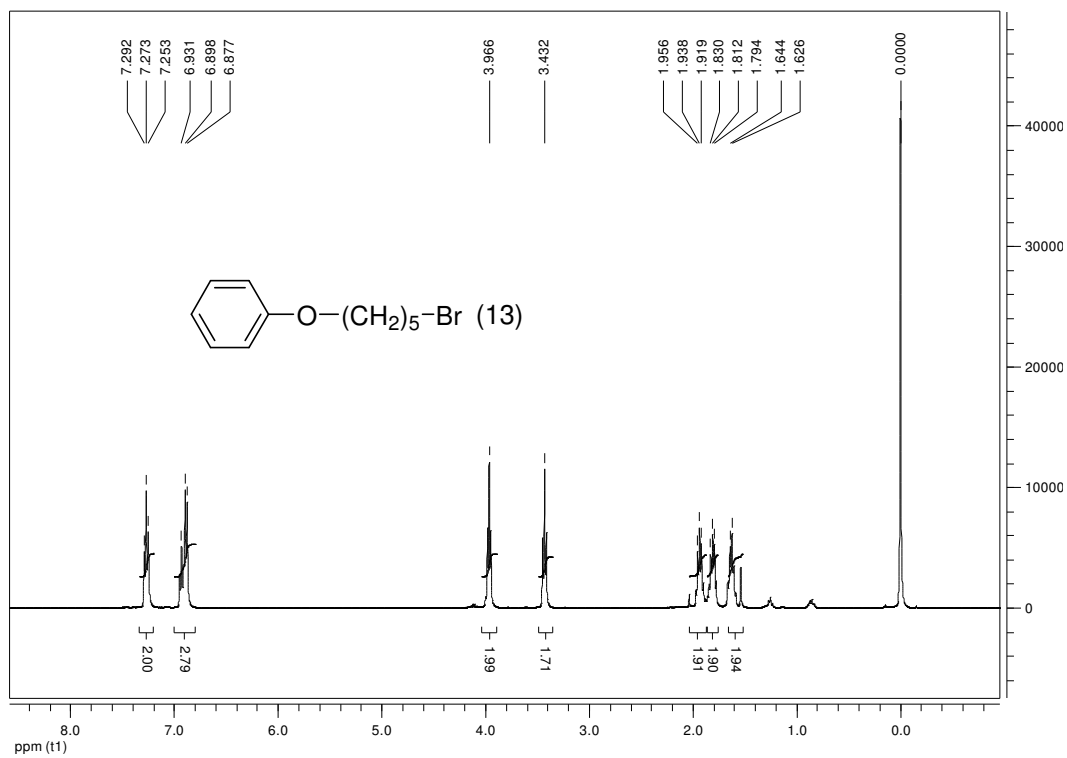


Figure 8.25 – Proton NMR spectrum of compound 13.

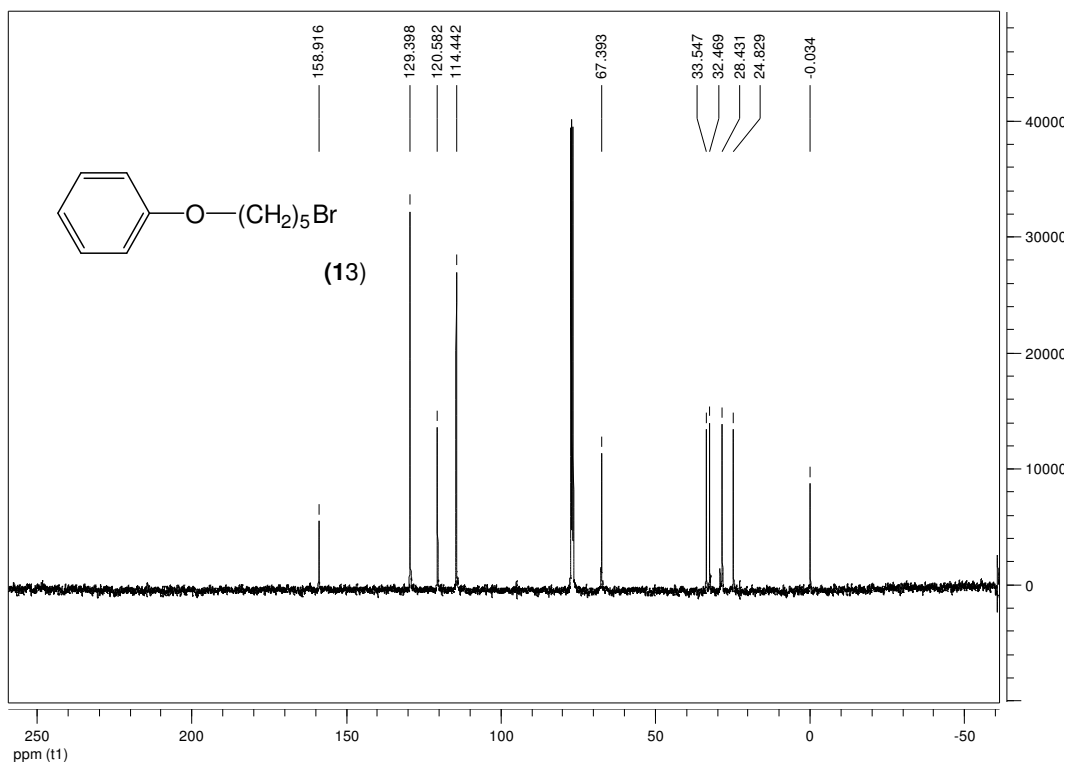


Figure 8.26 – Carbon NMR spectrum of compound 13.

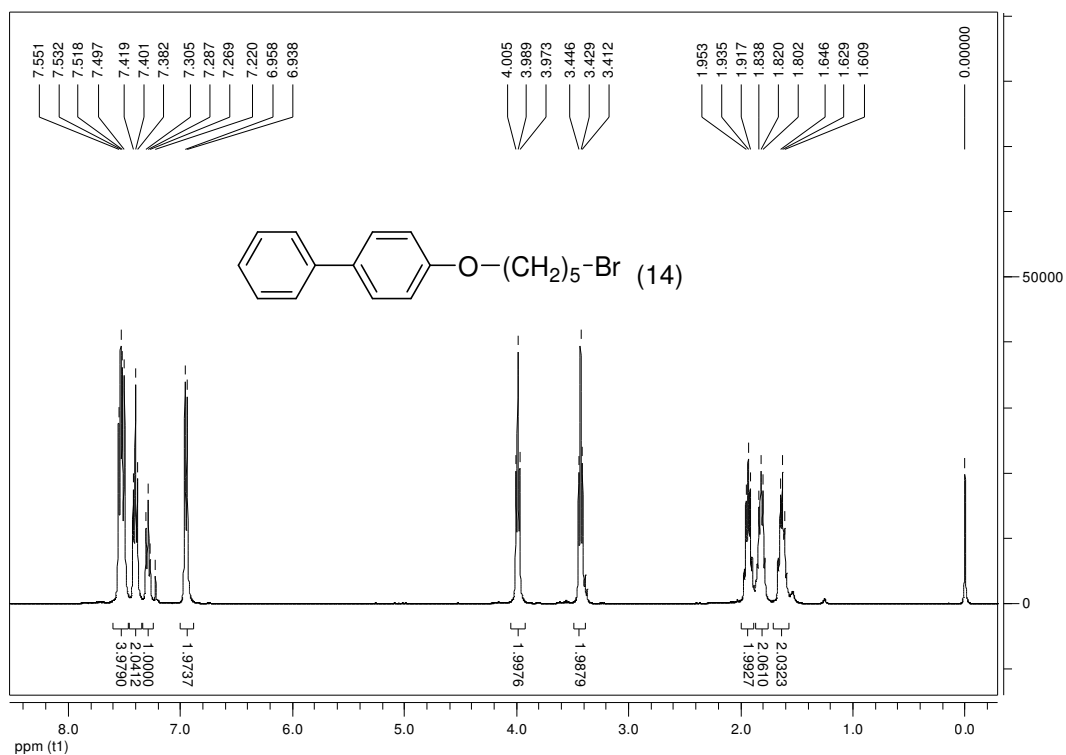


Figure 8.27 – Proton NMR spectrum of compound 14.

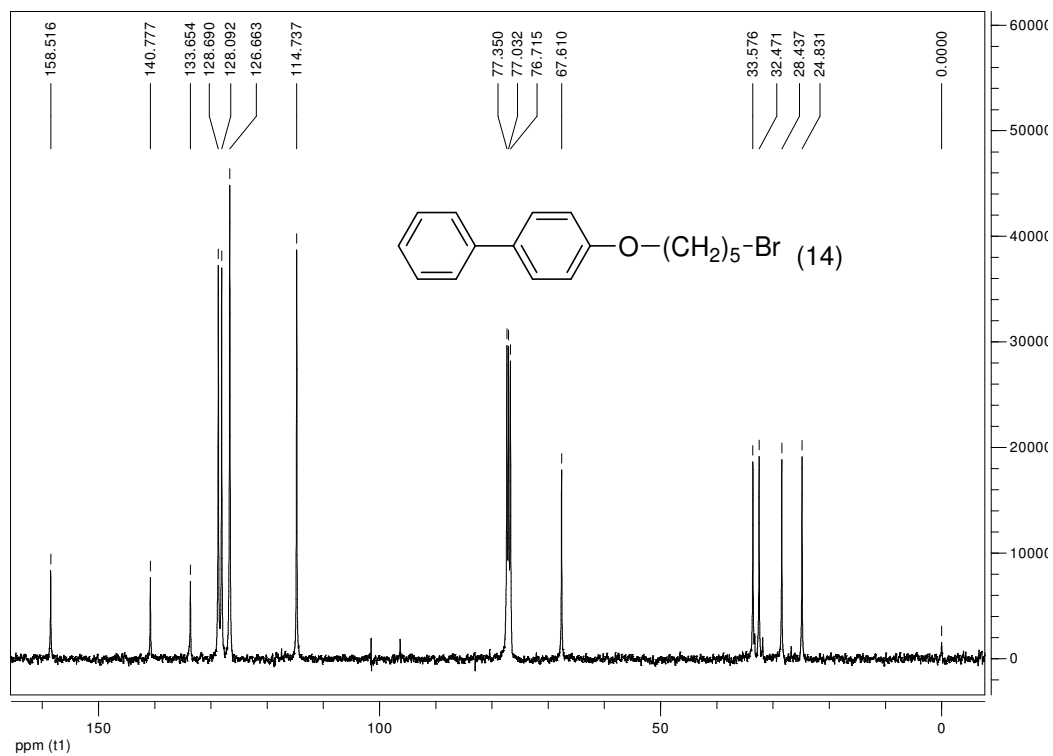


Figure 8.28 – Carbon NMR spectrum of compound 14.

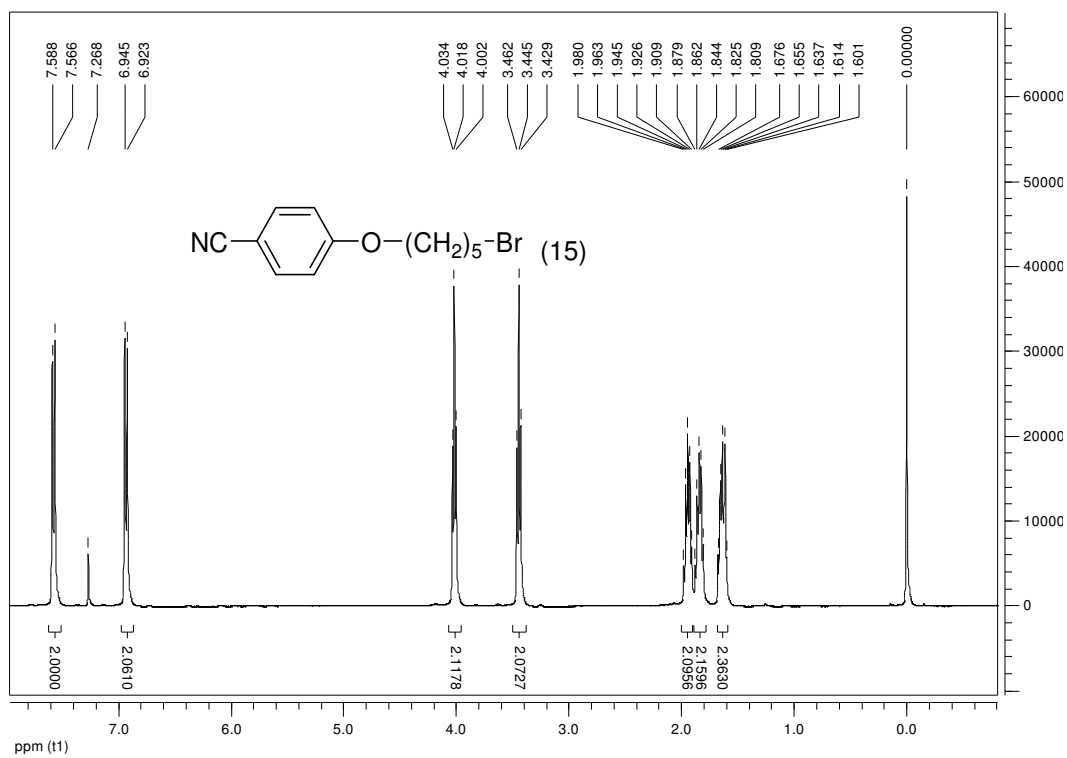


Figure 8.29 – Proton NMR spectrum of compound 15.

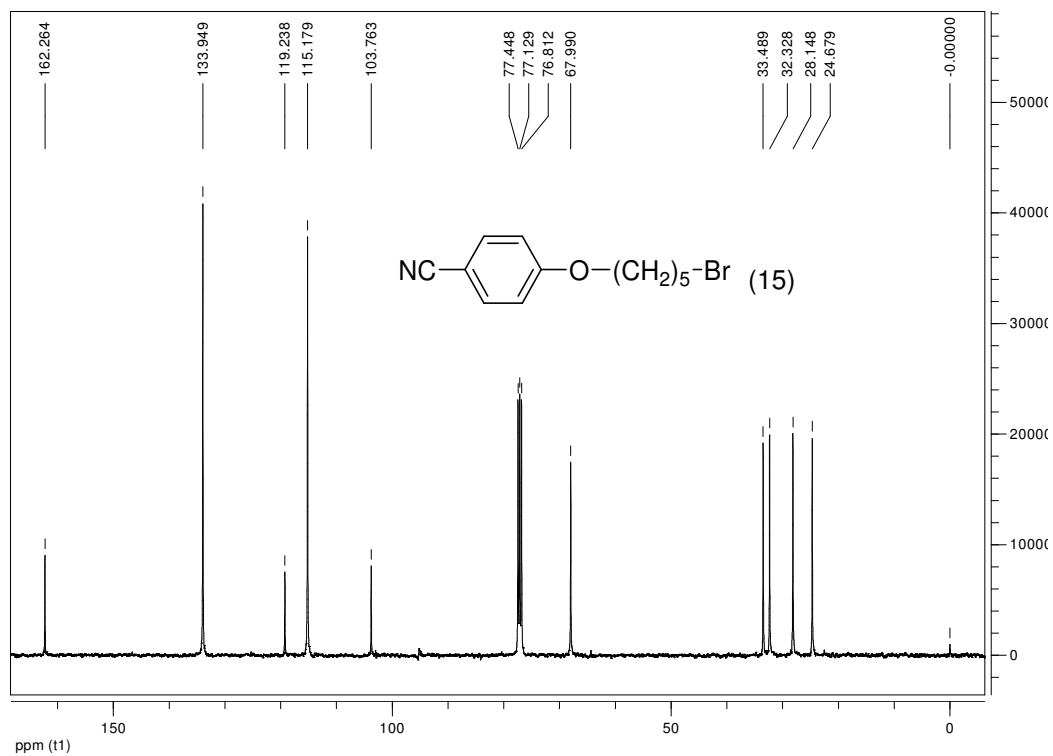


Figure 8.30 – Carbon NMR spectrum of compound 15.

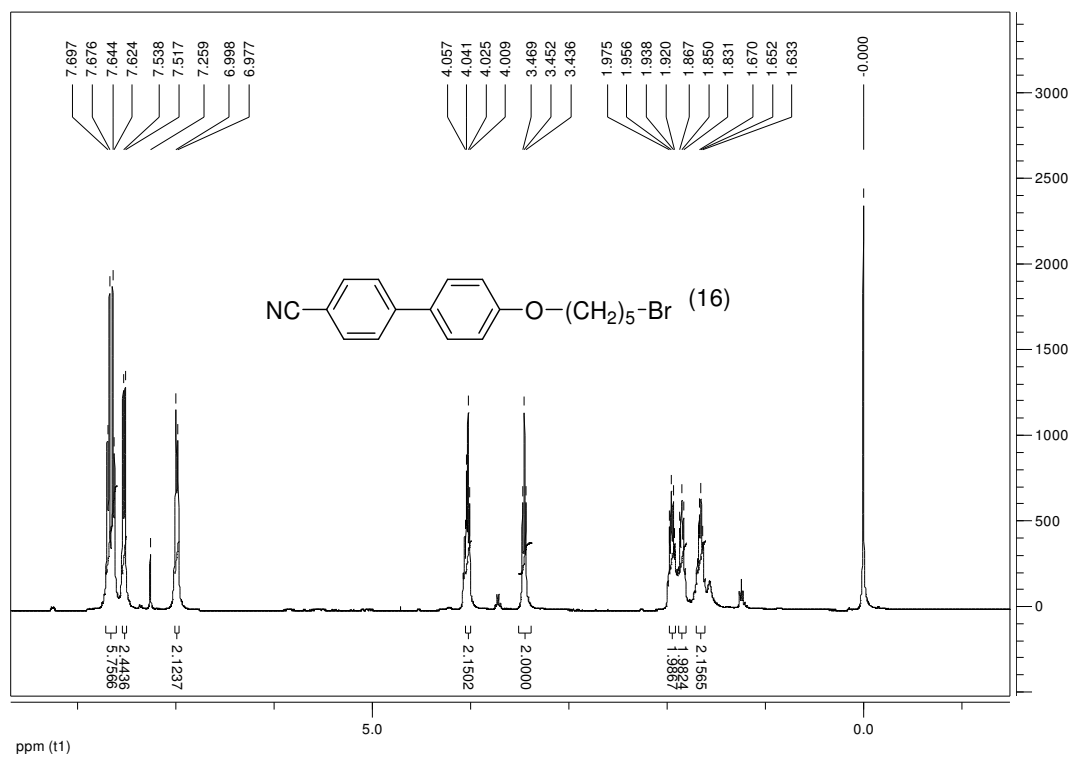


Figure 8.31 – Proton NMR spectrum of compound 16.

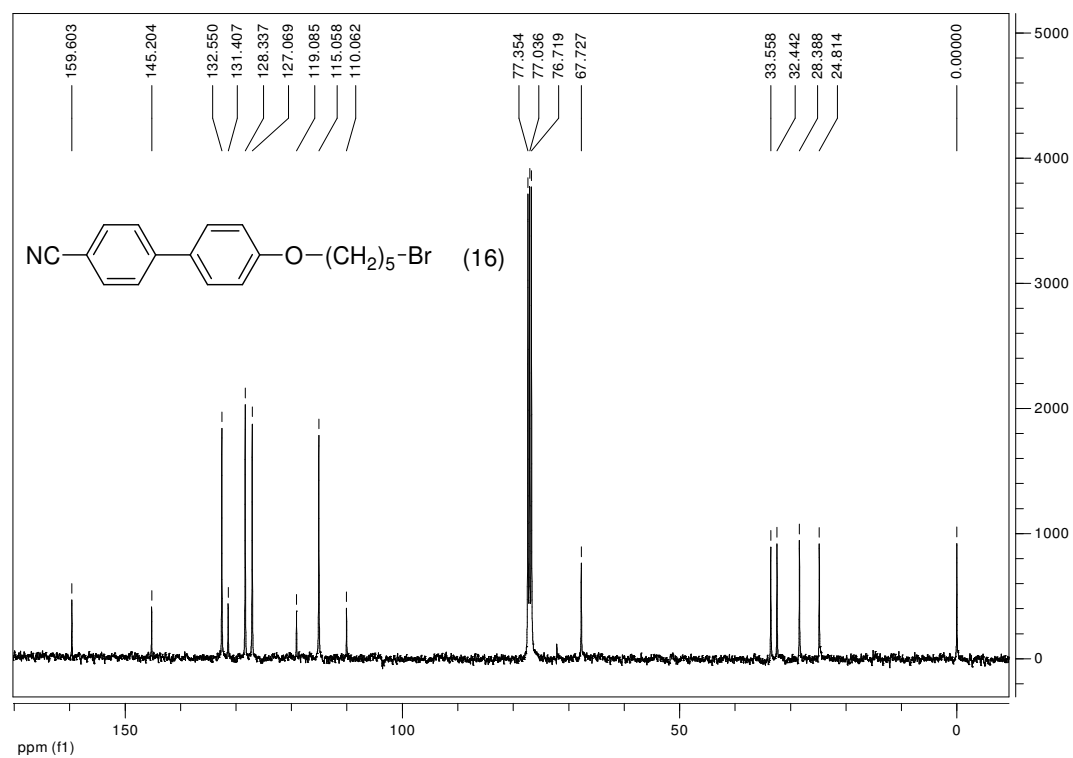


Figure 8.32 – Carbon NMR spectrum of compound 16.



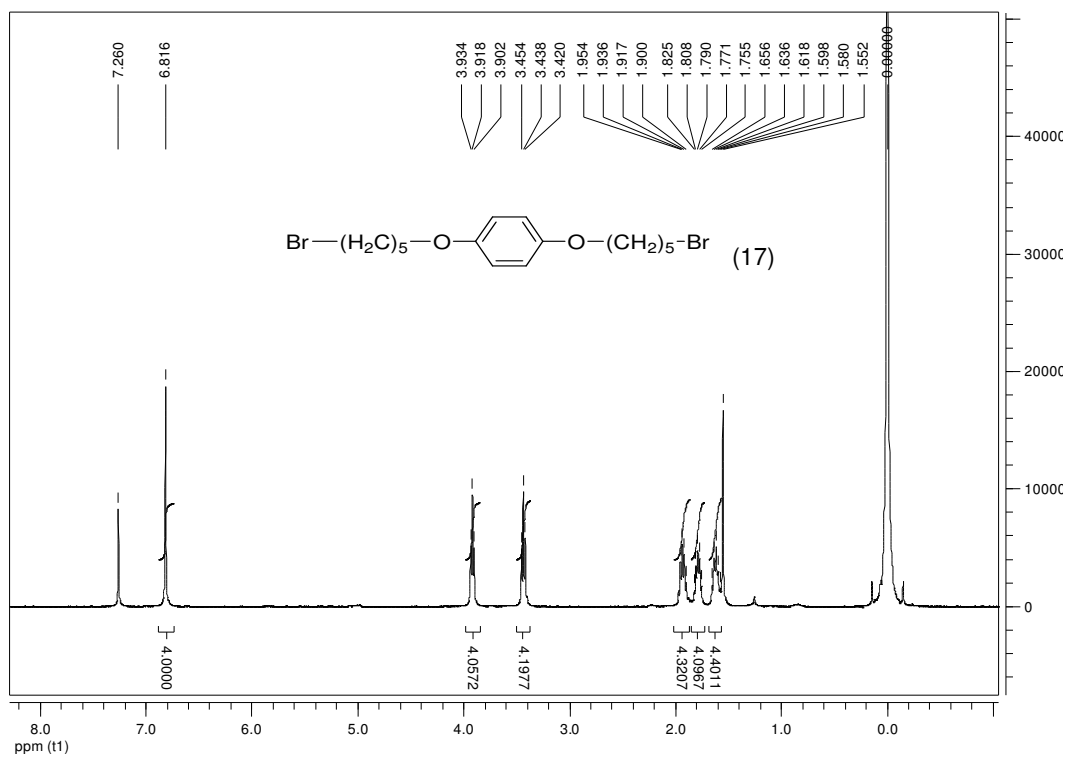


Figure 8.33 – Proton NMR spectrum of compound 17.

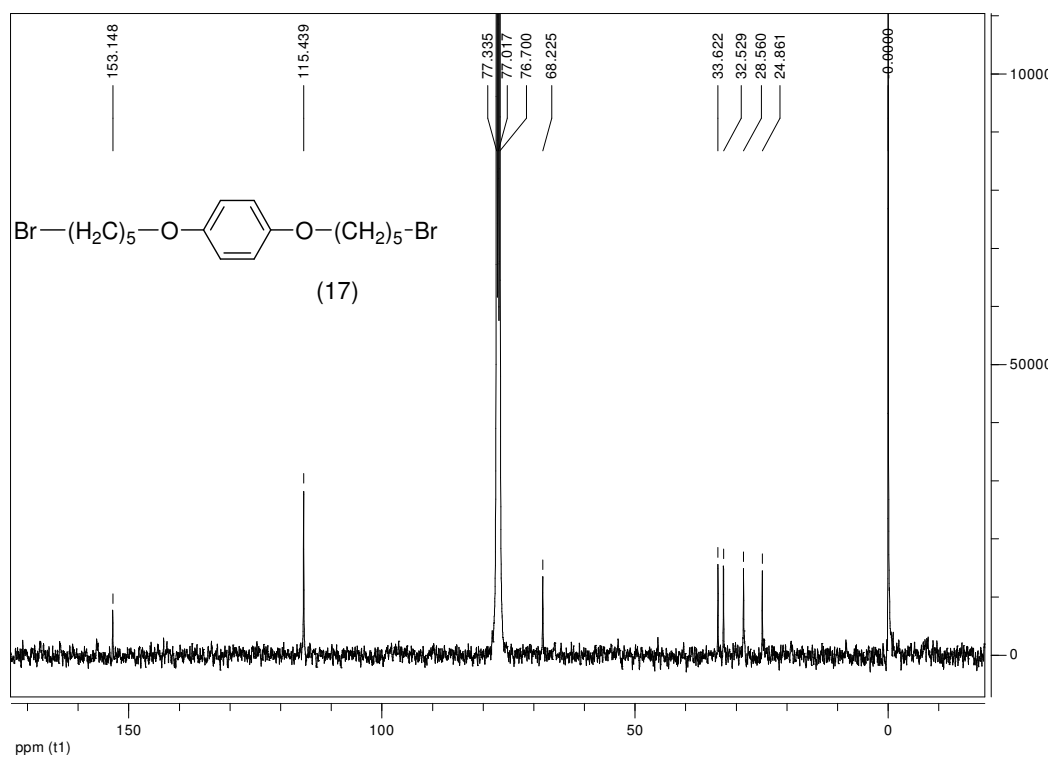


Figure 8.34 – Carbon NMR spectrum of compound 17.

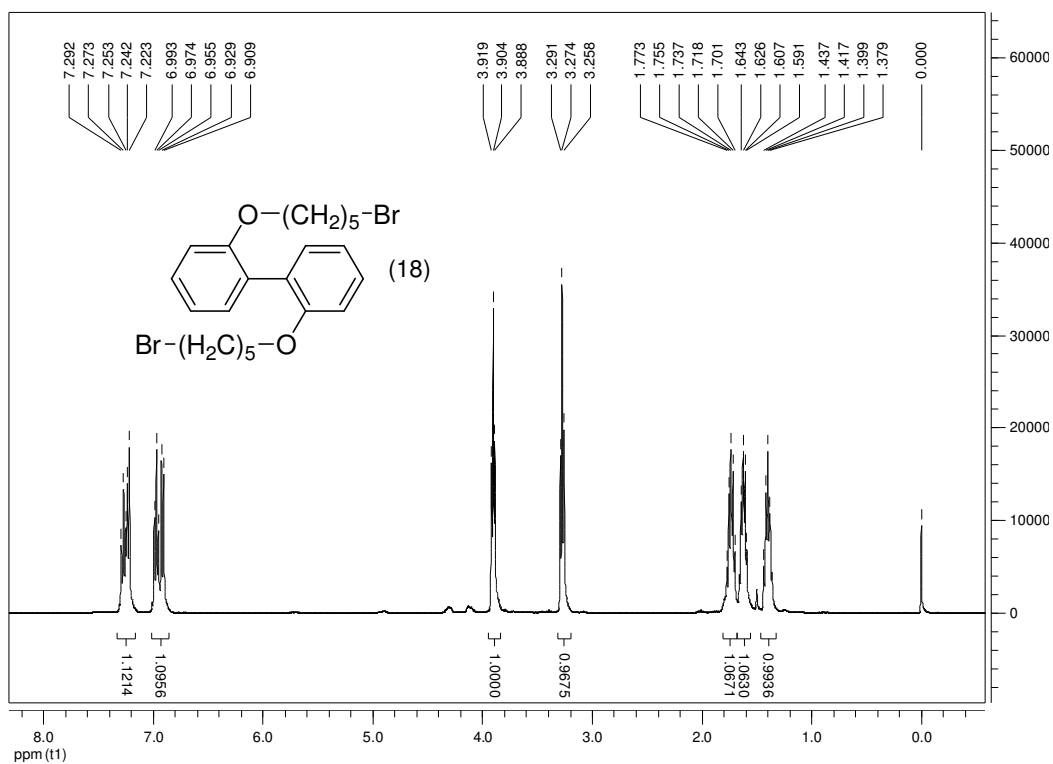


Figure 8.35 – Proton NMR spectrum of compound 18.

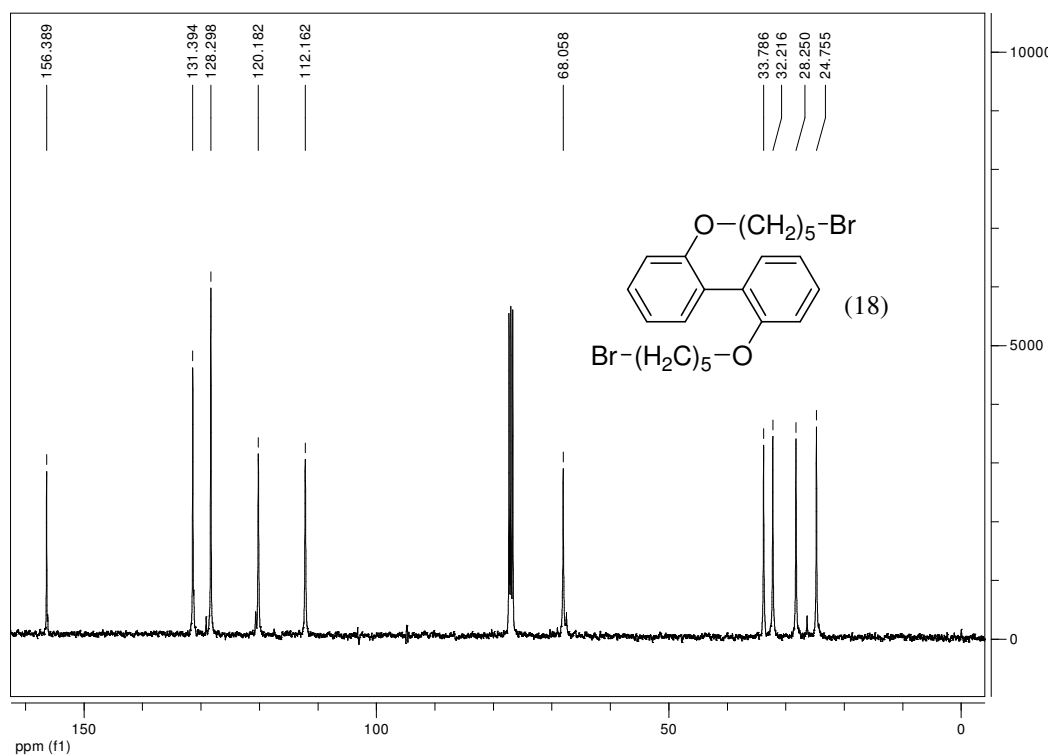


Figure 8.36 – Carbon NMR spectrum of monomer 18.

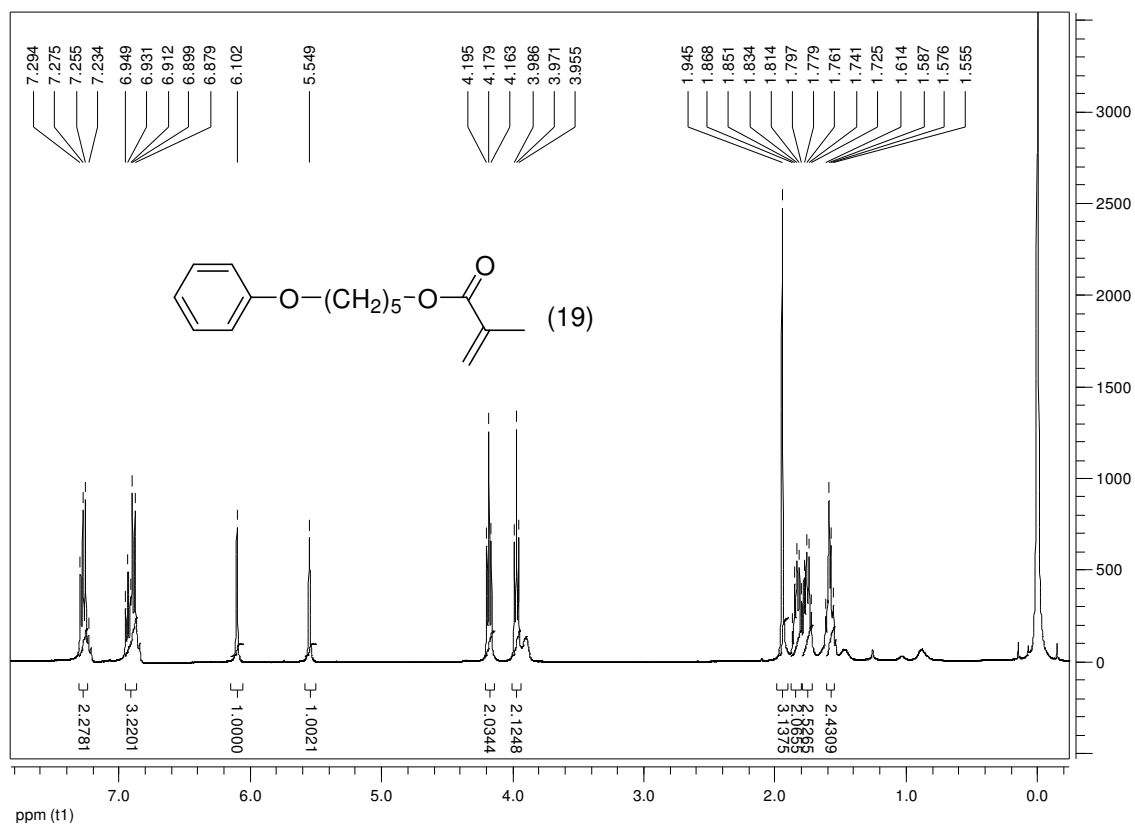


Figure 8.37 – Proton NMR spectrum of monomer 19.

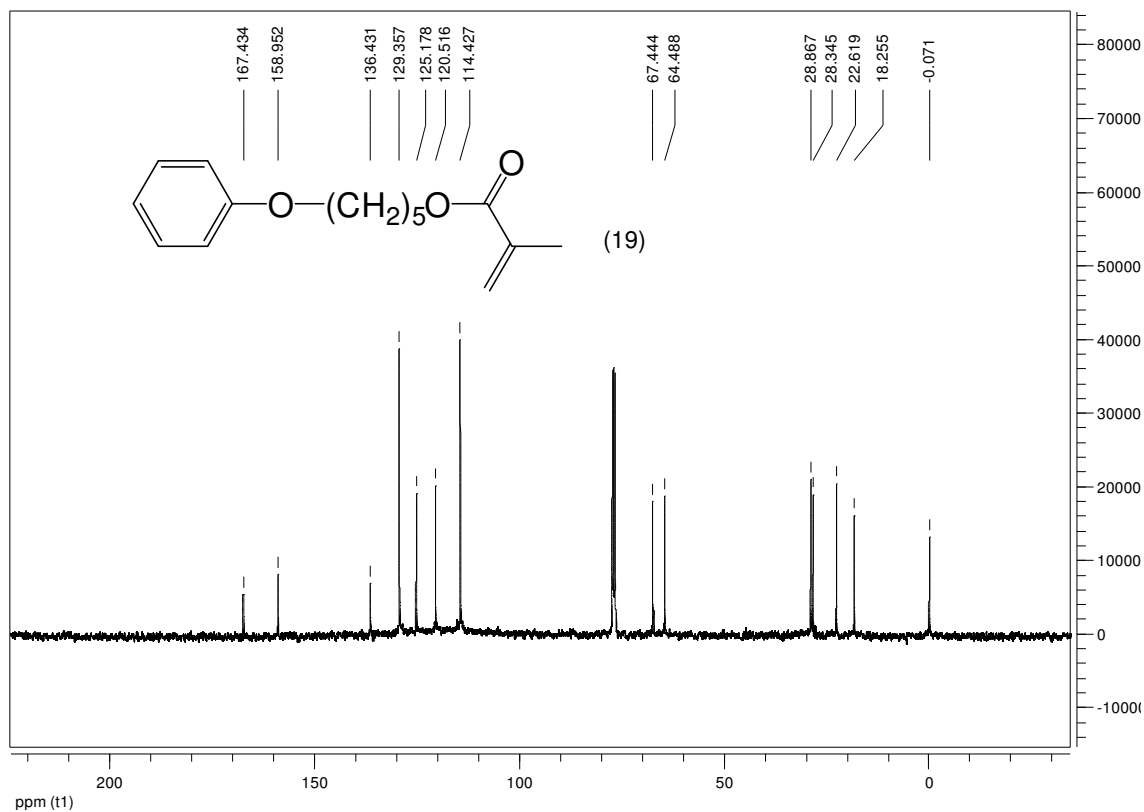


Figure 8.38 – Carbon NMR spectrum of monomer 19.

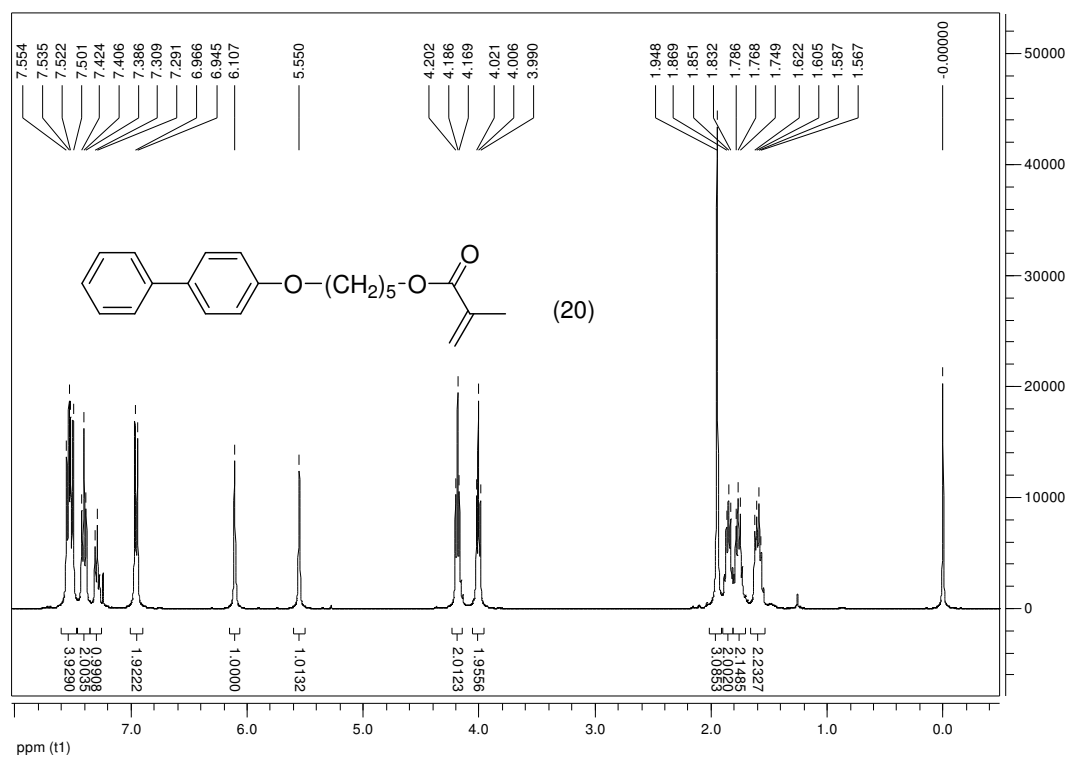


Figure 8.39 – Proton NMR spectrum of monomer 20.

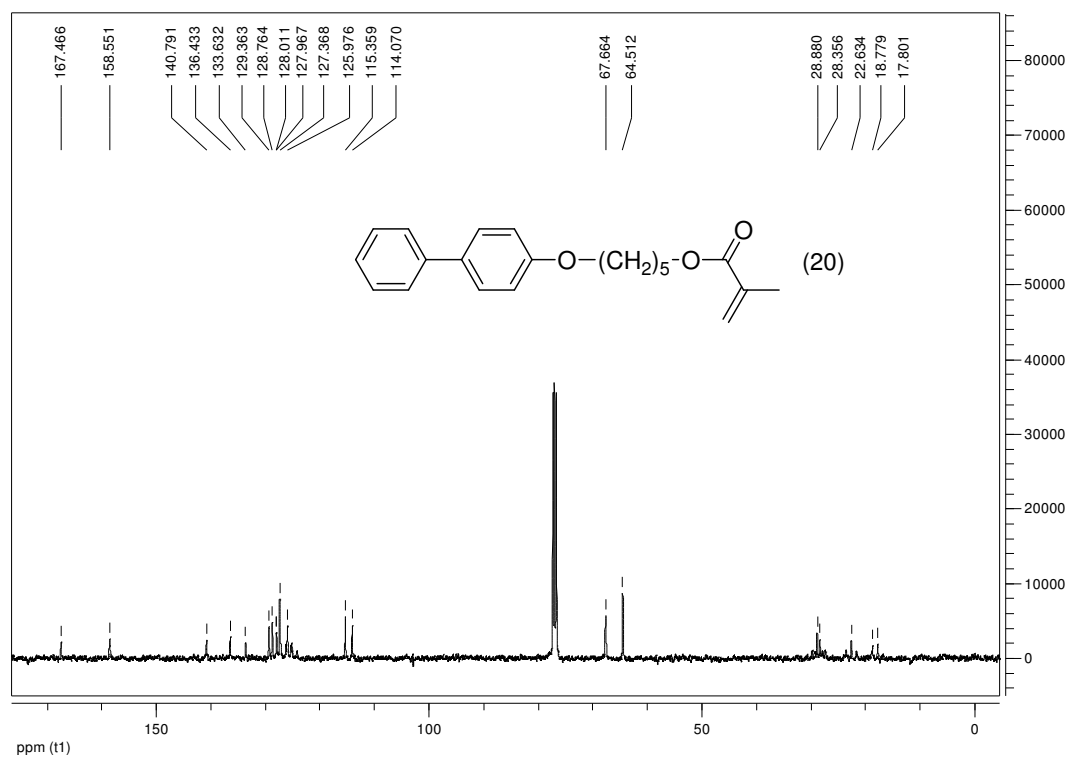


Figure 8.40 – Carbon NMR spectrum of monomer 20.

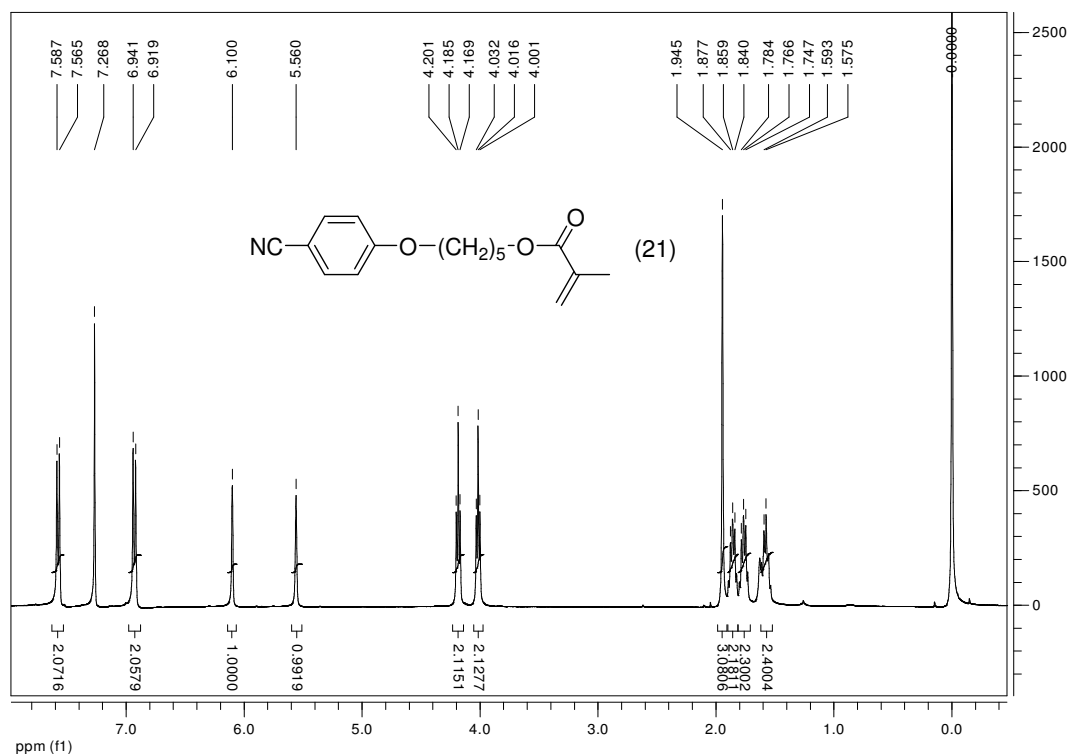


Figure 8.41 – Proton NMR spectrum of monomer 21.

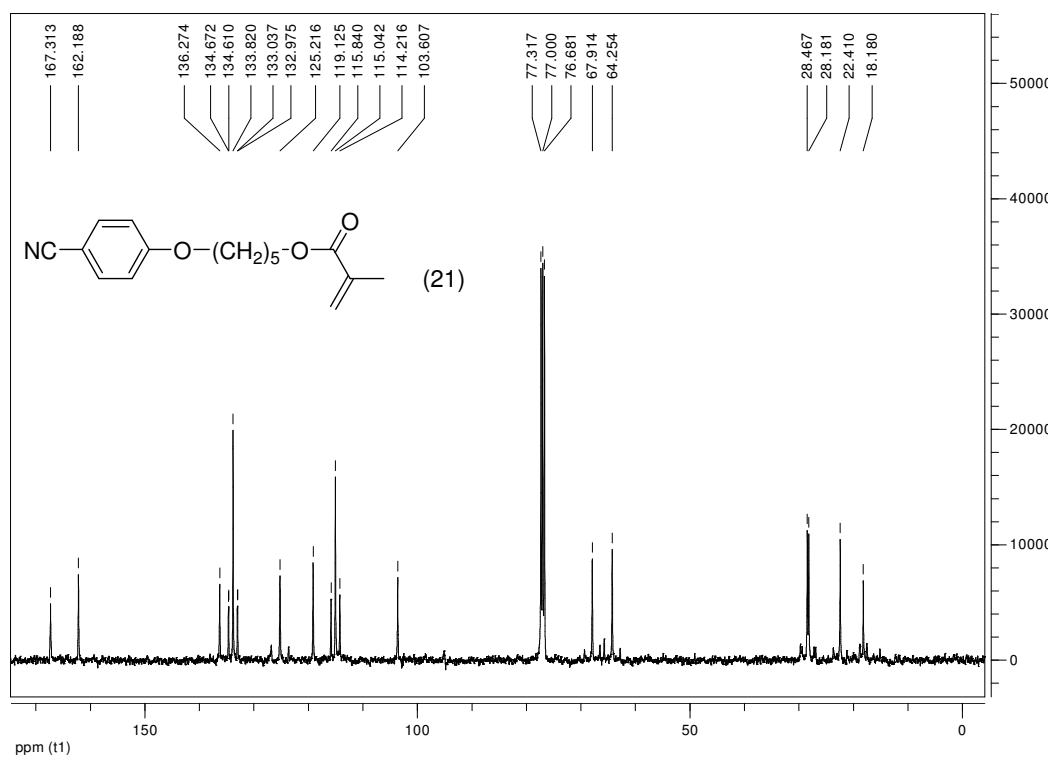
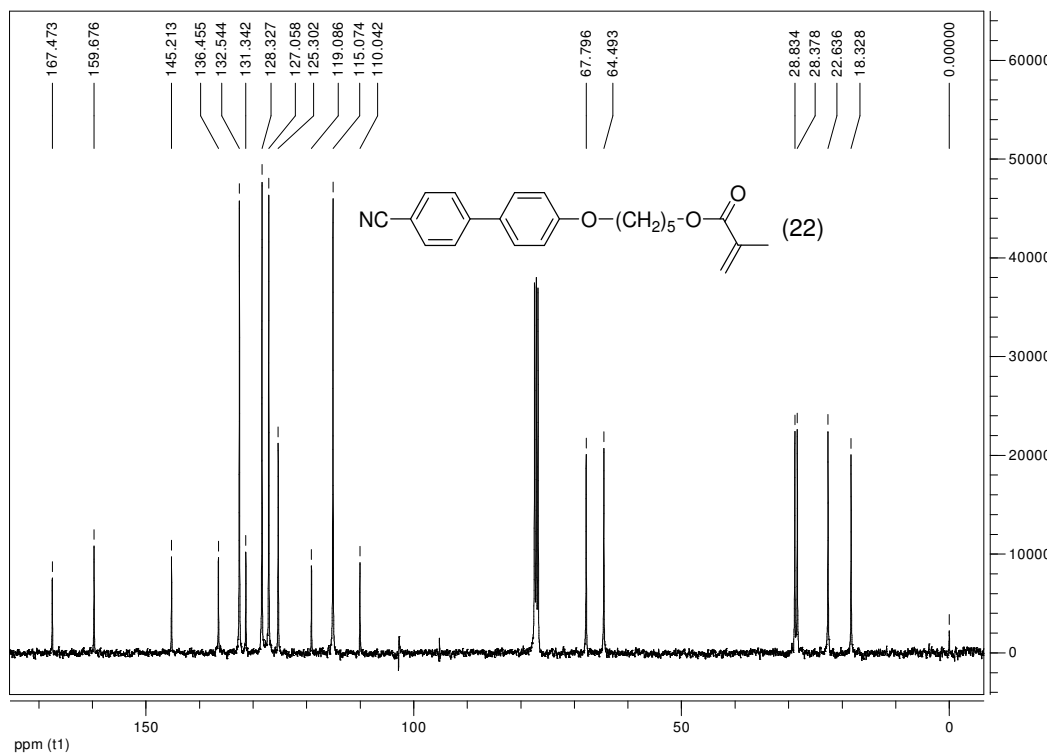
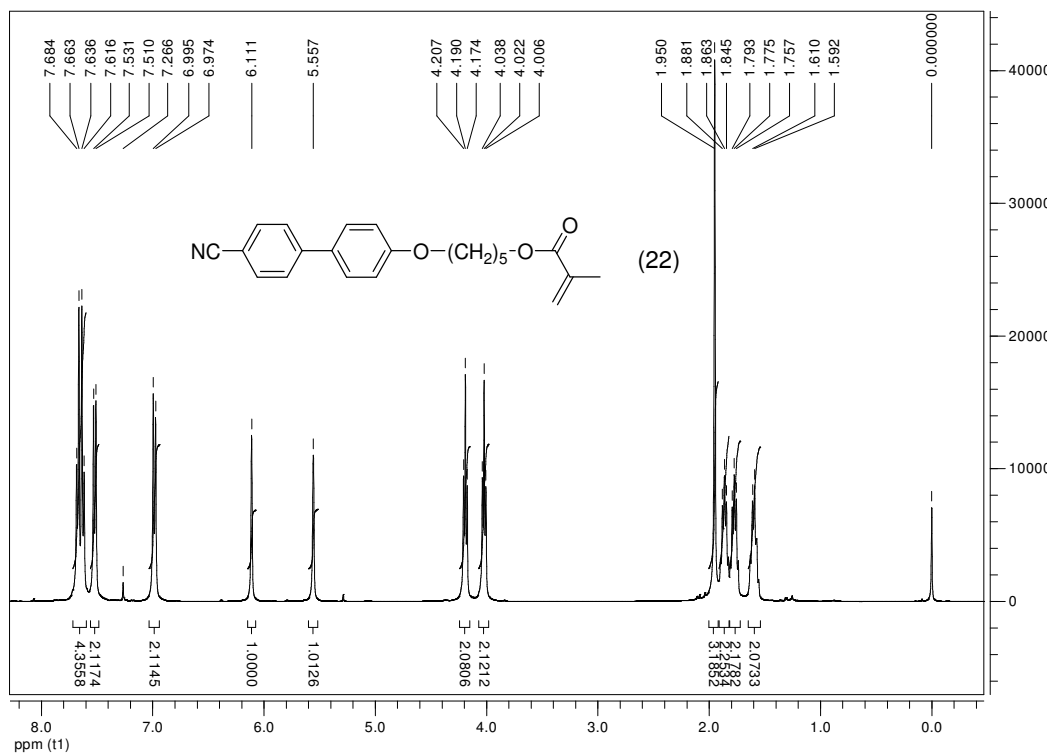


Figure 8.42 – Carbon NMR spectrum of monomer 21.



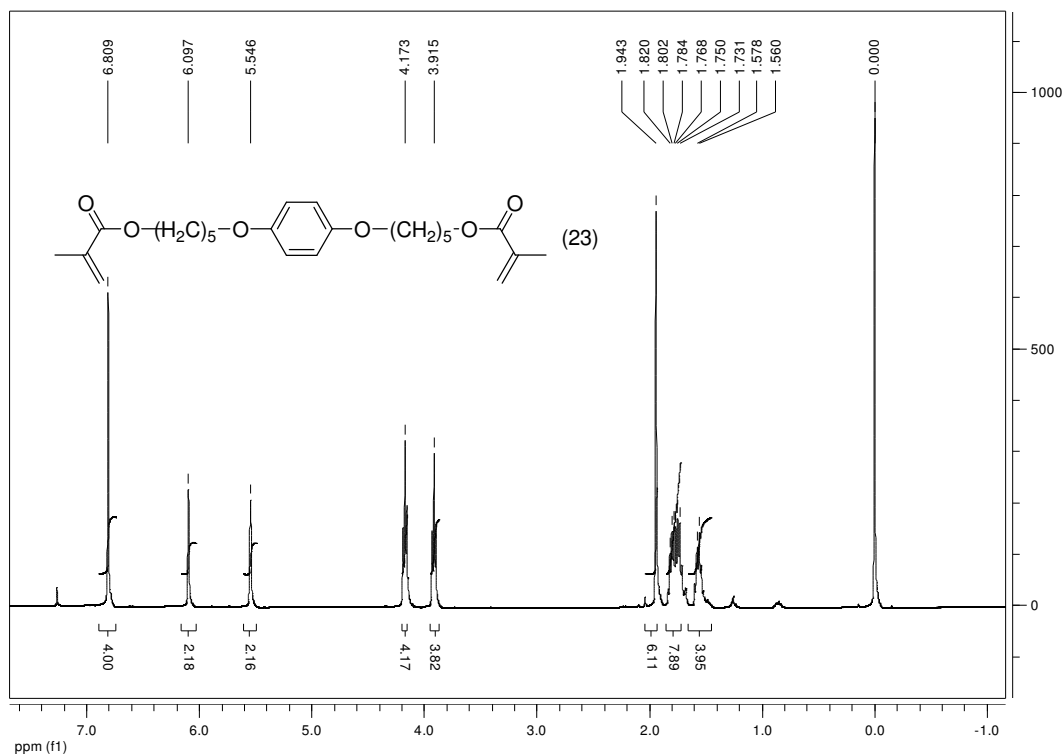


Figure 8.45 – Proton NMR spectrum of monomer 23.

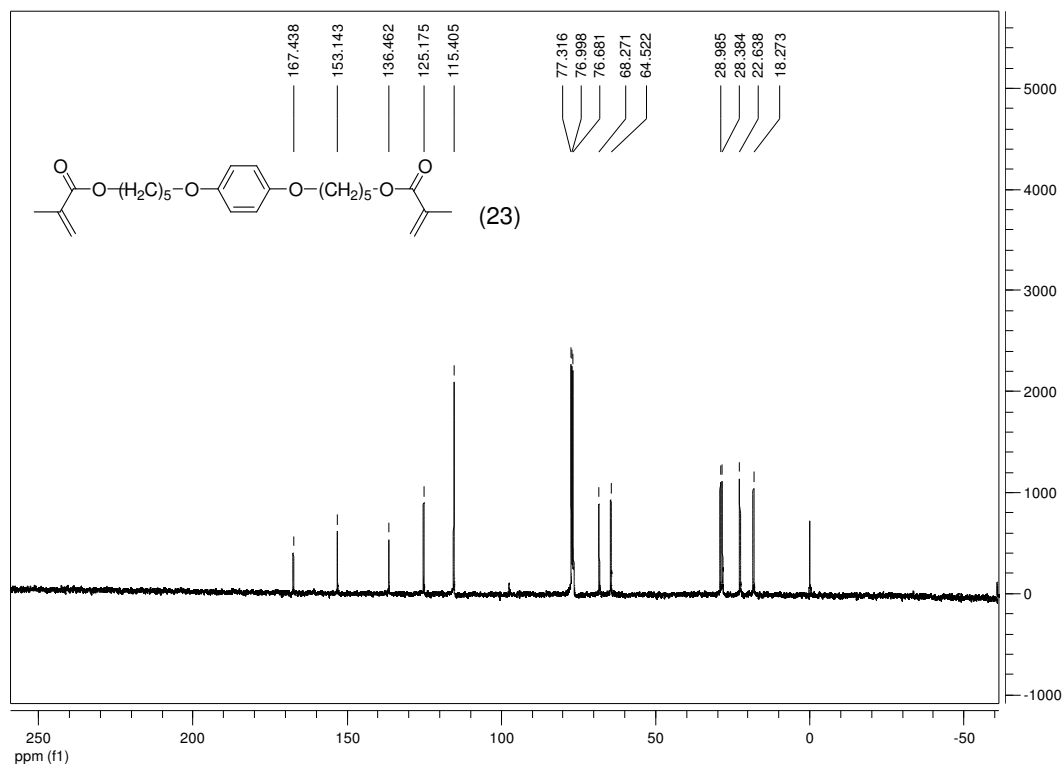


Figure 8.46 – Carbon NMR spectrum of monomer 23.

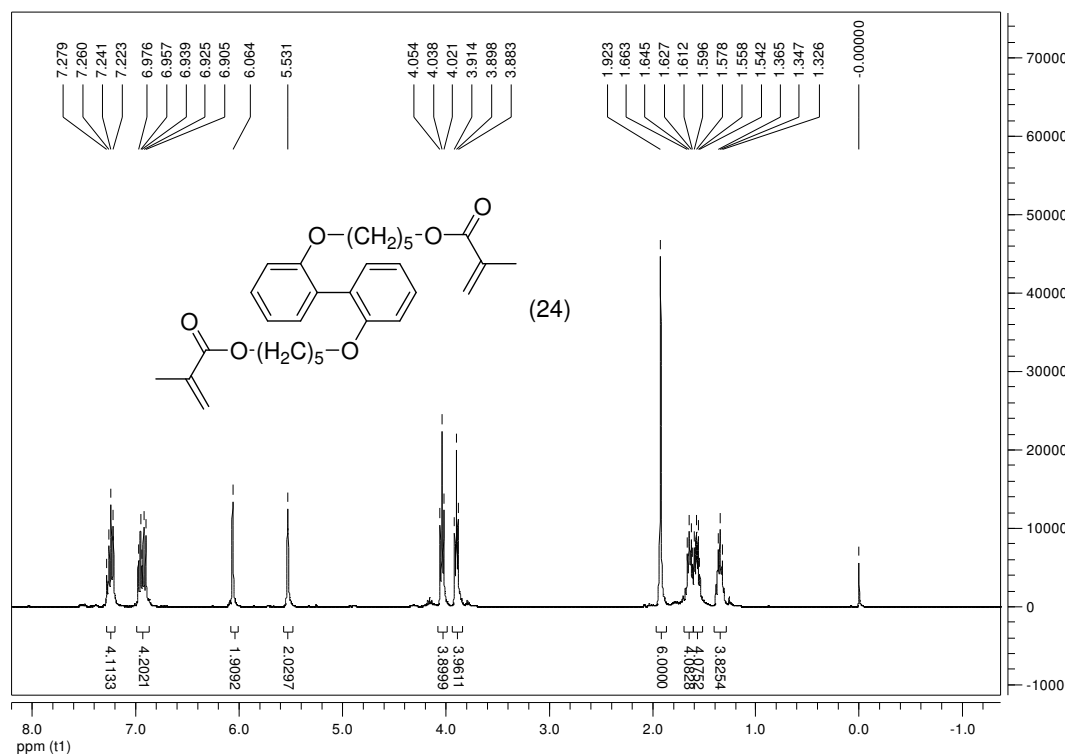


Figure 8.47 – Proton NMR spectrum of monomer 24.

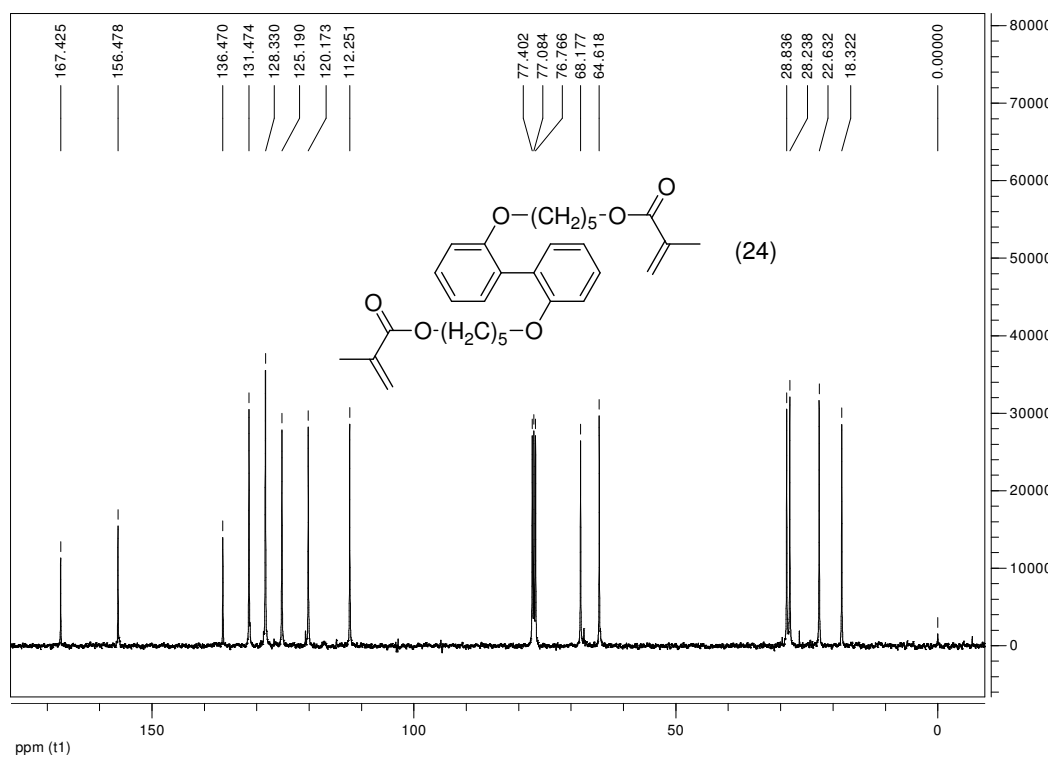


Figure 8.48 – Carbon NMR spectrum of monomer 24.



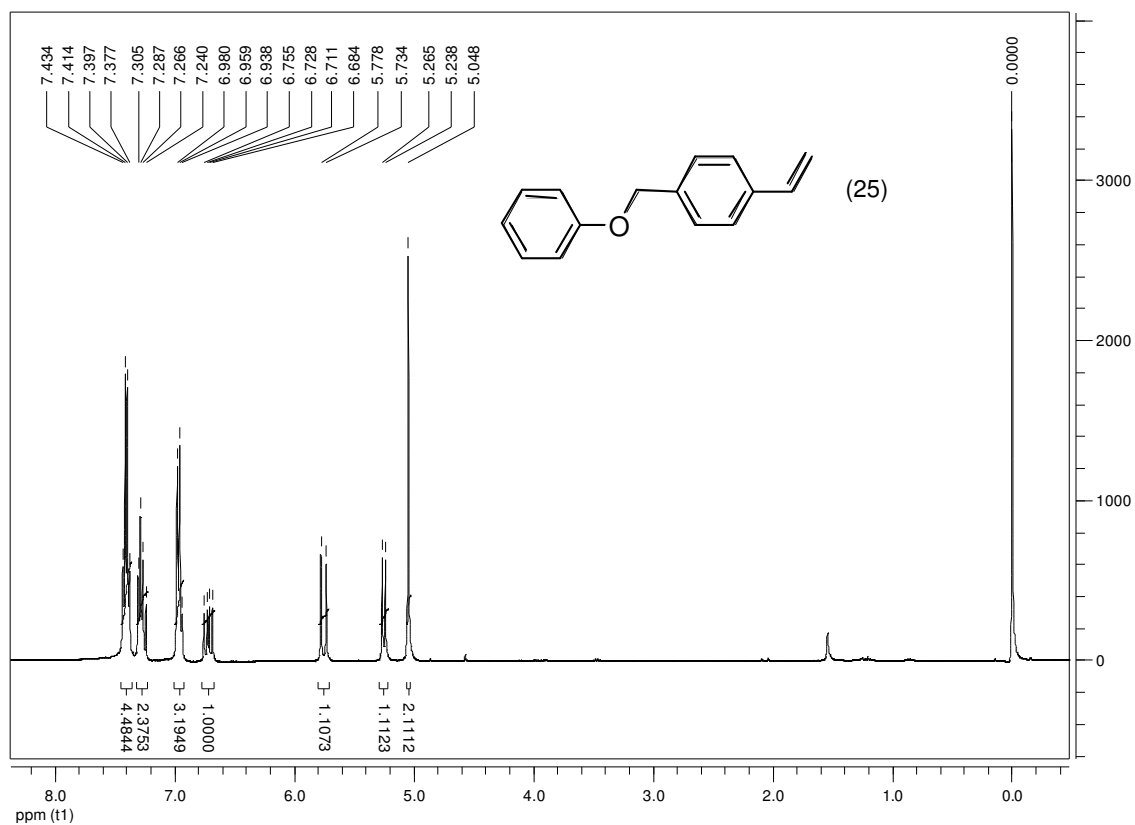


Figure 8.49 – Proton NMR spectrum of monomer 25.

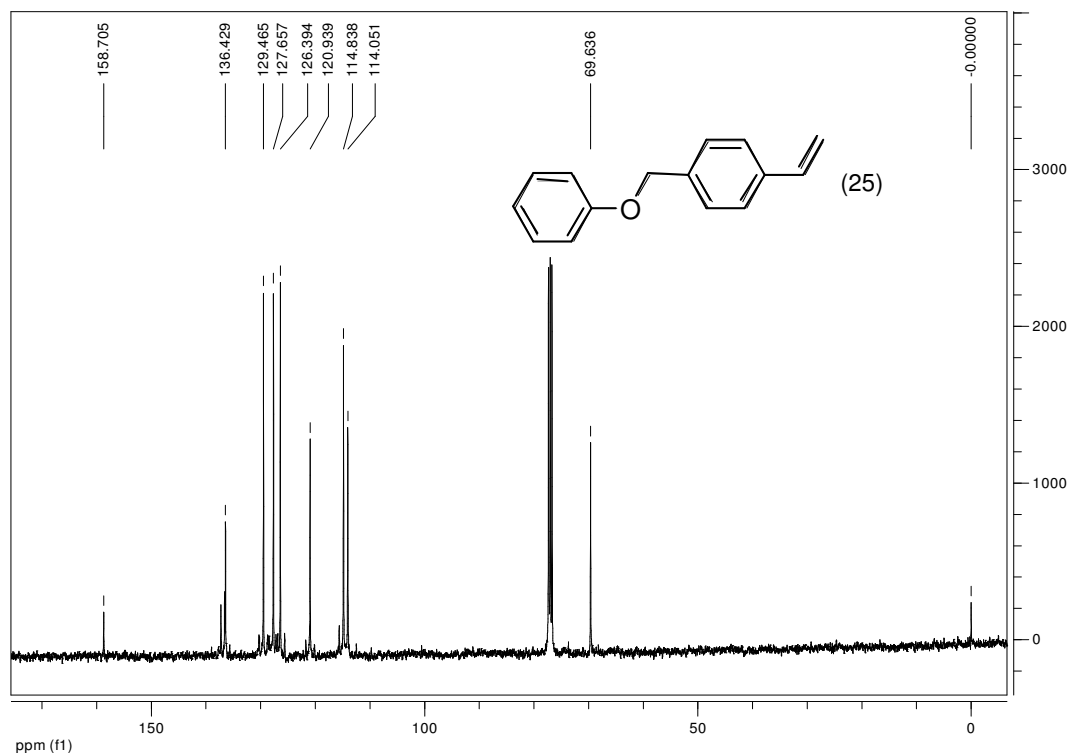


Figure 8.50 – Carbon NMR spectrum of monomer 25.

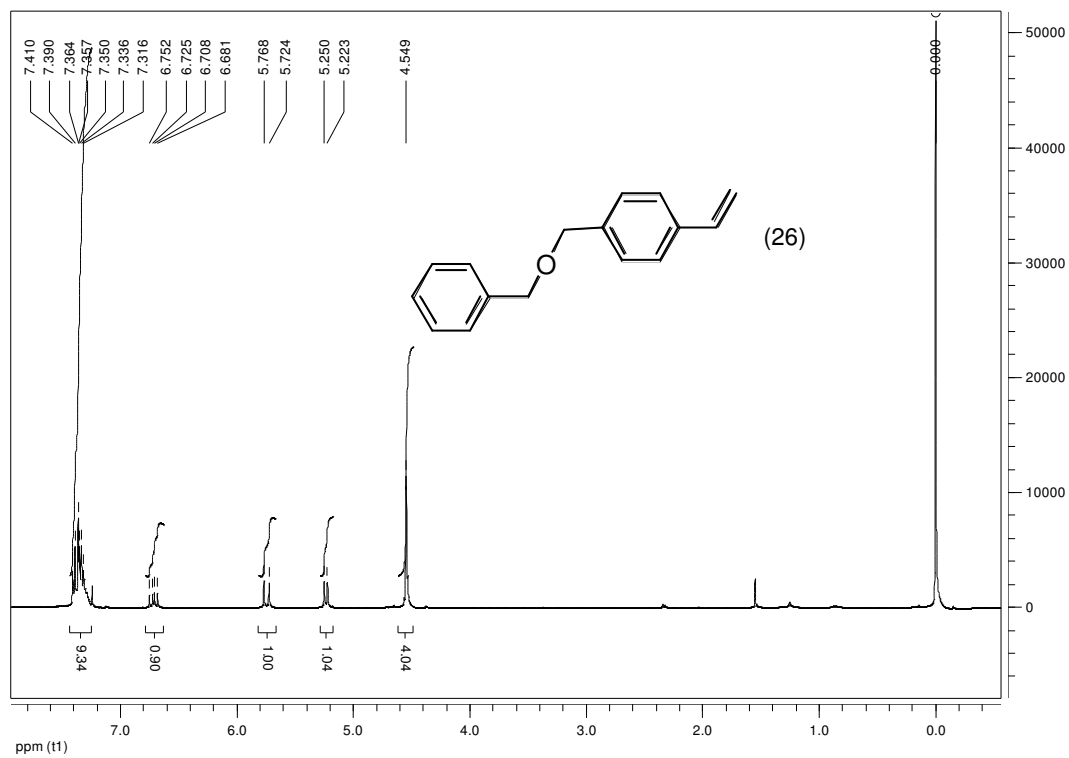


Figure 8.51 – Proton NMR spectrum of monomer 26.

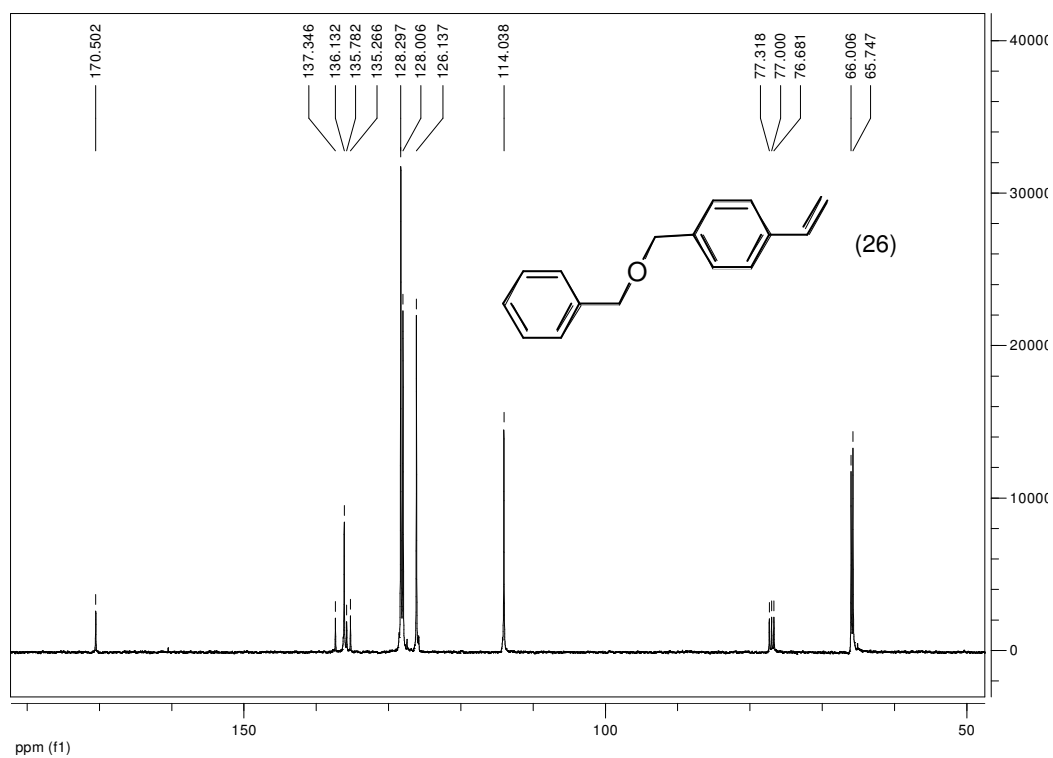


Figure 8.52 – Carbon NMR spectrum of monomer 26.